STRUCTURAL BASIS OF INTER-DOMAIN ELECTRON TRANSFER IN NCB5OR, A REDOX ENZYME IMPLICATED IN DIABETES AND LIPID METABOLISM

By

Bin Deng

Submitted to the graduate degree program in Rehabilitation Science and the Graduate Faculty of the University of Kansas in partial fulfillment of the requirements for the degree of Doctor of Philosophy

Hao Zhu, Ph.D. (co-chair, advisor)

Irina Smirnova, Ph.D. (co-chair)

David Benson, Ph.D. (co-advisor)

WenFang Wang, Ph.D.

Aron Fenton, Ph.D.

Date defended: August 17, 2011

The Dissertation Committee for Bin Deng
certifies that this is the approved version of the following dissertation

STRUCTURAL BASIS OF INTER-DOMAIN ELECTRON TRANSFER IN NCB5OR, A REDOX ENZYME IMPLICATED IN DIABETES AND LIPID METABOLISM

Hao Zhu, Ph.D. (co-chair, advisor)

Irina Smirnova, Ph.D. (co-chair)

Date approved: August 22, 2011

ABSTRACT

NADH cytochrome b5 oxidoreductase (Ncb5or) is a multi-domain redox enzyme found in all animal tissues and associated with the endoplasmic reticulum (ER). Ncb5or contains (from N-terminus to C terminus) a novel N-terminal region, the b5 domain (Ncb5or-b5), the CS domain, and the b5R domain (Ncb5or-b5R). Ncb5or-b5, the heme binding domain, is homologous to microsomal cytochrome b5 (Cyb5A) and belongs to cytochrome b5 superfamily. Ncb5or-b5R, the FAD (flavin adenine dinucleotide) binding domain, is homologous to cytochrome b5 reductase (Cyb5R3) and belongs to ferredoxin $NADP^+$ reductase superfamily. Both superfamilies are of great biological significance whose members have important functions. The CS domain can be assigned into the heat shock protein 20 (HSP20, or p23) family, whose members are known to mediate protein-protein interactions. Ncb5or is unique in containing these domains and employing a novel sequence as the N-terminal region.

Cyb5A and Cyb5R3 have been shown to form a complex to donate electrons to stearoyl-CoA desaturase (SCD) in fatty acid desaturation *in vitro*. Monounsaturated fatty acids are preferentially used in triglyceride synthesis for lipid storage. Mice with hepatic deletion of Cyb5A show no significant defect in lipid metabolism, whereas Ncb5or null mice exhibit diabetes, lipoatrophy and impaired SCD activity. We hypothesize that Ncb5or, as a fusion of both Cyb5A and Cyb5R3–like domains, serves as an alternative electron donor to SCD *in vivo*.

Ncb5or-b5 shows unique structural and functional features, such as, low sequence homology to other family members, displacement of the second heme-ligating His residue, a decrease in the number of surface-charged residues, and a much lower redox potential at the heme center

compared with Cyb5A. In order to understand how these differences between Ncb5or and Cyb5A contribute to their unique structural and functional properties in electron transfer, we solved the crystal structure of Ncb5or-b5 and performed kinetic assays by using various domain combinations. Our 1.25 Å crystal structure shows that Ncb5or-b5 has a general b5 fold. However, Ncb5or-b5 has a unique heme environment, namely the two heme-ligating His residues are nearly perpendicular to each other. The latter feature agrees with a large g_{max} value in electron paramagnetic resonance (EPR) spectra. This makes Ncb5or the first example with a tetragonally distorted heme environment in the cytochrome b5 superfamily. Lower density of charge on the surface of Ncb5or-b5 suggests weaker ionic interaction between Ncb5or-b5 and Ncb5or-b5R than that between Cyb5A and Cyb5R3. The lack of Ncb5or-b5/Ncb5or-b5R complex formation and lower rates of electron transfer than Cyb5A/Cyb5R3 are consistent with this hypothesis.

Low affinity between Ncb5or-b5 and Ncb5or-b5R prompted a search for other factors that facilitate the inter-domain electron transfer. Specifically, the role of the N-terminal region, a region rich in random coils but with little homology to known proteins, was explored. A reductionist approach was used to test various domains of Ncb5or with kinetic assays and spectral analyses, such as circular dichroism and nuclear magnetic resonance. I have unveiled the role of the N-terminal region for the first time: the N-terminal region facilitates inter-domain electron transfer by cooperatively interacting with the CS domain and the heme center of Ncb5or-b5. The formation of tertiary structure in the N-terminal region is governed by the region from Gly^{22} through Trp^{37}, especially Trp^{37}, and this region is essential for electron transfer. This feature suggests a potential mechanism to facilitate the inter-domain electron transfer in Ncb5or.

ACKNOWLEDGEMENTS

I would like to thank Dr. Hao Zhu (advisor), Dr. David Benson (co-advisor), Dr. Irina Smirnova, Dr. WenFang Wang and Dr. Aron Fenton for serving on my thesis committee and guiding me through the Ph.D. training.

I would like to thank Dr. Richard Schowen in University of Kansas (KU) for helpful suggestions in enzymology, Dr. Emily Scott for sharing equipments and Sudharsan Parthasarathy for the help in experiments.

I would like to thank Dr. Robert Hanzlik, Dr. Scott Lovell and Dr. Philip Gao in KU Center of Biomedical Research Excellence Protein Structure and Function (COBRE PSF) for facilitating protein preparation and crystallization, as well as solving crystal structure (S.L.).

I would like to thank Dr. Mark Hargrove and Ryan Sturms at Iowa State University for helping me with collecting stop-flow data.

I would like to thank Dr. Brian Gibney in Brooklyn College for collecting EPR data.

I would like to thank Dr. Susan Carlson for teaching me fatty acid profiling during my early graduate work.

I would like to thank Dr. Frank Bunn in Brigham and Women's Hospital for generous support to our laboratory and to my career.

TABLE OF CONTENTS

Chapter One

Introduction

Structural features of Ncb5or and homologues

NADH cytochrome b5 oxidoreductase (Ncb5or, also referred as Cyb5R4 or b5+b5R) was first identified during a bioinformatics search of the expressed sequence tag database (dbEST) for a putative hypoxia-sensing flavoprotein [1]. The amino acid sequence of classic cytochrome b5 reductase (Cyb5R3) containing FAD and NAD(P)H binding motifs was used as a query for the BLAST search [1]. Along with Ncb5or, two more novel homologues (b5R1 or Cyb5R1 and b5R2 or Cyb5R2) were identified (**Figure 1**).

Ncb5or contains four domains (from N terminus to C terminus): a novel N terminal region which has no homology with any known protein, a heme-binding b5 domain (Ncb5or-b5) which is homologous to microsomal cytochrome b5 (Cyb5A), a linkage CHORD-SGT1 domain (Ncb5or-CS) which is homologous to heat shock protein 20 (HSP20), and a FAD-binding b5R domain (Ncb5or-b5R) which is homologous to cytochrome b5 reductase (Cyb5R3) [1,2,3] (**Figure 2A**). Human Ncb5or has 521 amino acid residues. There are about 50, 90, 90 and 270 residues in the N-terminal region, Ncb5or-b5, Ncb5or-CS and Ncb5or-b5R, respectively.

Upon NAD(P)H binding, Ncb5or shuffles electrons flow from NAD(P)H to FAD (Ncb5or-b5R) and then to heme (Ncb5or-b5), reducing ferric iron to ferrous [1] (**Figure 2B**). Reduced heme in Ncb5or can donate electrons to multiple artificial acceptors, including cytochrome c, methemoglobin, ferricyanide and molecular oxygen [1,2]. The heme center in Ncb5or was identified to have a relatively low redox potential (-108 mV vs. the standard hydrogen electrode, SHE) in comparison to other members of the b5 superfamily [2], making Ncb5or a potent electron donor.

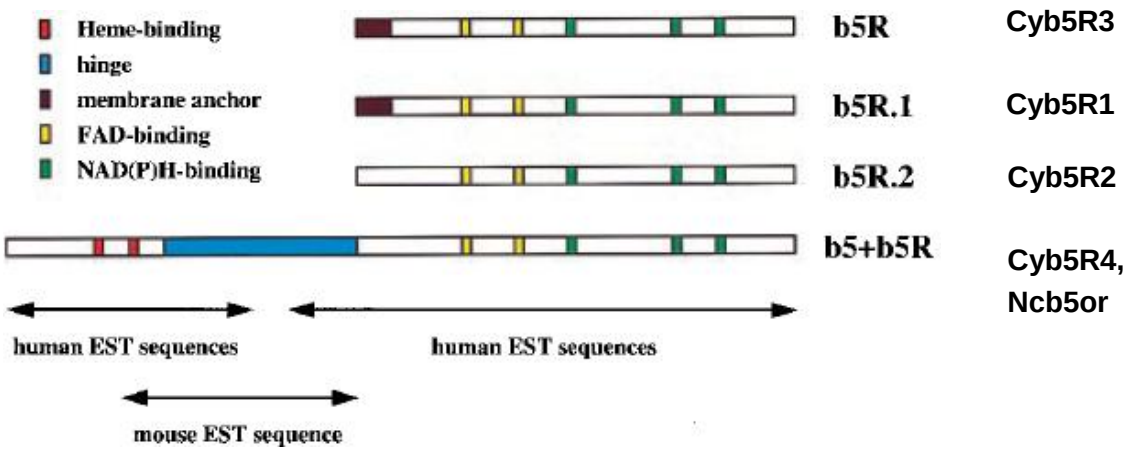

Figure 1. Schematic diagram of cDNA clones of Cyb5R1, Cyb5R2 and Ncb5or (Cyb5R4, b5+b5R) in human. The sequence of Cyb5R3 was used to search hypoxia-sensing flavoproteins, and three novel homologues were identified. Cyb5R1, Cyb5R2 and Ncb5or all contain a b5R domain, which binds FAD and NAD(P)H. Cyb5R3 and Cyb5R1 have an N-terminal membrane anchor, whereas none can be identified in Cyb5R2 and Ncb5or. Ncb5or has a heme-binding domain and a unique hinge domain that are not present in other isoforms. This figure is adapted from Zhu *et al.*[1].

A

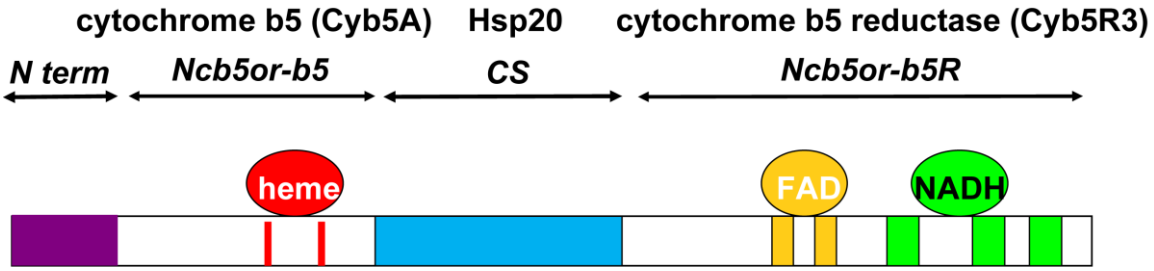

B

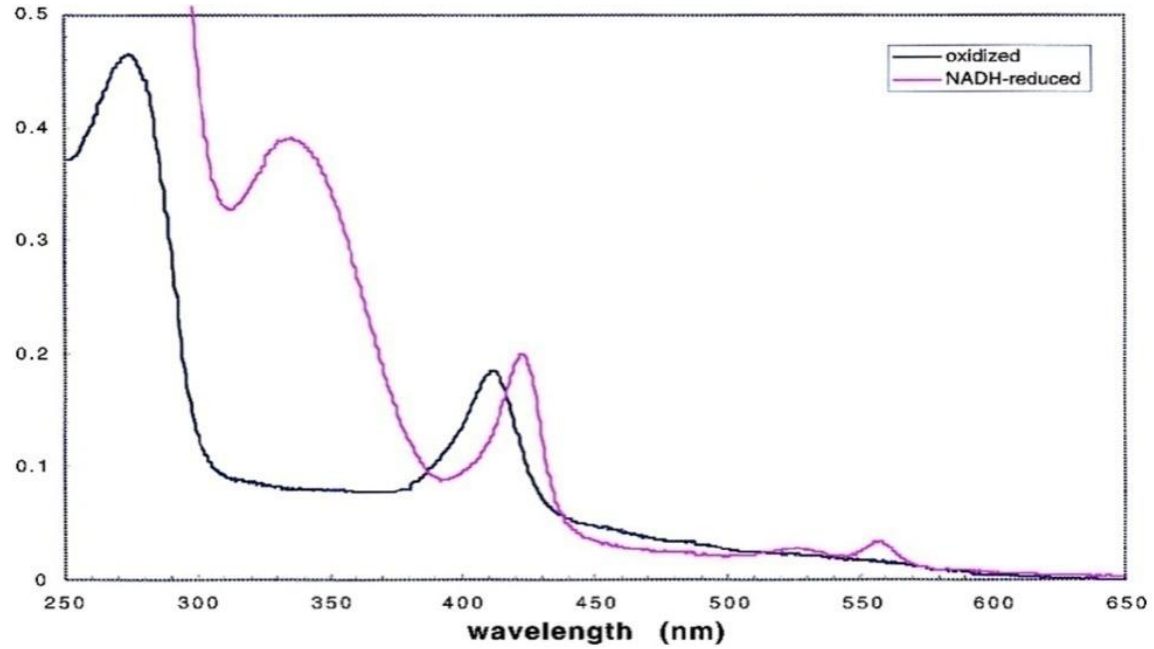

Figure 2. (A) Schematic diagram of individual domains in Ncb5or. Ncb5or contains a novel N-terminal region, a b5 domain, a CS linkage domain and a b5R domain. The last three are homologous to Cyb5A, HSP20 and Cyb5R3, respectively. Like Cyb5A and Cyb5R3, Ncb5or-b5 and Ncb5or-b5R employs heme and FAD, respectively, as prosthetic groups. (B) Action spectra of heme reduction (inter-domain electron transfer) in Ncb5or. By using NAD(P)H as electron source, Ncb5or can reduce its own heme by transferring electrons from the b5R domain to the heme of b5 domain. **Figure 2B** is adapted from Zhu *et al.*[1].

Besides Ncb5or, other b5-containing proteins are (**Figure 3**): (a) Δ5 and Δ6 desaturase in mammals have a b5 domain (cytochrome b5 domain) and a trans-membrane desaturase domain [4,5]. The latter employs a non-heme iron as cofactor. The b5 domain in Δ5 and Δ6 desaturase donates electrons to the iron in the desaturase domain, which catalyzes formation of a double bond at the Δ5 and Δ6 position of fatty acids, respectively. (b) Sulfite oxidase in mammals and birds, which contains a molybdenum-binding oxidase domain [6,7,8]. The molybdenum in the oxidase domain extracts electrons from sulfite and donates them to cytochrome c through the b5 domain. As a result, sulfite is oxidized to sulfate. (c) Yeast flavocytochrome b2 or lactate dehydrogenase is a fusion of the b5 domain and a dehydrogenase domain, which binds flavin mononucleotide (FMN) as a prosthetic group [9]. Electrons flow from lactate to the dehydrogenase domain, then to the b5 domain, and eventually to cytochrome c. Consequently, lactate is oxidized to pyruvate. (d) Nitrate reductase in algae and plants is a fusion protein of a b5 domain and a b5R domain [10,11,12]. This reductase also contains an extra reductase domain which is similar to the oxidase domain in sulfite oxidase and binds molybdenum. Nitrate reductase transfers electrons from the b5R domain to the b5 domain, and then to the molybdenum-binding domain, reducing nitrate to nitrite. Hinges are located between these domains in nitrate reductase. They contain fewer residues and are highly variable. The functions and localizations of these enzymes are summarized in **Table 1**.

Analyses of amino acid sequences of Ncb5or-b5R suggest that it is a member of ferredoxin-NADP reductase (FNR) superfamily. Cyb5R1, Cyb5R2, Cyb5R3, Ncb5or (Cyb5R4) and nitrate reductase belong to this superfamily [13,14,15]. Other members of FNR superfamily

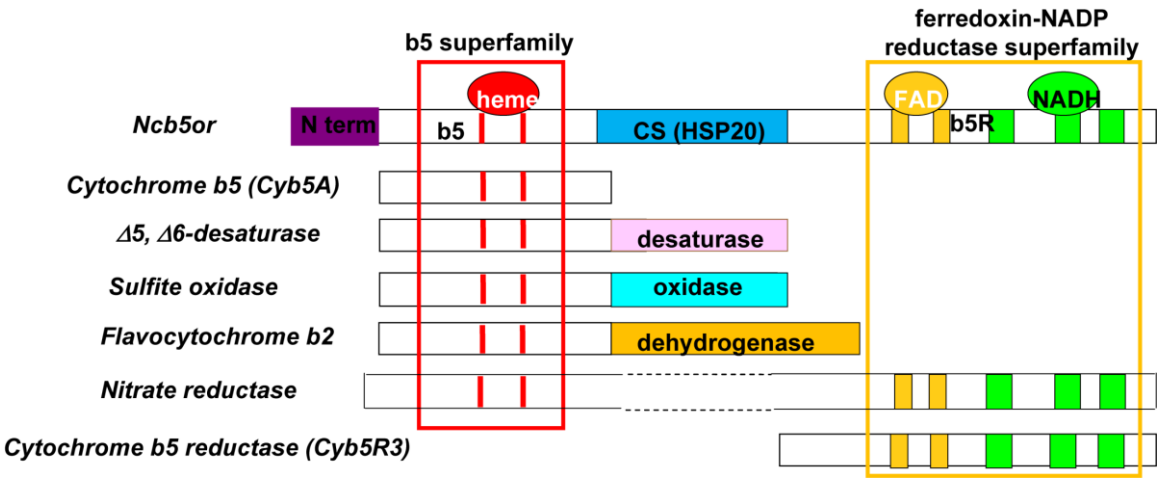

Figure 3. Schematic diagram of Ncb5or and its homologues. The b5 domain of Ncb5or is identified in members of the b5 superfamily, which usually contain a second redox-active domain, such as an iron-binding desaturase domain in $^{\Delta}5$ or $^{\Delta}6$ desaturase, a molybdenum-binding domain in sulfite oxidase or nitrate reductase, and a FMN-binding domain in flavocytochrome b2. The second redox-active domain serves to process the substrate, whereas the b5 domain either donates or accepts electrons from the second redox-active domain.

Table 1. Functions of Ncb5or and its homologues

Protein	Function	Localization
Ncb5or	Putative electron donor of (stearoyl-CoA desaturase) SCD *in vivo*	Endoplasmic reticulum (ER)
Cyb5A	Electron donor to SCD and P450	ER
Cyb5B	Synthesis of androgens	Outer-mitochondrial membrane
Desaturase (b5 fusion)	$^{\triangle}5$, $^{\triangle}6$ fatty acid desaturation	ER
Sulfite oxidase (b5 fusion)	Oxidation of sulfite to sulfate	Mitochondria
Cytochrome b2 (b5 fusion)	Oxidation of lactate to pyruvate	Mitochondria
Nitrate reductase (b5-b5R fusion)	Reduction of nitrate to nitrite	Cell-wall and tonoplast/cytoplasmic membranes
Cyb5R2	Reduction in spermatozoa	
Cyb5R3	Reduction of Cyb5A and Cyb5B	ER and mitochondria
Soluble Cyb5A and Cyb5R3	Reduction of methemoglobin	Cytosol in red blood cell

include cytochrome P450 reductase, nitric oxide synthase, sulfite reductase, and flavohemoglobin [13]. The function of Cyb5R1 and Cyb5R2 remain unclear, although Cyb5R2 was shown to be involved in redox reactions in spermatozoa [16].

Crystal structures of Cyb5A (PDB code 1CYO), Cyb5B (PDB code 3MUS; 3NER), yeast flavocytochrome b2 (PDB code 1FCB) and b5 domain of sulfite oxidase (PDB code 1MJ4) have been solved [8,17,18,19]. Although sequence variation exists across these proteins, their heme-binding regions share a similar b5 fold, (**Figure 4**). Cyb5A and Cyb5B have highly similar folds. In all of these four proteins, heme is sandwiched between two helix-loop-helix motifs with ligation to heme iron provided by the side chains of two histidine residues. However, the differences among them are: 1) position of the fourth helix (lower-left in each panel); 2) relative orientation of heme inside the pocket; 3) conformation and total number of β sheets; and 4) a second hydrophobic core at the back side of the β–sheet (**Figure 4**). Their common properties determine their function as electron transfer agents, whereas their variations allow specificity for their partners.

Comparison between the crystal structure of Cyb5R3 [20] (PDB code 1UMK) and a structure predicted for Ncb5or-b5R using the I-TASSER server [21] reveals a similar fold of backbone (**Figure 5**, cyan for Cyb5R3 and purple for Ncb5or-b5R). However, in the FAD-binding region, Ncb5or-b5R has a shorter loop to wrap FAD than that in Cyb5R3, which may result in looser FAD binding in Ncb5or-b5R. It is also noteworthy that Ncb5or-b5R contains fewer charged residues compared to Cyb5R3. This difference can decrease the solubility of Ncb5or-b5R in an aqueous environment. Asp371 and Leu424 are conserved residues, of which point mutations have

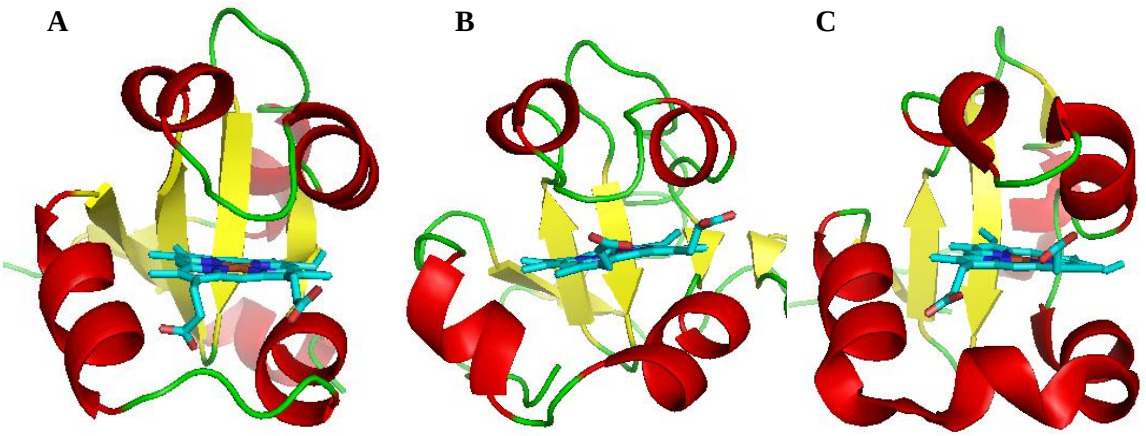

Figure 4. Crystal structures of bovine Cyb5A (A, PDB code 1CYO), the b5 domain of yeast flavocytochrome b2 (B, PDB code 1FCB) and the b5 domain of human sulfite oxidase (C, PDB code 1MJ4). They have similar b5 folds in the core heme-binding region, which contains two helix-loop-helix motifs. Heme is sandwiched between these two motifs.

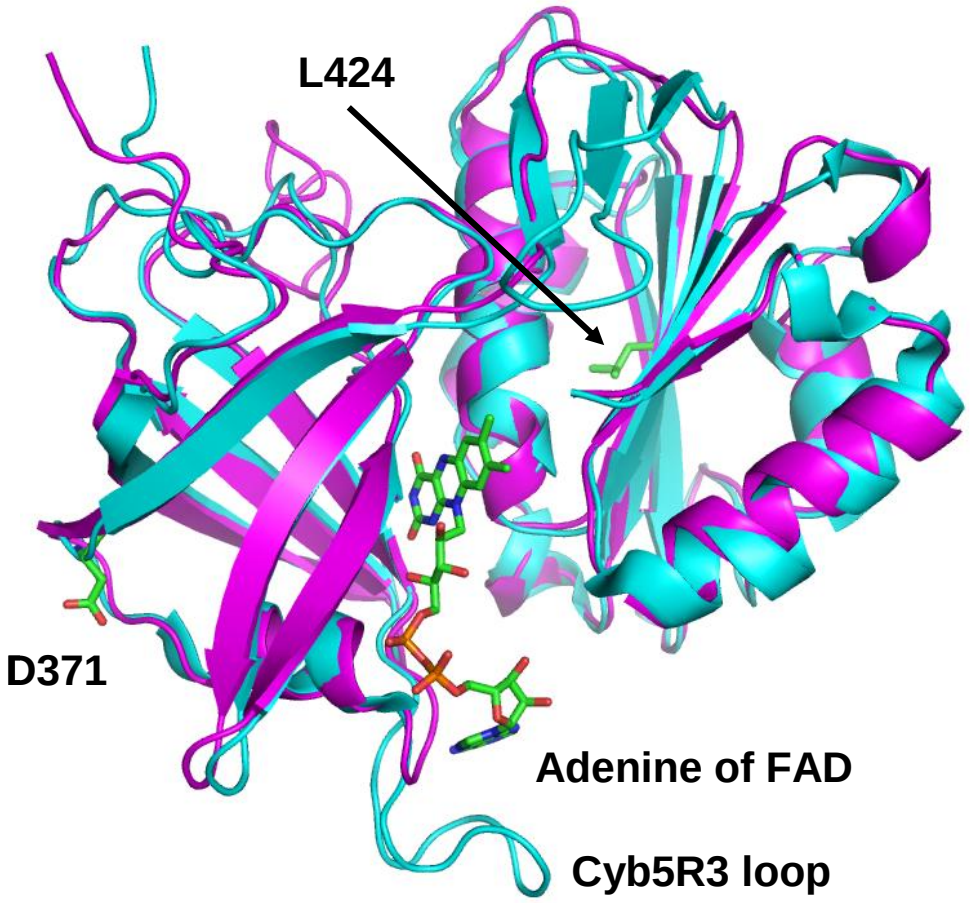

Figure 5. Overlay of crystal structure of Cyb5R3 (PDB code 1UMK) with the predicted structure of Ncb5or-b5R. Cyb5R3 is cyan and Ncb5or-b5R is purple. The two structures have similar folds, but in the FAD-binding region Cyb5R3 contains a longer loop to wrap FAD. FAD, Asp371 and Leu424 are labeled.

been found in human breast cancer specimens [22].

The CS domain of Ncb5or has been identified as a member of the HSP20 or p23 family [3], which is involved in protein-protein interactions. HSP20 binds to the ATP-bound form of HSP90 and stabilizes this state, and the complex facilitates folding of various client proteins [23]. Among family members, Sgt1 has the highest homology with the CS domain in Ncb5or (~30% sequence identity). Sgt1 works with HSP90 to mediate an innate immune response in animals [24]. A crystal structure of the plant Sgt1-HSP90 complex has been solved [25]. Tyr157, Phe168, Lys221 and Glu223 in Sgt1 are shown to interact with HSP90, suggested by the crystal structure and results of mutagenesis studies [25,26]. In the HSP20 family, the folds of all members can be fit into a model of seven β sheets [3]. Crystal structures of human p23 [27] and plant (Arabidopsis) Sgt1 [25], and the predicted structure of Ncb5or-CS [21] all match to this model (**Figure 6**). Notably, residues Phe173, Tyr184, Lys239 and Glu241 in Ncb5or correspond to Tyr157, Phe168, Lys221 and Glu223 in Sgt1, respectively, which are responsible for interaction with HSP90. In addition, Ncb5or-CS contains conserved residues, such as Lys188 and Arg 205, which are not found in Sgt1. Based on these sequence features it is interesting to speculate that Ncb5or-CS may be involved in interaction with specific partner(s).

In summary, Ncb5or is a unique natural fusion protein containing a novel N terminal region, a heme-binding domain, a linkage domain and a FAD-binding domain. Ncb5or-b5, Ncb5or-b5R and Ncb5or-CS belong to the b5 superfamily, FNR superfamily and p23 family, respectively. Members of each family fulfill important biological functions. Electrons can flow from Ncb5or-b5R to Ncb5or-b5, and then to acceptor(s). Multiple artificial ones have been identified.

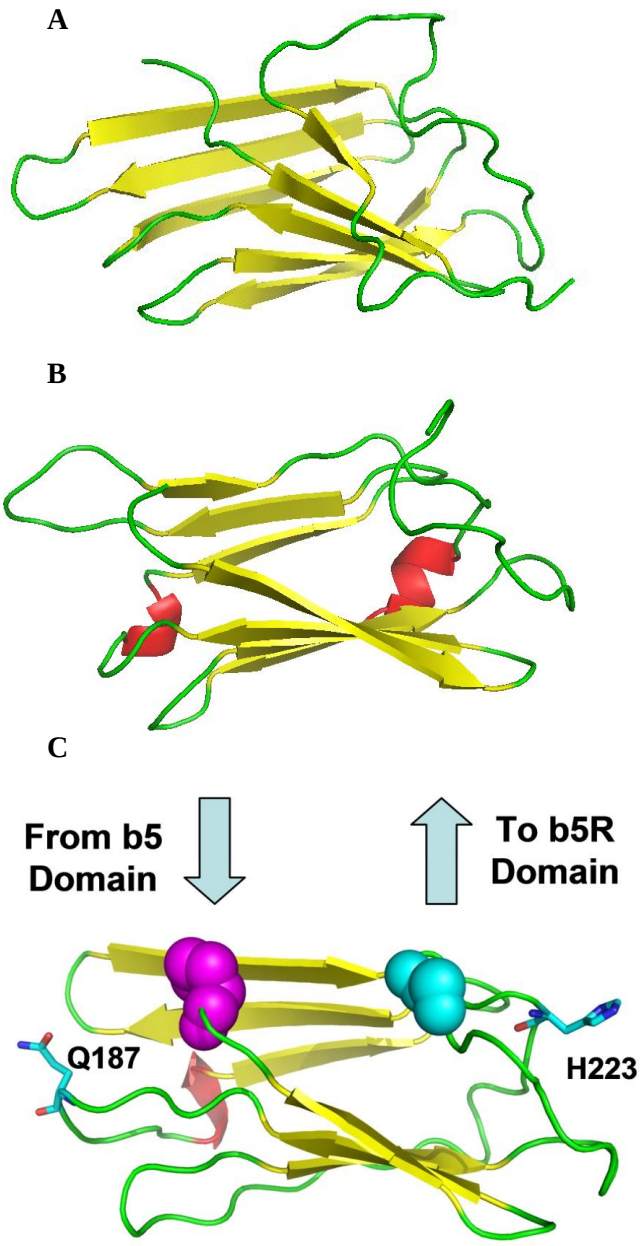

Figure 6. Crystal structures of human p23 (A, PDB code 1EJF) and Arabidopsis Sgt1 (B, PDB code 2XCM), and predicted structure of Ncb5or-CS (C). All of them show seven anti-paralleled β sheets plus multiple turns. Both p23 and Sgt1 are involved in protein-protein interaction. It is likely that Ncb5or-CS is also responsible for protein-protein interaction. Gln187 and His223 were previously identified residues for polymorphism [28].

Biological function of Ncb5or and its redox homologues

There are two isoforms of cytochrome b5: Cyb5A and Cyb5B (28) (**Figure 7**). Cyb5A is tail-anchored to the ER membrane, whereas Cyb5B is tail-anchored to the outer-mitochondrial membrane. These two isoforms are encoded by separate genes [29] but have virtually identical folds [18]. Both contain a C-terminal hydrophobic region, which is responsible for membrane anchoring. The ten residues at the C terminus determine the intracellular localization [30]. Membrane-bound Cyb5R3 from both mitochondria and ER have identical sequences [31]. Cyb5R3 contains an N-terminal hydrophobic region which is responsible for membrane anchoring, and the first glycine is myristoylated [32,33].

Microsomal Cyb5A donates electrons to stearoyl-CoA desaturase (SCD) in fatty acid desaturation, as demonstrated by *in vitro* reconstitution [34]. *In vitro* and *in vivo* studies also show that Cyb5A facilitates cytochrome P450 reactions [35,36] and is involved in the biosynthesis of cholesterol [37] and androgen [38]. Although its biological role is unclear, Cyb5B has been shown to modulate synthesis of androgens in Leydig cells [39]. Soluble forms of Cyb5A and Cyb5R3 are found in the cytosol of red blood cell. Both are encoded by the same genes and generated by alternative splicing. They compose the major enzyme complex responsible for methemoglobin reduction [40] (**Figure 7**). More than thirty mutations in Cyb5R3 have been identified in methemoglobinemia patients [41], in contrast to only one documented case of a mutation in Cyb5A gene [42].

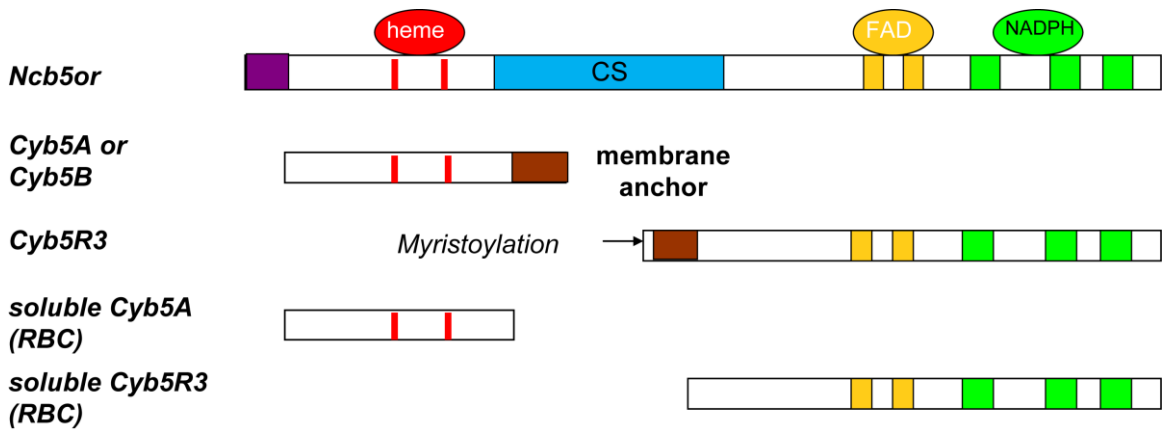

Figure 7. Different forms of cytochrome b5 and cytochrome b5 reductase. Motifs for bindings of heme, FAD and NADPH are red, yellow and green, respectively. Membrane anchor regions in Cyb5A/B and Cyb5R3 are brown. Cyb5A is anchored to ER membrane, and Cyb5B is anchored to outer-mitochondrial membrane. They are encoded by different genes. Cyb5R3 is found in both ER and mitochondria, and its first Gly residue is myristoylated. The same genes encode, through alternative splicing, soluble forms of Cyb5A and Cyb5R3 in red blood cell (RBC) that function as methemoglobin reductase.

Cyb5A and Cyb5R3 are localized on the cytoplasmic side of the ER [43], similar to SCD [44]. Cyb5R3, Cyb5A and SCD can form a trimeric complex in fatty acid desaturation, as demonstrated by reconstitution *in vitro* [34] with individual Cyb5R3, Cyb5A and SCD that are purified from animal tissues. Detergents are required to solubilize these integral membrane proteins, and phospholipid is required to form membrane structure. The reaction requires NADH and oxygen. Once NADH is added, reduced flavin in Cyb5R3 shuttles electrons to heme in Cyb5A, which passes electrons to the iron center in SCD to convert stearoyl-CoA to oleoyl-CoA in the presence of oxygen (**Figure 8**). Results from *in vitro* studies suggest that Cyb5A is essential for fatty acid desaturation. However, this view has been challenged by recent *in vivo* findings of Cyb5A null mice. Mice with liver-specific deletion of Cyb5A show no defect in fatty acid composition of hepatic microsomal lipids, and mice with global deletion of Cyb5A show only a mild lipid phenotype [35,45,46] **(Figure 9**). The major phenotype in both hepatic and global Cyb5A null mice is deficiency of P450 function in drug metabolism [35,45]. In parallel, inhibitors of SCD exhibit differential effects on cellular desaturation depending on the source of the fatty acid substrate [47], suggesting that fatty acid desaturation pathways are compartmentalized within cells. Based on the above evidence, it is reasonable to speculate the presence of an alternative electron donor of SCD *in vivo*.

We hypothesize that Ncb5or functions as an electron donor for SCD *in vivo*. This hypothesis is supported by the following evidence: (a) Ncb5or is associated with ER [2], similar to Cyb5A, Cyb5R3 and SCD; (b) Ncb5or contains the essential redox domains, Ncb5or-b5 and Ncb5or-b5R; (c) Ncb5or null mice show impaired fatty acid desaturation *in vivo* [48].

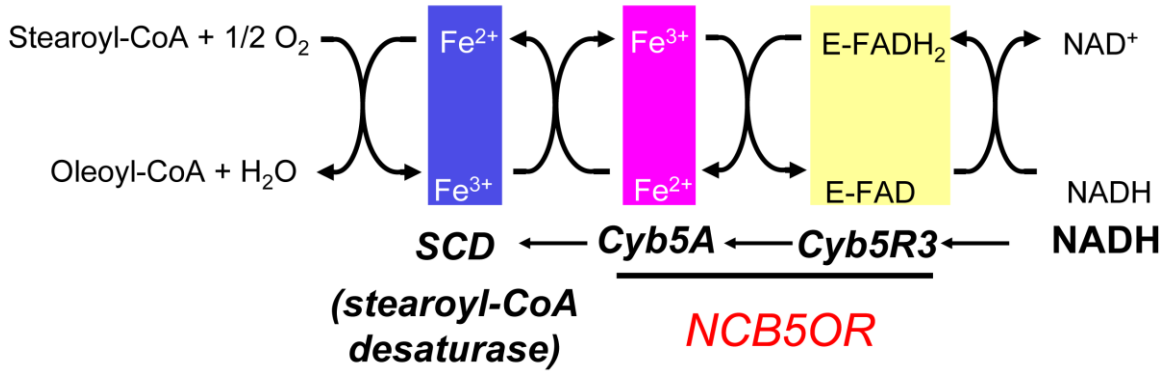

Figure 8. Fatty acid desaturation. Electrons flow from NADH to Cyb5R3 to Cyb5A, and then to SCD during the reconstitution of fatty acid desaturation system *in vitro*. Once receiving electrons from Cyb5A, SCD will introduce a double bond at $^{\Delta}9$ position and convert 18:0 to 18:1(n-9). Ncb5or contains both b5 and b5R domains and is likely to function as an alternative electron donor for SCD *in vivo*.

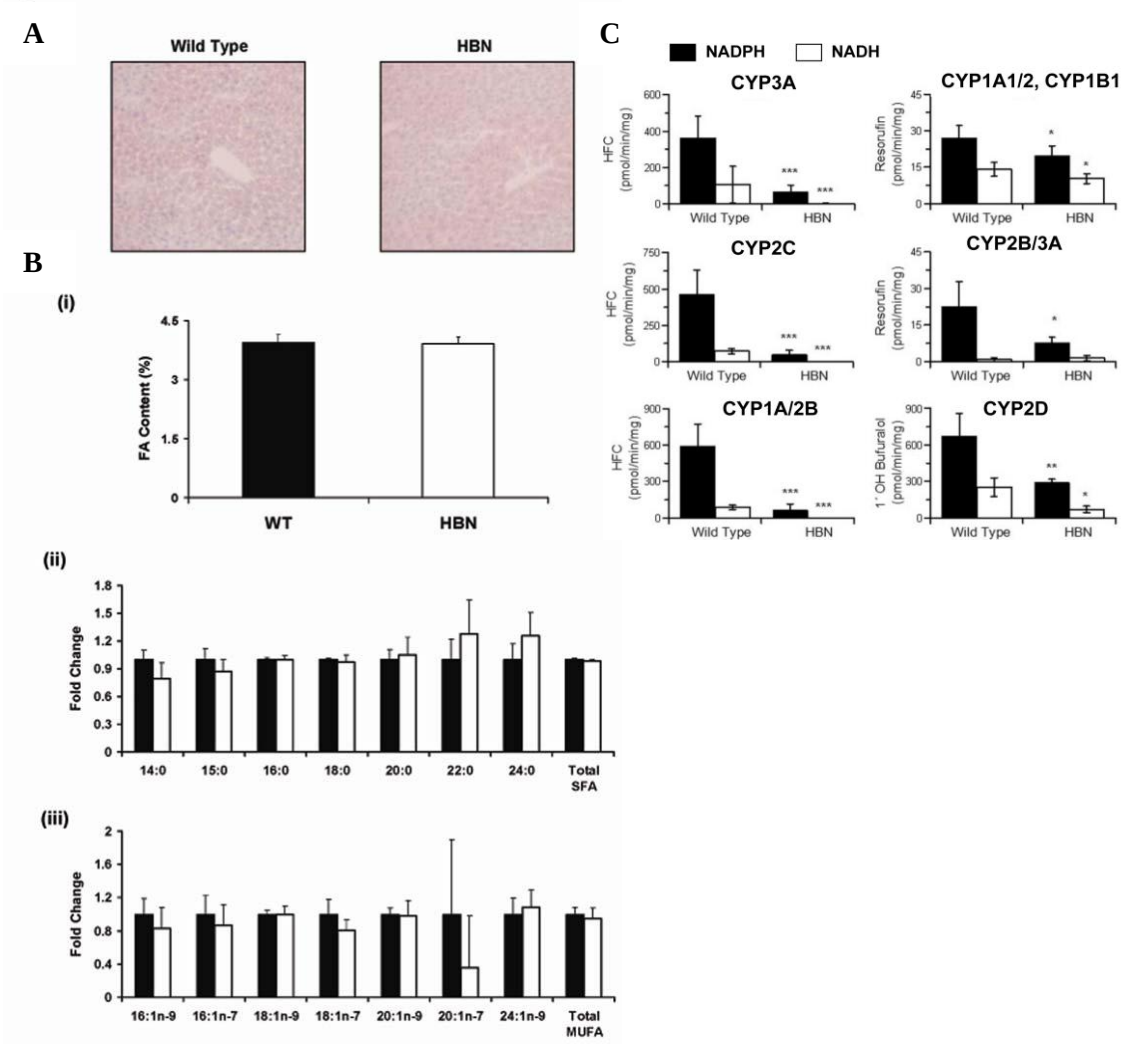

Figure 9. (A) Oil Red staining for neutral lipid in liver of wild-type and hepatic b5 null (HBN) mice. No significant difference is found between genotypes. (B) Fatty acid composition of microsomal lipids in liver of wild-type and HBN mice. No significant difference can be found between genotypes in total content (i) and levels of saturated (ii) and monounsaturated (iii) fatty acids. (C) Decreased P450 activity in HBN mice. HBN: hepatic b5 null or hepatic deletion of Cyb5A. This figure is adapted from Finn *et al*. [35].

Ncb5or is co-localized with the ER marker calreticulin during fractionation of intact subcellular organelles and confocal microscopic analyses [2] (**Figure 10**). However, no segment in Ncb5or can be recognized as a transmembrane region by PHD prediction [49], and recombinant Ncb5or is soluble in aqueous solution [1]. Therefore, Ncb5or is associated with ER potentially through interaction with the ER membrane or with an ER membrane protein. Truncation of the first 34 N-terminal residues of Ncb5or seems not to alter the localization of Ncb5or in the ER (**Figure 10**).

Ncb5or null mice develop early-onset diabetes [50,51], namely, hyperglycemia and low blood insulin level at age seven weeks (**Figure 11**). Ncb5or null mice with diabetes are sensitive to insulin, as shown by insulin tolerance test, or ITT (**Figure 11**). Furthermore, *in situ* insulin staining reveals a progressive loss of β cells during the development of diabetes in Ncb5or null mice. No lymphocyte infiltration has been observed in these mice, suggesting this type of insulin-dependent diabetes is not identical to Type 1 diabetes. No apoptosis of β cells has been detected by terminal deoxynucleotidyl transferase dUTP nick end labeling (TUNEL).

Lipoatrophy is another primary phenotype of Ncb5or null mice [48,52,53], similar to that observed in SCD null mice [54], Ncb5or null mice exhibit lower body weight, smaller fat mass in epididymal white adipose tissue, and lower levels of hepatic triglyceride than wild-type (**Figure 12**). In agreement with the phenotypes stated above, hepatocytes from Ncb5or null mice exhibit enhanced fatty acid oxidation and are more susceptible to saturated fatty acid-induced lipotoxicity than wild-type cells [52].

A

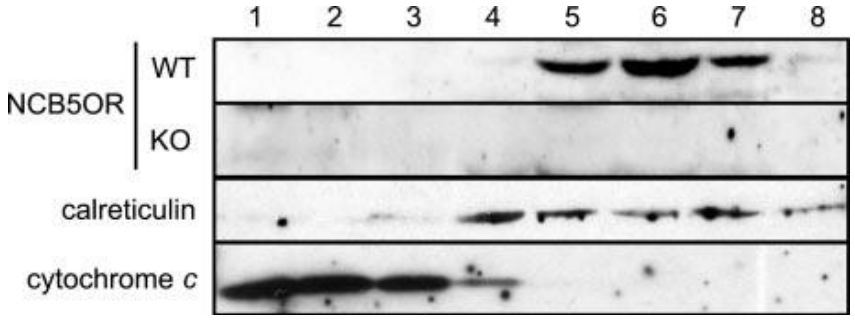

B

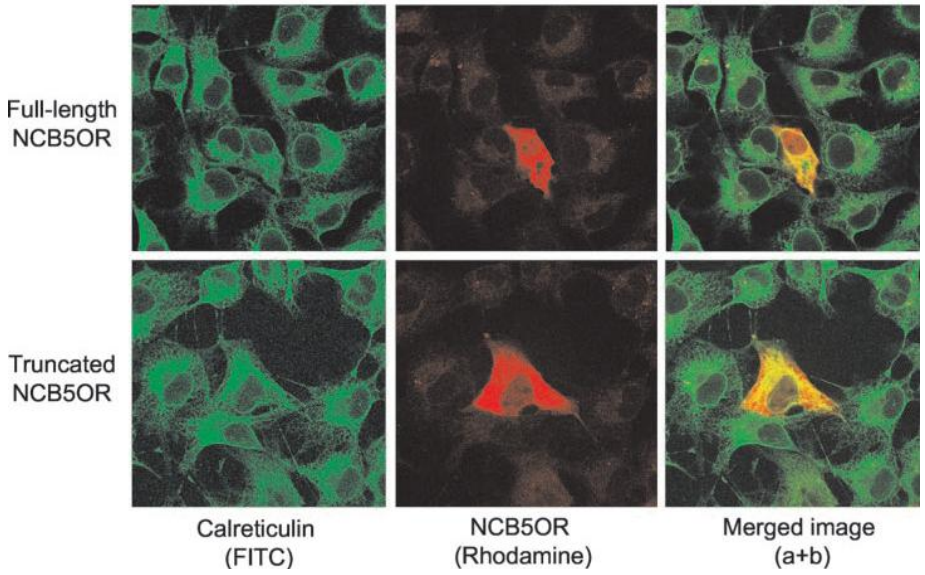

Figure 10. (A) Localization of Ncb5or through fractionation of subcellular organelles from liver of wild-type and Ncb5or-null mice. Cell organelles were separated through density gradient, #1 (heavy) through #8 (light). Immuno-blot analyses were performed to characterize each fraction using antibodies against calreticulin and cytochrome c, which are the marker for ER and mitochondria, respectively. Ncb5or colocalizes with calreticulin, an ER maker. (B) Intracellular localization of Ncb5or in COS7 by confocal microscopy. Full-length and truncated Ncb5or (lacking the first 34 residues) have similar calreticulin colocalization in ER. This figure is adapted from Zhu *et al*. [2].

A

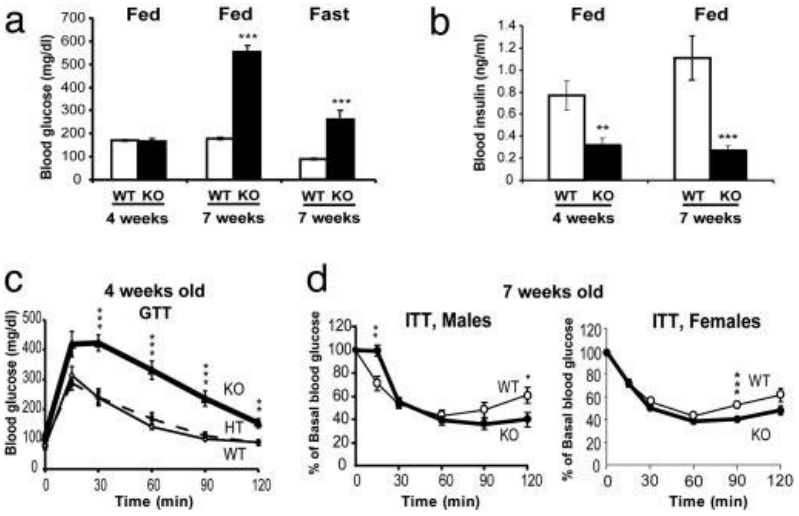

B

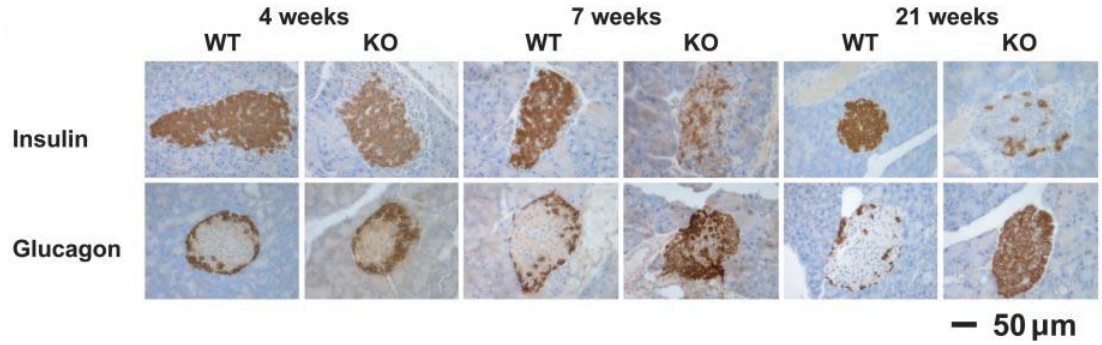

Figure 11. (A) Ncb5or null mice exhibit hyperglycemia at age seven weeks (a) decreased blood insulin levels (b) and impaired glucose tolerance (c) at age 4 weeks, but remain insulin-sensitive at the onset of diabetes (d). (B) Insulin staining of mouse islets shows a gradual loss of β cells during the development and progression of diabetes, in parallel to the expansion of α cells, as shown by glucagon staining. GTT: glucose tolerance test; ITT: insulin tolerance test. This figure is adapted from Xie *et al*. [50].

In addition to Ncb5or deficiency-induced lipid defect in mice, two polymorphisms and two missense mutations of the Ncb5or gene have been identified in human (**Figure 5, 6 and 13**). Q187R and H223R are two polymorphisms that have been identified in both patients with non-inflammatory diabetes and normal sub-population [28]. These two residues are in the CS domain and not conserved in Ncb5or. Two missense mutations in Ncb5or, D371Y and L424M, have been identified in 7% of human breast cancer specimens, which are heterozygous of these mutations [22]. D371 and L424 are well conserved in Ncb5or orthologs. It is postulated that D371Y could alter the local environment due to the striking difference of chemical property between Asp and Tyr, whereas L424M is more likely to subject Ncb5or to oxidative modification. Both mutations potentially decrease the stability of Ncb5or or the efficiency of electron transfer.

Physical interaction and electron transfer between Cyb5A and Cyb5R3

Numerous biochemical and structural studies have been carried out to determine the physical interaction between Cyb5A and Cyb5R3. The rate of electron transfer from Cyb5R3 to Cyb5A decreases with increasing ionic strength, suggesting electrostatic interaction mediated by pairs of charged residues between Cyb5A and Cyb5R3 [55] (**Figure 14)**. The increasing strength of ions forms a shield and disrupts the interaction between charge pairs. Cross-linking studies identified negatively charged residues like Glu47, Glu48, Glu52, Glu60 and Asp64 from Cyb5A, and positively charged residues, namely, Lys41, Lys125, Lys 162 and Lys 163 from Cyb5R3, which are potentially involved in interaction between Cyb5A and Cyb5R3 [56]. Mutagenesis studies have confirmed the role of these positively charged residues of Cyb5R3 in interaction with

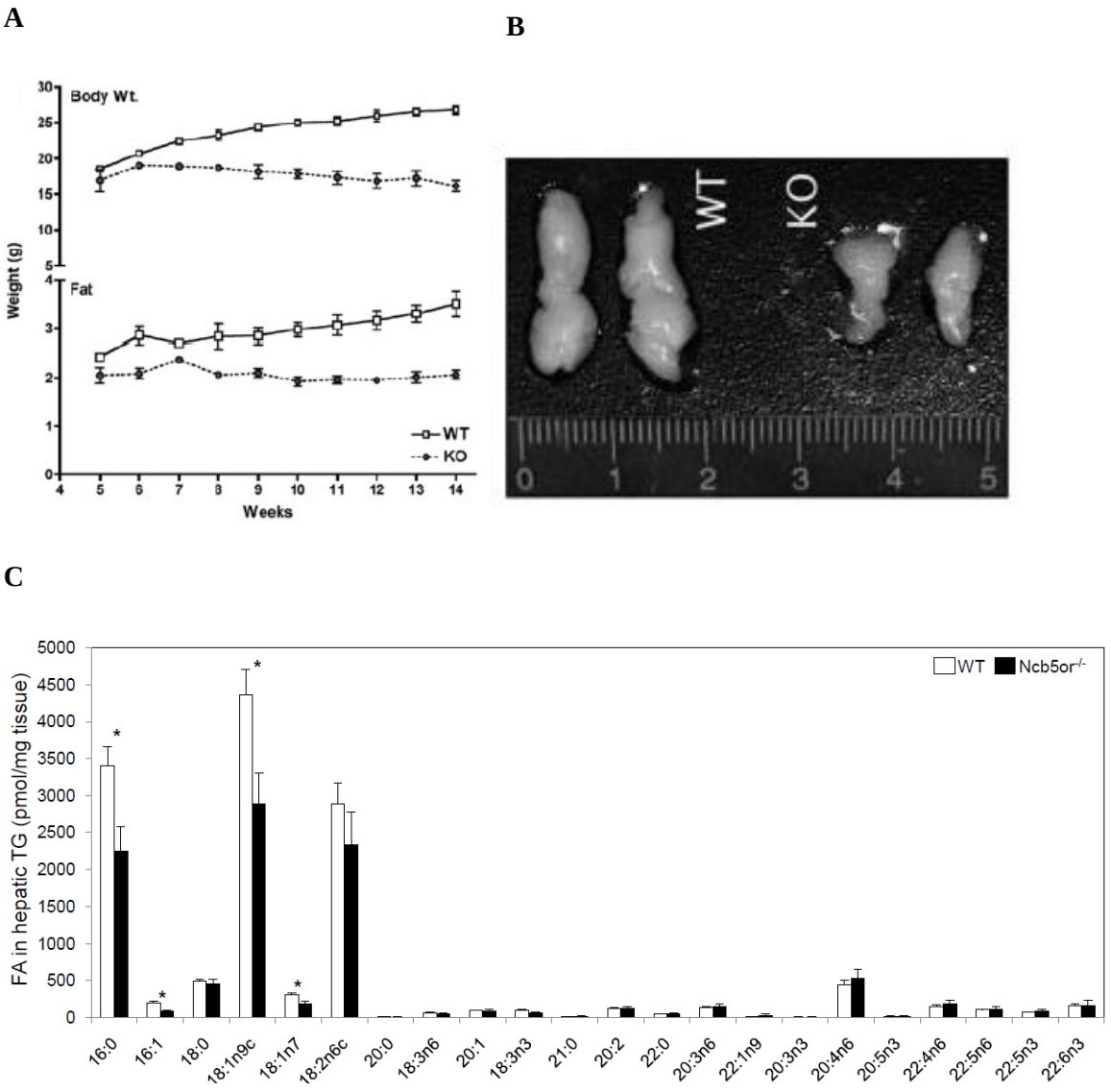

Figure 12. (A) Lipoatrophy in Ncb5or null mice with lower body weight and body fat than the wild-type. (B) Decreased amount of white adipose tissue in Ncb5or null mice. (C) Altered fatty acid composition of hepatic triglyceride of prediabetic Ncb5or null mice. Levels of 16-carbon and 18-carbon fatty acids are lower in Ncb5or null mice, as well as the desaturation index 18:1/18:0 (not shown). Figures A and B are adapted from Larade *et al*. [48]; Figure C is adapted from Xu *et al*. [52].

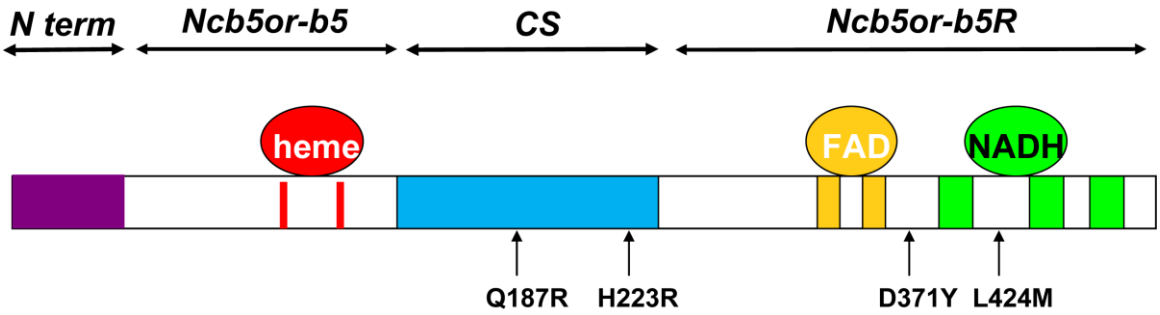

Figure 13. Ncb5or variants in human. Two polymorphisms, Q187R and H223R in the CS domain, have been identified in early onset diabetic patients and normal individuals [28]. Two heterozygous mutations, D371Y and L424M, are found in 7% of breast cancer specimens. Both are conserved residues in the b5R domain [22].

Cyb5A, but not negatively charged residues of Cyb5A [57]. However, mutation of either Glu42 or Asp70 in Cyb5A causes decreased affinity in Cyb5A-Cyb5R3 [58]. The positions of these residues are modeled in **Figure 14**. Glu42 and Asp70 from Cyb5A are in the helices around the heme center, whereas Lys residues from Cyb5R3 are along the side of FAD.

Unique structural features of Ncb5or

Ncb5or has several unique structural features and biochemical properties, despite the sequence similarity with other members of the b5 superfamily (**Figure 15**): (a) Displacement of heme-ligating His112, corresponding to a deletion before and an insertion after by a single residue; (b) a lower redox potential in Ncb5or-b5 (-108 mV vs. SHE) than Cyb5A (-9 mV vs. SHE) [2]; (c) Fewer surface charged residues than Cyb5A. The novel features of Ncb5or-b5 potentially endow this domain with a special fold, a unique heme environment and distinct properties. Ncb5or-b5 is functionally important for shuttling electrons between Ncb5or-b5R and a downstream partner. Hereby our investigation started from Ncb5or-b5 (see Chapter Two).

The role of the N-terminus of Ncb5or remains mysterious. This 50-residue N-terminal region has no homology with any known proteins. The N-terminal region is predicted by PONDR VL-XT (predictors of natural disordered regions) to be disordered [59,60,61]. This N-terminus is rich in positively charged (Lys and Arg) residues and is therefore likely to be highly soluble. Truncation of the first 34 residues does not change the localization in ER, but accelerates the rate of auto-oxidation [2]. A detailed description of the role of the N-terminal region in protein function is included in Chapter Three.

A

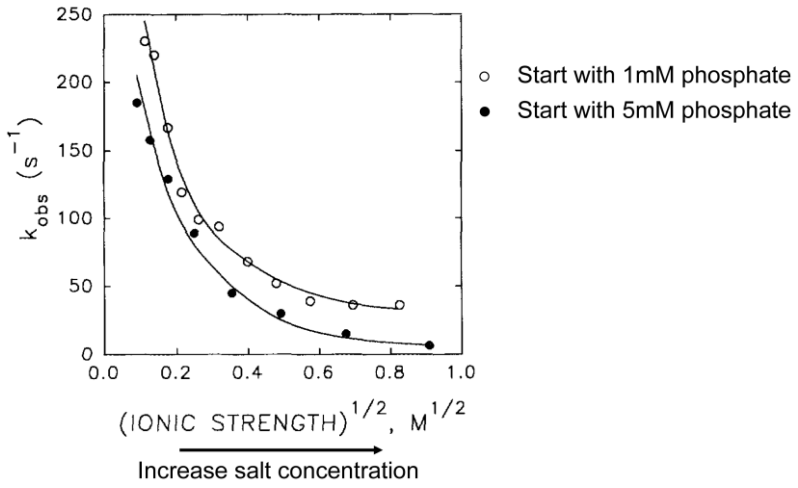

B

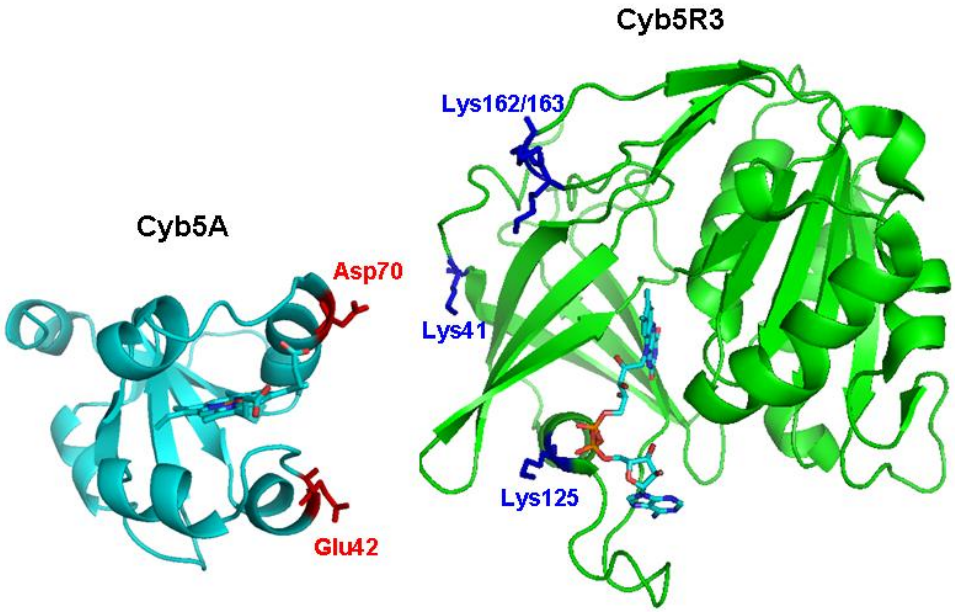

Figure 14. (A) Electrostatic interactions between Cyb5A and Cyb5R3. The rate constant for electron transfer from Cyb5R3 to Cyb5A decreases with increasing ionic strength. The reaction under a lower concentration of phosphate (1 mM) is faster than that under higher concentration (5 mM). (B) Mapping of the key charged residues implicated in interaction between Cyb5A and Cyb5R3. Mutation in any of these residues increases K_M, i.e, decreases the Cyb5A-Cyb5R3 affinity. Figure 14A is adapted from Meyer *et al*. [55].

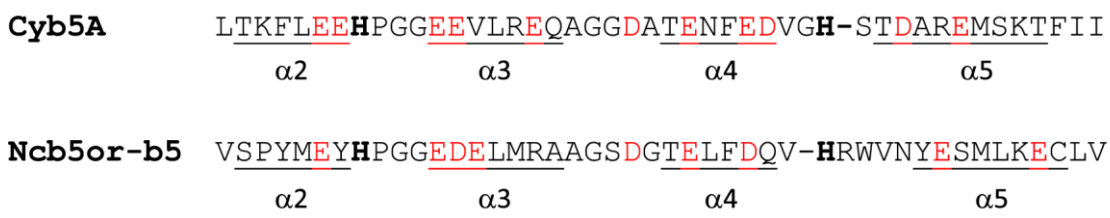

Figure 15. Partial sequence alignment of human Cyb5A and Ncb5or-b5. The heme binding motifs in both Cyb5A and Ncb5or-b5 contain four helices (α2-α5). Two heme-ligating His residues are in bold, and negatively charged residues in red. The sequence identify between the two proteins is approximately 30%. The second heme-ligating His is shifted by one position. Fewer surface charged residues are found in Ncb5or-b5.

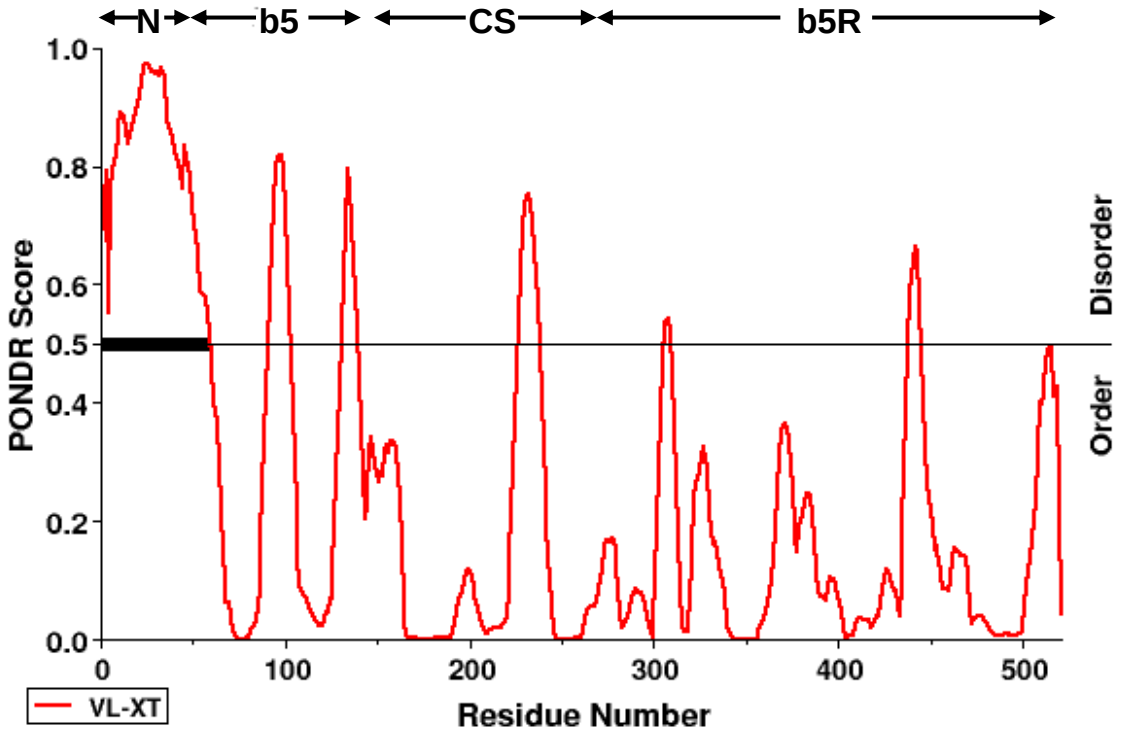

Figure 16. Prediction of disordered regions in Ncb5or by PONDR VL-XT [59,60,61]. The N-terminal region (50 residues) is considered a disordered or unstructured region.

Chapter Two

Study of the Individual Cytochrome b5 and Cytochrome b5 Reductase Domains of Ncb5or Reveals a Unique Heme Pocket and a Possible Role of the CS Domain

Abstract

NADH cytochrome b_5 oxidoreductase (Ncb5or) is found in animals and contains three domains similar to cytochrome b5 (b5), CHORD-SGT1 (CS) and cytochrome b5 reductase (b5R). Ncb5or has an important function as suggested by the diabetes and lipoatrophy phenotypes in Ncb5or null mice. To elucidate the structural and functional properties of human Ncb5or, we generated its individual b5 and b5R domains (Ncb5or-b_5 and Ncb5or-b5R, respectively) and compared them with human microsomal b5 (Cyb5A) and b5R (Cyb5R3). A 1.25 Å X-ray crystal structure of Ncb5or-b5 reveals nearly orthogonal planes of the imidazolyl rings of heme-ligating residues His^{89} and His^{112}, consistent with a highly anisotropic low-spin (HALS) EPR spectrum. Ncb5or is the first member of the cytochrome b5 family shown to have such a heme environment. Like other b5 family members, Ncb5or-b5 has two helix-loop-helix motifs surrounding heme. However, Ncb5or-b5 differs from Cyb5A with respect to location of the second heme ligand (His^{112}) and of polypeptide conformation in its vicinity. Electron transfer from Ncb5or-b5R to Ncb5or-b5 is much less efficient than from Cyb5R3 to Cyb5A, possibly as a consequence of weaker electrostatic interactions. The CS linkage likely obviates the need for strong interactions between b5 and b5R domains in Ncb5or. Studies with a construct combining the Ncb5or CS and b5R domains suggest that the CS domain facilitates docking of the b5 and b5R domains. Trp^{114} is an invariant surface residue in all known Ncb5or orthologs but appears not to contribute to electron transfer from the b5R domain to the b5 domain.

Introduction

NADH cytochrome b5 oxidoreductase (Ncb5or, also named Cyb5R4, b5/b5R or b5+b5R) was cloned from human as a natural fusion protein containing structural homolog of both cytochrome b5 (b5) and cytochrome b5 reductase (b5R) [1]. Ncb5or is found only in animals and is expressed in a wide range of tissues and cells. Human Ncb5or contains 521 amino acid residues and three structural domains. The N-terminal b5 domain and the C-terminal b5R domain are linked by a CS (CHORD-SGT1) domain comprising approximately 90 residues (**Figure 1A**). Several natural fusion proteins are known that contain a cytochrome b5 domain and a second redox-active domain. Examples include sulfite oxidase [6,7,8] and Δ5 and Δ6 fatty acid desaturases [4,5] in animals, nitrate reductase in algae [10] and plants [11,12], flavocytochrome b2 or lactate dehydrogenase [9] and Δ9 fatty acid desaturase [62] in baker's yeast. However, Ncb5or is the only member of the cytochrome b5 superfamily known to contain three distinct domains. The function of the non-redox-active CS domain is presently unknown, although its primary sequence is distantly homologous to those in human heat shock protein 20 (HSP20, a co-chaperone of HSP90) and other CS family members [3].

The cytochrome b5 family includes two isoforms in vertebrates, one anchored to the membrane of the endoplasmic reticulum (Cyb5A) and the other anchored to the outer mitochondrial membrane (Cyb5B) [29]. The heme-binding domains of Cyb5A and Cyb5B have identical folds with six α helice and a five-strand β-sheet [17,18]. There are two hydrophobic cores: core 1 includes α2 - α5 in heme binding packet; core 2 includes α1 and α6 close to the C terminus. Fold of both proteins can be described as two hydrophobic cores separated by the five-strand β-sheet [63]. All cytochrome b5

proteins contain a redox active heme. Heme binding core is composed of two helix-loop-helix motifs (α2 - α5), between which heme is sandwiched by two His residues. The first heme-ligating His is located in the loop between α2 and α3, and the second His is located in the loop between α4 and α5 (**Figure 1B**). The amino acid sequence homology of the b5 cores is very high among vertebrate orthologs of Cyb5A (**Supplemental Fig. 1**), among Cyb5B family members (data not shown), and among Ncb5or orthologs (**Supplemental Fig. 2**). In contrast, the b5 cores of human Cyb5A and the human Ncb5or-b5 domain share only 31% identity and 52% similarity, and in Ncb5or, there are a deletion before and an insertion after heme ligand His^{112} (**Figure 1B**). Compared to Cyb5A, Ncb5or-b5 contains fewer surface-charged residues (**Figure 1B).** All of these suggest substantial divergence of structural, biophysical and functional properties of these two members of the cytochrome b5 superfamily.

Four b5R isoforms have been identified in humans, Cyb5R1-Cyb5R4 [1,64]. These and all other b5R family members belong to the ferredoxin-NADP+ reductase superfamily [13], and contain conserved amino acid residues responsible for FAD and NAD(P)H binding. Microsomal b5R (Cyb5R3) associates with both endoplasmic reticulum (ER) and outer-mitochondrial membranes via a myristoyl group [31], and is the cognate reductase for both Cyb5A and Cyb5B [65]. Ncb5or (Cyb5R4), the only b5R isoform in animals that contains more than one domain, is localized in the ER [2]. Previous studies have shown that recombinant Ncb5or is soluble and that its heme is reduced instantaneously when excess NADH (or NADPH) is present [1]. Kinetic measurements have revealed that human and mouse Ncb5or can reduce a number of artificial substrates in vitro, such as cytochrome c, methemoglobin, ferricyanide, and even molecular oxygen [1,2].

Biochemical studies with in vitro reconstitution show that the Cyb5R3/Cyb5A pair serves as an electron source for stearoyl-CoA desaturase (SCD) in fatty acid desaturation [34]. Studies comparing normal and liver-specific Cyb5A knockout mice have revealed no difference in the SCD index of liver microsomal lipids [35], and global Cyb5A knockout mice do not display any major phenotype in lipid metabolism [45], suggesting that other redox protein(s) may play this role in vivo. Notably, mice lacking the Ncb5or gene exhibit impaired SCD activity and develop early-onset diabetes and lipoatrophy [48,50,53], suggesting that Ncb5or functions in vivo as an electron donor in the SCD reaction. These discoveries have motivated us to further characterize the structural and functional properties of Ncb5or. Herein we describe the results of studies with recombinant proteins representing the individual b5 and b5R domains of human Ncb5or (designated as Ncb5or-b5 and Ncb5or-b5R, respectively), as well as one containing both the CS and b5R domains (Ncb5or-CS/b5R). We report a 1.25 Å X-ray crystal structure of Ncb5or-b5 which reveals a heme environment that is unique among known cytochrome b5 superfamily members. We also report kinetic data showing that Ncb5or-b5 can be reduced by Ncb5or-b5R in the presence of excess NADH, albeit much less efficiently than the corresponding reaction in full-length Ncb5or or in Cyb5A/Cyb5R3. Finally we provide evidence that the CS domain plays a role in facilitating interactions between the b5 and b5R domains.

Material and methods

Molecular cloning and site-directed mutagenesis. On the basis of structure predictions using the online I-TASSER server [21], we assigned Lys^{51}-Lys^{137} for Ncb5or-b5, Lys^{260}-Ala^{521} for Ncb5or-b5R,

and Gly^{164}-Ala^{521} for Ncb5or-CS/b5R (schematic diagram in **Figure 1A**). The cDNA fragment of wild-type Ncb5or-b5 (no poly-histidine tag) was synthesized and cloned into pET22b vector by Genscript Inc. (Piscataway, NJ). For comparison purposes we required soluble proteins representing human Cyb5A and Cyb5R3. An expression plasmid for human erythrocyte cytochrome b5, which is identical to the soluble heme-binding domain of human Cyb5A with the exception of the C-terminal residue, was kindly provided to us by Dr. Grant Mauk [66] and is herein referred as Cyb5A. Its cDNA was subcloned into pET19b vector. An expression construct of human Cyb5R3 (residues Ile^{34}-Phe^{301} was generated in our laboratory on the basis of previously published reports [67]. A 6x histidine tag was added to the NH_2-terminus of Ncb5or-b5R, Ncb5or-CS/b5R, and human Cyb5R3 through respective PCR primers and cloned into pET19b vector. Site-directed mutagenesis was performed to generate Ncb5or-b5 mutants, R113A and W114A, with the Stratagene QuikChange mutagenesis kit (La Jolla, CA) and the full-length wild-type Ncb5or cDNA as the PCR template. The mutated DNA fragment was then subcloned into the pET22b. Primers with the desired codon change were designed with Stratagene's software online. All oligonucleotides were synthesized by Integrated DNA Technology (Coralville, IA) and the sequences are available upon request.

Protein preparation. Soluble forms of each recombinant protein were generated in *E.coli* BL21(DE3) cells that were transformed with the respective expression construct. For Ncb5or-b5 and Cyb5A, cells were grown at 37^{o}C in LB media to an OD_{600} of approximately 1.0 before IPTG induction (1 mM) for 6 hours at 25^{o}C. Cells were collected by centrifugation at 5000g (4^{o}C) for 30 minutes and used immediately or the pellet was kept at -80^{o}C until ready for use. Human Cyb5A and Ncb5or-b5 were initially obtained as mixtures of holo (heme-bound) and apo

(heme-free) forms. Hemin was added to the crude cell lysate in order to convert the apo forms to the holo forms [68]. The holo protein was purified to homogeneity by ion-exchange, hydrophobic-interaction and size-exclusion column chromatography consecutively using HiTrap Q HP, HiTrap Phenyl HP and Superdex 200 columns at a flow rate of 1.0, 1.0 and 0.5 ml/min., respectively. For HiTrap Q HP, a linear gradient between 0 and 1 M NaCl in 20 mM Tris-HCl (pH 7.2) was used to elute all proteins in 20 column volumes. The fractions with red color were collected, pooled and loaded directly onto HiTrap Phenyl HP to collect flow-through. For Superdex 200, the running buffer was 20 mM Tris-HCl (pH 7.2). All purifications were conducted using an ÄKTAxpress purification system (GE Healthcare Life Sciences) at 4^{o}C. SDS polyacrylmide gel electrophoresis (PAGE) was used to determine protein purity, and native PAGE was to confirm the absence of residual apoprotein upon the completion of holo Ncb5or-b5 and Cyb5A purification [69]. Small aliquots of concentrated Ncb5or-b5 and Cyb5A samples were flash frozen in liquid nitrogen and stored at -80^{o}C until use. For Ncb5or-b5R, Ncb5or-CS/b5R and Cyb5R3, the same conditions were used except cells were grown in TB media and supplemented with 0.1 mM riboflavin [70], expression was induced with 0.5 mM IPTG overnight at 15^{o}C. Both Ncb5or-b5R and Cyb5R3 proteins were purified to homogeneity with Ni-NTA chelation and size-exclusion column chromatography using HisTrap HP and Size Exclusion 100 columns at a flow rate of 1.0 and 0.5 ml/min., respectively. For HisTrap HP, the sample was loaded in 20 mM Tris-HCl, 500 mM NaCl, 10 mM imidazole (pH 8), washed with 20 mM imidazole for 10 column volumes and then eluted with a linear gradient of 20 - 500 mM imidazole in 10 column volumes. The fractions with yellow color were collected and pooled. For

Size Exclusion 100, the running buffer was 20 mM Tris-HCl, 500 mM NaCl, 0.1 mM EDTA (pH 7.2) and the yellow fractions were collected. The Ncb5or-CS/b5R was purified one-step with affinity chromatography by Ni-NTA beads (QIAGEN). The sample was loaded in 50 mM Tris-HCl, 300 mM NaCl (pH 8), washed with 10 mM imidazole (10 column volumes), and then eluted in 200 mM imidazole. The yellow fractions were collected and dialyzed exhaustively against 20 mM Tris-HCl, 500 mM NaCl, 0.1 mM EDTA (pH 7.2). Final yields of purified protein were 5-10 mg/L for Ncb5or-b5, ≥ 20 mg/L for Cyb5A, 2 mg/L for Ncb5or-b5R, 1 mg/L for Ncb5or-CS/b5R and 10 mg/L for Cyb5R3. All polypeptide products have the expected molecular weights by electrospray ionization mass spectrometry (KU Mass Spectrometry Laboratory). UV/visible spectra showed A413:A280 ratios of 4.1 and 6.4 for holo-Ncb5or-b5 and holo-Cyb5A, respectively. The FAD contents of Ncb5or-b5R, Ncb5or-CS/b5R and Cyb5R3 were determined by A461 and used to represent enzyme concentrations.

Spectroscopy. UV/visible spectra were obtained using a Varian Cary 50 Bio spectrophotometer or a Varian 100 Bio equipped with a Peltier-thermostated multiple cell holder and a dedicated temperature probe accessory (± 0.1 °C). The concentrations of heme and FAD were determined by the following ε values ($mM^{-1}cm^{-1}$): 130 (413 nm) of oxidized heme in Ncb5or-b5 and Cyb5A [2], 10.5 (461 nm) of FAD in Ncb5or-b5R, Ncb5or-CS/b5R and Cyb5R3 [70]. Electron paramagnetic resonance (EPR) spectroscopy was performed on a Bruker Elexys E500 spectrometer operating at X-band frequencies. Temperature control was maintained by an Oxford ESR 900 continuous flow liquid helium cryostat interfaced with an Oxford ITC 503

temperature controller. Typical EPR parameters were as follows: sample temperature, 7K; microwave frequency, 9.382 GHz; microwave power, 1 mW; modulation frequency, 100 kHz; modulation amplitude, 5G. These conditions provided clean spectra without saturation of the signals. EPR data acquisition and background subtraction were performed using *XeprView* software (Bruker).

Crystallization and structure solution. Concentrated human Ncb5or-b5 (20 mg/ml in 20 mM Tris-HCl pH 7.0) was screened for crystallization in Compact Jr. (Emerald Biosystems) sitting drop plates using 0.5 μl of protein and 0.5 μl crystallization solution equilibrated against 100 μL of the latter. Red plate shaped crystals were obtained in approximately 3 days from the Wizard 2 screen (Emerald Biosystems) condition #45 (2 M $(NH4)_2SO_4$, 100 mM Tris-HCl pH 7.0, 200 mM Li_2SO_4) at 4^{o}C. Crystal growth conditions were optimized using the pH buffer screen (Emerald Biosystems). Large single plate shaped crystals were obtained from 2 M $(NH_4)_2SO_4$, 100 mM Na/K phosphate pH 6.2, 200 mM Li_2SO_4 after approximately 1 week at 4^{o}C. Crystals were equilibrated for 30 seconds in the same solution plus 25% glycerol and frozen for data collection at APS. Initial diffraction data were collected in-house at 93K using a Rigaku RU-H3 rotating anode generator (Cu-Kα) equipped with Osmic Blue focusing mirrors and a Rigaku Raxis IV^{++} image plate detector (KU Protein Structure Laboratory). Crystals obtained from the initial crystallization screen were used for data collection. The Matthew's coefficient [71] (Vm=2.2, 44.4% solvent) suggested that there were 2 molecules in the asymmetric unit. Additionally, the self rotation function yielded a peak on the $\kappa = 180^o$ section at $\omega = 55.1^o$, $\phi = 180^o$ indicating the presence of a non-crystallographic 2-fold axis. Structure solution was carried

out by molecular replacement with BALBES [72] in the space group $P2_1$, which produced a homology model for the rotation and translation searches from a high-resolution structure of rat Cyb5B (Protein Data Bank or PDB ID: 1EUE [73]. No solution was found in the space group *P*2. Initial refinement of the model following molecular replacement converged at R = 38.8%. The model was improved by automated building with BUCANNEER [74] which converged at R = 31.4%. A final model was obtained from subsequent rounds of structure refinement and manual model building. Atomic resolution diffraction data were collected at 100K at the Advanced Photon Source (APS) IMCA-CAT beamline 17ID using an ADSC Quantum 210r CCD detector. Crystals obtained from the optimized growth conditions described above were used for synchrotron data collection. Intensities were integrated and scaled with the XDS [75] software package and the model obtained from in-house diffraction data was used for molecular replacement with MOLREP [76]. Refinement and model building were carried out with REFMAC [77] and COOT [78], respectively, and the final model was refined with anisotropic displacement parameters. Structure validation was conducted with Molprobity [79] and figures were prepared with the RIBBONS and CCP4MG packages [80,81]. There were two molecules in the asymmetric unit related by a non-crystallographic 2-fold axis. The final model was refined to 1.25 Å resolution and contained, in addition to the two polypeptide chains (denoted A and B), 2 heme molecules, 2 sulfate ions and 73 water molecules. Both heme molecules in subunit A and B of Ncb5or-b5 adopt two orientations, as shown by a 2Fo-Fc electron density map (**Supplemental Figure 3**). The coordinates of human Ncb5or-b5 have been deposited in the Protein Data Bank (PDBID: 3LF5). Crystallographic data are summarized in **Supplemental Table 1**.

Electrostatic map. The electrostatic maps of human Ncb5or-b5 and bovine Cyb5A were calculated from their X-ray structures using the Adaptive Poisson- Boltzmann Solver (APBS) software plugin [82] in Pymol (http://www.pymol.org). The necessary PQR files were generated from the PDB files using the PDB2PQR server (http://nbcr.sdsc.edu/pdb2pqr/) [83] and the pKa values were assigned using the PROPKA software [84]. The parameters set for a typical calculation are as follows; internal dielectric constant = 2.0, external dielectric constant = 80.0, solvent probe radius = 1.4 Å and Temperature = 298 K. Visualization of electrostatic maps was performed with Pymol.

Inter-domain electron transfer. Inter-domain electron transfer was measured under oxygen-free conditions in a regulated gas-flow device that has been previously described [2]. The substrate and reductant mixture (final volume 1.5 ml) was equilibrated with a slow stream of moisturized nitrogen (purity 99.999%, from Linweld, Kansas City, MO) for 30 minutes in a reaction vessel. Upon the injection of a small aliquot of reductase (< 2 ul), the complete mixture was pushed by N_2-flow into a sealed quartz cuvette in a Varian Cary 50 spectrophotometer. Data collection was initiated after a dead time of < 20 seconds due to mixing and reaction transfer. Reduction of heme was monitored by the increase of absorbance at the Soret band (ε_{424} = 120 $mM^{-1}cm^{-1}$, Ncb5or-b5 or 134 $mM^{-1}cm^{-1}$, Cyb5A). Data were fit to a single exponential function and the resulting pseudo-first order rate constant was dissolved by the appropriate enzyme concentration to obtain the reported observed rate constants ($min^{-1}\mu M^{-1}$). Two buffer conditions were examined: (*i*) 5 mM sodium phosphate, and (*ii*) 50 mM sodium phosphate, pH 7.0, with ionic strength (μ) of 0.009 and 0.108 M, respectively.

Measurement of Michaelis-Menten parameters. Ncb5or-b5 (0.7 - 100 μM) or Cyb5A (1.4 - 50 μM) was reduced by Ncb5or-b5R (140 nM) or Cyb5R3 (0.56 nM), respectively, in the presence of excess NADH (100 μM) in 5 mM sodium phosphate (pH 7.0, no air). All reactions were monitored by the absorbance increase of the Soret band (A_{424}) when the concentration of substrate [S] ≤ 10 μM, or the β-peak (ε_{558} = 17.5 $mM^{-1}cm^{-1}$, Ncb5or-b5 or ε_{556} = 18.1 $mM^{-1}cm^{-1}$, Cyb5A) when [S] ≥ 10 μM. The Michaelis-Menten equation was used to fit V_0 (initial rate constant) and [S] (substrate concentration) with SigmaPlot 10.0 software to generate K_M and V_{max}. Both V_0 and the corresponding [S] are the actual values at the beginning of data collection.

$$V_0 = V_{max}*[S]/(K_m+[S])$$

All data points of the Cyb5A/Cyb5R3 pair fit well to the non-linear function, and the same results were obtained for Cyb5A/Cyb5R3 pair whether a Vo = 0; [S] = 0 point was included or not. However, this was not the case with the Ncb5or pair, and consequently the (0,0) point was omitted for data fitting. For reasons that have not been determined, a *y* intercept of 0.0061±0.0011 was observed for the Ncb5or pair. The substrate is either Cyb5A or Ncb5or-b5, and the enzyme is either Cyb5R3 or Ncb5or-b5R.

Cytochrome c reduction. Reduction of ferric horse cytochrome c (1.4 μM, Sigma) by the protein constructs described herein was performed in the presence of excess NADH (50 μM) in 5 mM phosphate (pH7.0, no air). Reduction of heme was monitored by the increase of absorbance at 416 nm (Soret band). Data were fit to a single exponential function and the resulting pseudo-first order rate constant was dissolved by the appropriate enzyme concentration (28 nM each was used in all cases) to obtain the reported observed rate constants ($min^{-1}\mu M^{-1}$).

Results

Generation and initial characterization of individual redox domains of human Ncb5or. Recombinant proteins representing the individual redox domains of human Ncb5or (**Figure 1A**), designated herein as Ncb5or-b5 and Ncb5or-b5R, were generated in order to (a) characterize the structure of the Ncb5or-b5 core, and (b) compare the nature of Ncb5or-b5/Ncb5or-b5R interactions with those exhibited by the well-known Cyb5A/Cyb5R3 pair. We also generated a construct comprising the CS and b5R domains of Ncb5or (Ncb5or-CS/b5R) in order to explore possible roles played by the CS domain in interactions between the b5 and b5R domains. Human Ncb5or-b5 and human Cyb5A are virtually identical in stability, with thermal denaturation midpoints (T_m values) of 72°C and 73.5°C, respectively (**Supplementary Figure 4**). In contrast, Ncb5or-b5R is considerably less stable than Cyb5R3 as evidenced by its much lower expression yield and its much greater tendency to form polypeptide aggregation during concentration following purification unless high salt levels were maintained (20 mM Tris-HCl, 500 mM NaCl, 0.1 mM EDTA, pH 7.0). Despite being obtained in a lower yield, Ncb5or-CS/b5R is more stable than Ncb5or-b5R. This suggests the possibility of favorable interactions between the CS and b5R domains, perhaps like those in full-length Ncb5or.

EPR spectroscopy indicates different heme environments in Cyb5A and Ncb5or-b5. UV/vis spectra of Ncb5or-b_5 [1] and Cyb5A [66] show similar and characteristic spectra for low-spin, bis-histidine heme ligation. However, a previously reported study comparing rat Cyb5A and Ncb5or revealed distinctly different EPR spectra [70]. In the present study, we observed differences in EPR spectra between human Cyb5A and Ncb5or (**Figure 2**), which are consistent

A.

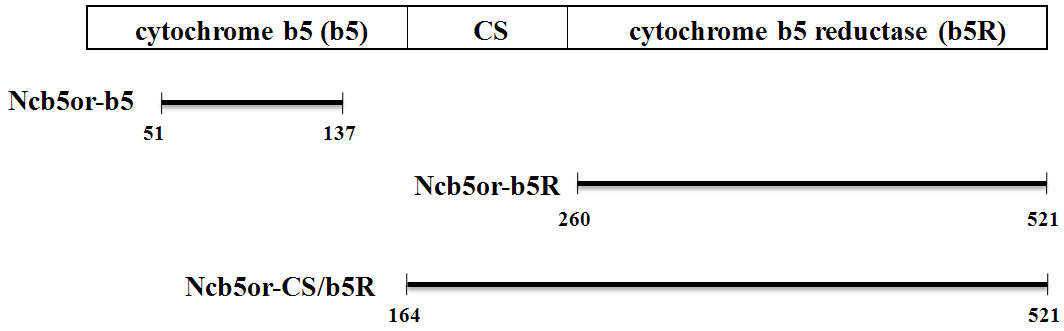

B.

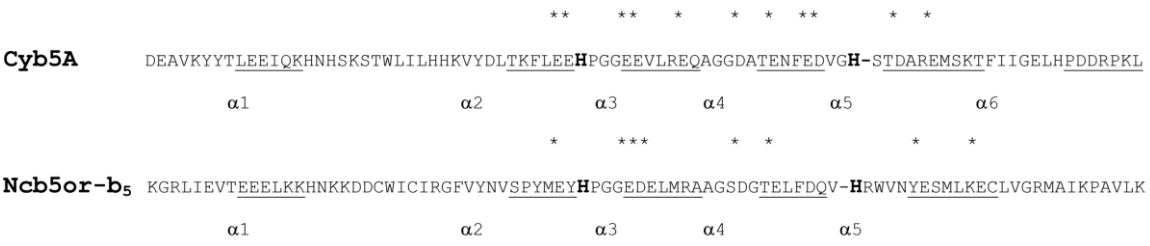

Figure 1. (A) Schematic diagram of individual domains in human Ncb5or. Cytochrome b5 and cytochrome b5 reductase domains are at NH_2- and COOH-terminus, respectively, with the CS domain in between. Ncb5or-b5 and Ncb5or-b5R are two constructs used in this study. (B) Sequence alignment of human Ncb5or (bottom) and human Cyb5A (top) showing all helical segments, i.e., α1-α6 in Cyb5A and α1-α5 in Ncb5or-b5, as well as negatively charged surface residues in core 1 that are conserved in all vertebrate orthologs of each protein (asterisks). In bold are heme-ligating residues, His^{44} and His^{68} in Cyb5A and His^{89} and His^{112} in Ncb5or-b5. These figures are adapted from Deng *et al*. [85].

with the previous EPR spectra for rat proteins [70]. The EPR signals of Cyb5A giving g values of 3.03, 2.21 and 1.40 (**Figure 2**, bottom) are typical among cytochrome b5 superfamily members and among most low-spin, bis-histidine ligated ferric heme proteins (**Supplemental Table 2**). Such a spectrum represents a rhombically distorted heme environment which is caused by the small dihedral angle between the planes of the His imidazolyl groups (< 57°) [86]. In contrast, the EPR spectrum of ferric human Ncb5or-b5 shown a spectrum dominated by a signal at g=3.56 (**Figure 2**, top). This kind of spectrum, called to as a highly anisotropic low spin (HALS) or "large g_{max}" spectrum [87,88], is unique in cytochrome b5 superfamily and indicative of iron in a tetragonally distorted environment [89,90]. HALS EPR spectra are defined as those in which the value of g_z (g_{max}) is ≥ 3.2 and is caused by the large dihedral angle between the imidazolyl planes (> 57°) [86].

Atomic structure of human Ncb5or-b5. A 1.25 Å X-ray crystal structure was obtained for Ncb5or-b5 with two protein molecules in the asymmetric unit. Although a solution structure of human Cyb5A determined by NMR is available in the Protein Data Bank (PDBID: 2I96), it may not be comparable to crystal structure. Therefore we use the 1.5 Å crystal structure of the bovine Cyb5A lipase fragment (PDBID: 1CYO) [17] for comparison with our structure of Ncb5or-b5. The heme-binding domains of human and bovine Cyb5A are almost identical, and differ at only four of the 87 residues that are involved in specific packing interactions in the bovine Cyb5A crystal structure (residues 6-92, **Supplemental Figure 1**). Two of these residues are localized in the heme-binding pocket (α2-α5), which are the major part for comparison in this study. As

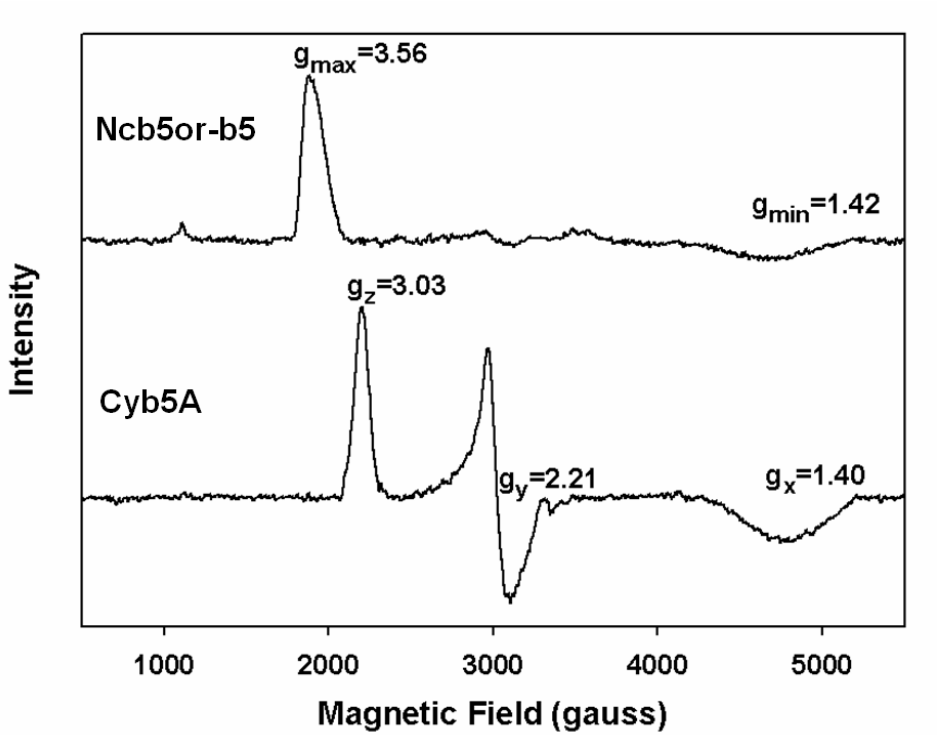

Figure 2. EPR spectra of human Ncb5or-b5 (top) and human Cyb5A (bottom). Ncb5or-b5 exhibits a highly anisotropic low-spin (HALS) signal with g_{max} = 3.56 and g_{min} = 1.42 (1866 and 4683 gauss, respectively). Cyb5A shows a classic low-spin axial heme spectrum with g values of 3.03 (z), 2.21 (y) and 1.40 (x), at 2183, 3016, 4800 gauss, respectively. EPR data were collected by Dr. Brian Gibney. This figure is adapted from Deng *et al*. [85].

indicated by the previous studies [57,58], the two residues was not identified to interact with Cyb5R3. The mutations at the two sites are available, but seem to cause no significant changes in chemical property and local environment. We consider it valid to compare crystal structures between human Ncb5or-b5 and human Cyb5A. Notably the residue numbers used for Cyb5A in this report reflect those in the native protein sequences in which Met1 is set as the first residue, while in the commonly employed numbering system that was devised by Mathews for the bovine Cyb5A lipase fragment, Ser^{6} is designated Ser^{1} [91,92].

The structural overlay in **Figure 3A** reveals that Ncb5or-b5 shows similar b5 fold to Cyb5A, and the fold can be also described as two hydrophobic cores separated by a five-stranded β-sheet. Similarly as compared to Cyb5A, heme in Ncb5or-b5 is ligated by His^{89} and His^{112}, with His^{89} localized in the first helix-loop-helix motif (α2 and α3) and His^{112} localized in the second helix-loop-helix motif (α4 and α5). The fold of region from α2 to α4 in Ncb5or-b5 are almost identical to the corresponding region in Cyb5A (**Figure 3A)**. "HPGG" motif that is invariant in all known eukaryotic members of the cytochrome b5 superfamily constructs the loop between α2 and α3. The first heme-ligating His^{89} in Ncb5or-b5, corresponding to His^{44} in Cyb5A, resides at the beginning of the loop. Ncb5or-b5 has three Cys residues in comparison with no Cys in Cyb5A; however, none of the Cys residues in Ncb5or-b5 are involved in disulfide bridges or covalent linkages to heme, and all of them are buried.

Two distinct differences in polypeptide conformation between Ncb5or-b5 and Cyb5A are observed. First, the C-terminal α6 in Cyb5A is absent in Ncb5or-b5. Second and more importantly, in Ncb5or-b5 the orientation of the second heme-ligating His^{112}, and the fold of the

A.

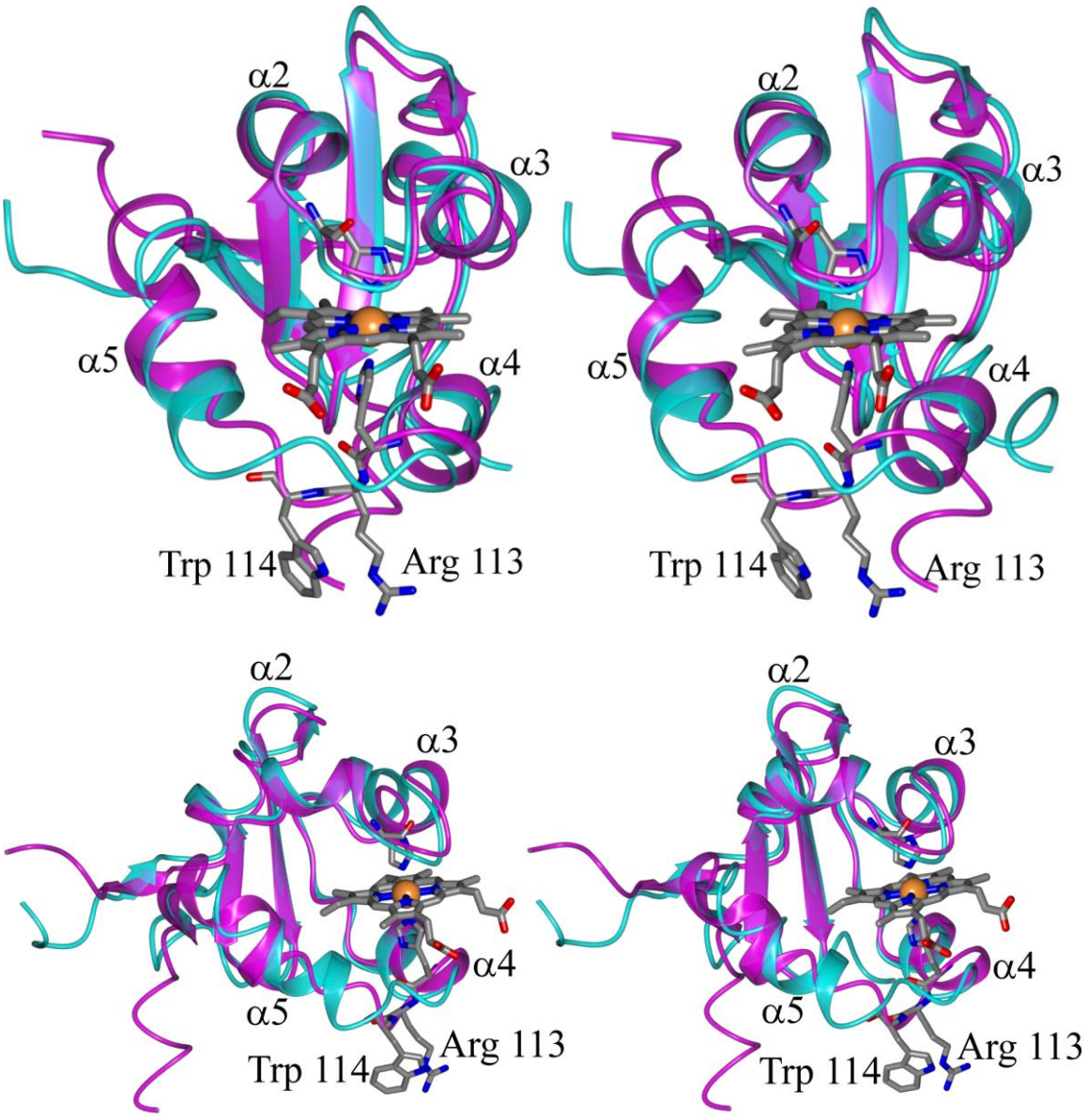
α2
α3
α5
α4
Trp 114
Arg 113
α2
α3
α5
α4
Trp 114
Arg 113
α2
α3
α4
α5
Trp 114
Arg 113
α2
α3
α4
α5
Trp 114
Arg 113

B.

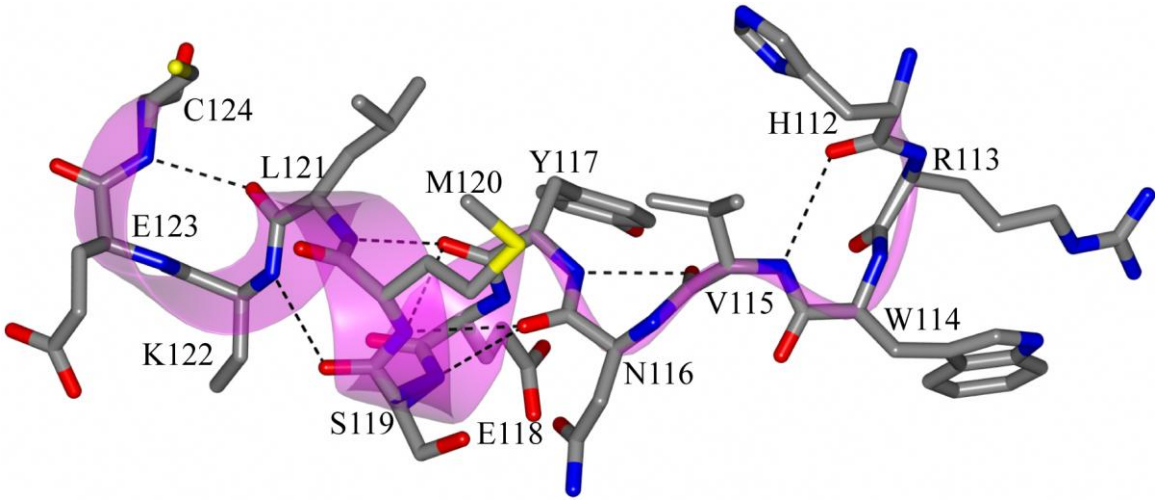
C124
L121
M120
Y117
H112
R113
E123
V115
W114
K122
N116
S119
E118

C.

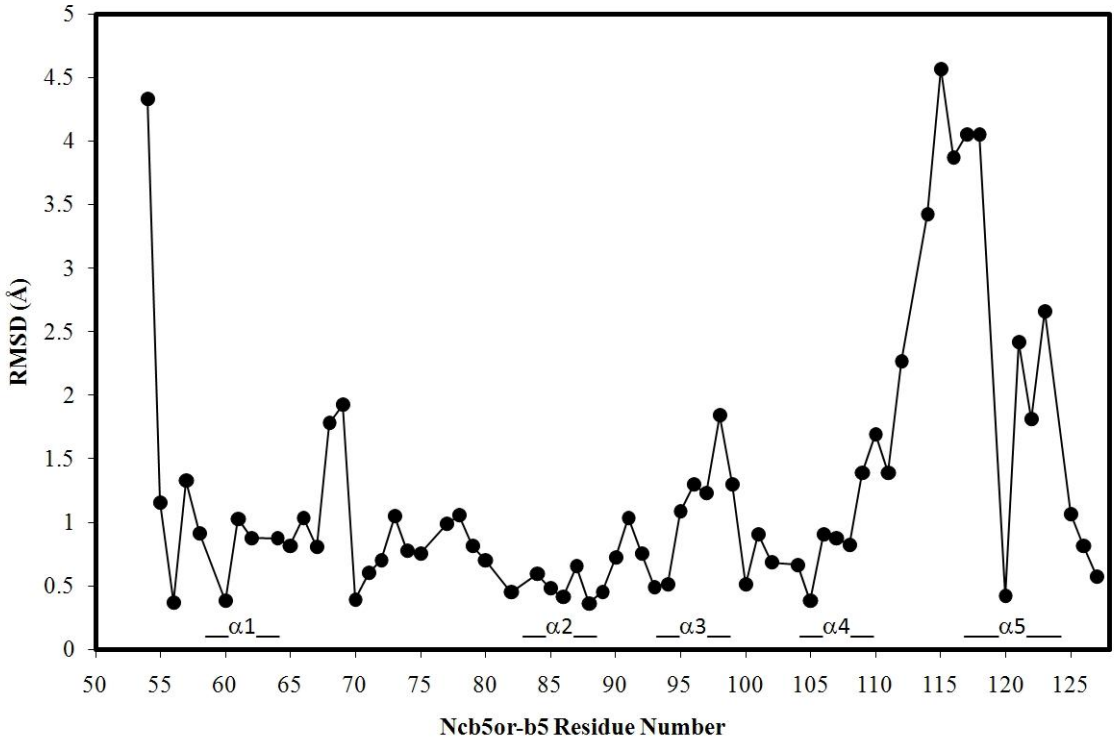
RMSD (Å)
Ncb5or-b5 Residue Number
__α1__
__α2__
__α3__
__α4__
___α5___

D.

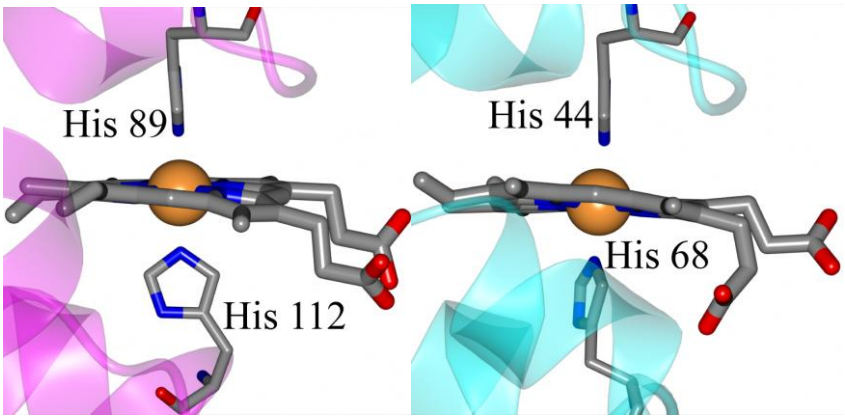

Ncb5or-b5 **Cyb5A**

Figure 3. (A) Stereo views of the overlay of human Ncb5or-b5 (magenta) and bovine Cyb5A (PDB: 1CYO, cyan). The helices are labeled using the standard notation (α2-α5) of Cyb5A. Top panel is viewed perpendicular to the face of the heme binding pocket with the heme propionates clearly visible, and the bottom panel is rotated approximately 45°. (B) Loop and α5 region of Ncb5or-b5. Hydrogen bonds are indicated by dashed lines. Electron density for K122 was not observed therefore the side chain was truncated. Secondary structure is represented as a magenta ribbon. (C) Root mean square deviations (RMSD, Å) between Cα atoms of Ncb5or-b5 (chain A) reported here and bovine Cyb5A (PDB: 1CYO). The helices in the heme binding core of Ncb5or (α1-α5) are marked. For this comparison, residues Val4 to Gly77 of 1CYO were superimposed onto Leu54 to Gly127 of Ncb5or-b5. (D) Zoomed in view of the heme binding pockets for Ncb5or-b5 (left) bovine Cyb5A [93]. The imidazole rings of the histidine residues that ligate the heme Fe atom in Ncb5or-b5 are nearly orthogonal to each other. The structure was solved and figures were prepared by Dr. Scott Lovell. The figures were adapted from Deng *et al*. [85].

subsequent region are different from Cyb5A. In Cyb5A, the second heme-ligating His^{68} is located in a highly conserved $V^{66}GHS^{69}$ loop, which is followed by a 9-residue helix α5. In Ncb5or-b5, the second heme-ligating His^{112} is located in an invariant sequence $H^{112}RWVNYESMLKEC^{124}$. The alignment with Cyb5A (**Figure 1B**) reveals a deletion of Gly before His^{112} and an insertion of Arg after. This confers the formation of a hydrogen bond between the amide NH of Val^{115} and the carbonyl group of His^{112} (**Figure 3B**). Variations in the vicinity of the second heme ligating residue, His^{112}, and the hydrogen bond in Val^{115} and His^{112} of Ncb5or, contribute to the rotation of His^{112} to the orientation nearly orthogonal to His^{89}, resulting in the tetragonally distorted heme environment and large g_{max} in EPR spectrum.

The Helix α5, which is composed of Tyr^{117}-Cys^{124}, is a kink helix (**Figure 3B**). Asn^{116} forms hydrogen bonds with Ser^{119} and Met^{120}. Tyr^{117} forms hydrogen bonds with Met^{120} and Leu^{121}. The kink is at Leu121. The following helix is canted at about 45º relative to the helix α5 in Cyb5A (**Figure 3A**). The irregular pattern of hydrogen bonds in the region from His^{112} to Cys^{124}, instead of i/i+4 hydrogen bonds, endows the special fold in this region. This is determined by the unique primary sequence in this region in Ncb5or-b5 (**Figure 1B**). According to the comparison of root mean square deviation (RMSD) of Cα atoms in Ncb5or-b5 and Cyb5A, the conformations differ significantly from Arg^{113} to Ser^{119} (**Figure 3C**). The fold of Ncb5or-b5 can be also described as an adaptable module, like the folds of other members in the b5 superfamily [15].

The bis-histidine ligands in Ncb5or are nearly orthogonal to each other. As revealed before, Cyb5A and Ncb5or-b5 exhibit quite similar fold from α2 to α4, and the first heme-ligating His is within this region. Consequently the imidazolyl ring of His^{44} in Cyb5A and His^{112} in Ncb5or-b5

orients similarly in the heme pocket (**Figure 3D**). However, the imidazolyl ring of His^{112} in Ncb5or-b5 is substantially rotated relative to that of His^{68} in Cyb5A. In comparison of sequences between Ncb5or-b5 and Cyb5A (**Figure 1B**), in regard to this His residue, there is a deletion of Gly before and an insertion of Arg after. The displacement of His in Ncb5or-b5 may cause the rotation of His^{112}.

The dihedral angle of imidazolyl rings of His^{89} and His^{112} in Ncb5or-b5 are 83.2º and 81.3º in molecules A and B of the asymmetric unit, respectively, (**Supplemental Table 2)**, consistent with HALS EPR signal in **Figure 2,** top. In contrast, the imidazolyl rings of His^{44} and His^{68} in bovine Cyb5A is almost coplanar to each other, with a dihedral angle of 21.2° (**Figure 3D**, right panel), similar to values in other structurally characterized Cyb5A orthologs and consistent with the rhombic EPR spectrum in **Figure 2**, bottom (**Supplemental Table 2**). It is noteworthy that the redox potential of Ncb5or-b5 (-108 mV) [2] is quite low compared to human Cyb5A (-9 mV) [66], and probably is lowest so far in cytochrome b5 superfamily. Such a unique heme center in Ncb5or-b5 may a factor to contribute to its low redox potential.

Differences in solvent-exposed residues in core 1 of Cyb5A and Ncb5or-b5. A number of studies have shown that interaction between Cyb5A and Cyb5R3 is electrostatic in nature between the side chains of negatively charged residues in Cyb5A and positively charged residues in Cyb5R3 [56,57,58]. The negatively charged residues in Cyb5A are located the four helices α2-α5 packing heme, and around the opening of heme packet. In this region, there are eleven invariant negatively charged residues (Glu and Asp) in mammalian Cyb5A compared to eight conserved Glu and Aps residues in Ncb5or-b5 (**Figure 1B)**. Accordingly in the electrostatic map

A. **B.**

(Cyb5A) **(Ncb5or-b5)**

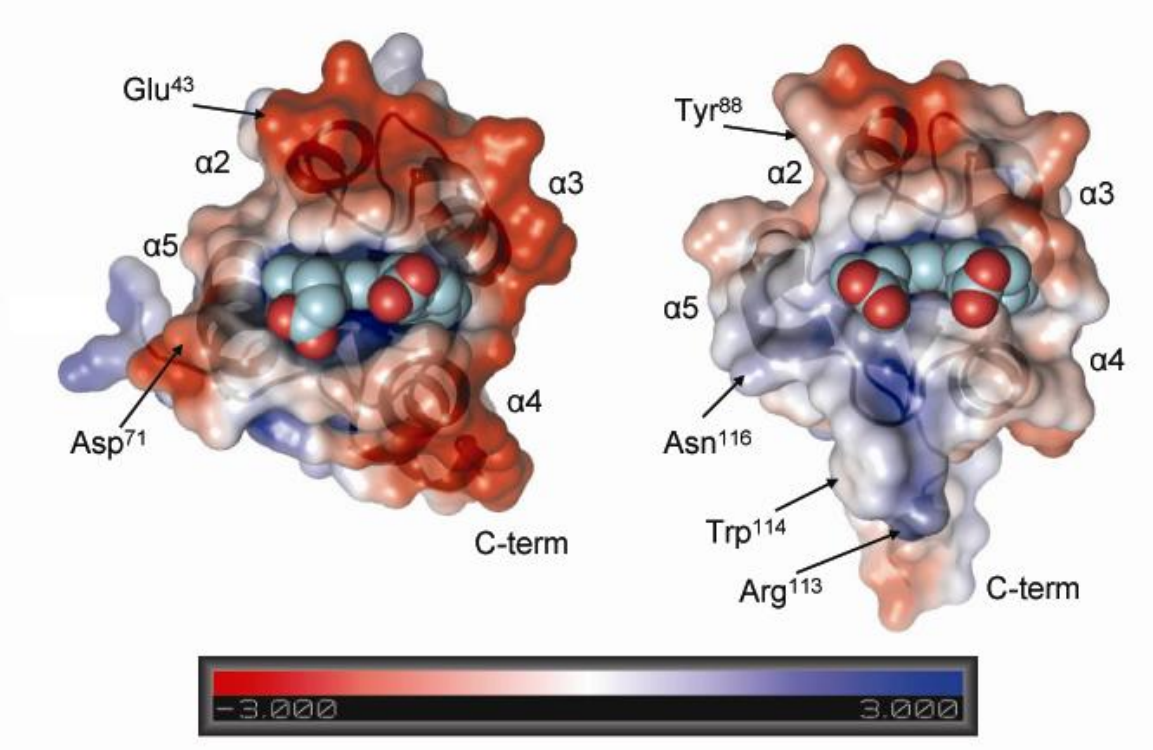

Figure 4. Electrostatic surface maps of bovine Cyb5A (A) and human Ncb5or-b5 (B) show the two proteins in the same orientation as that in Figure 3A-left. The negatively charged surface in Cyb5A interacting with Cyb5R3 is shown along with a much weaker charged corresponding surface in Ncb5or-b5. Both proteins are oriented identically with the heme propionates clearly visible. The figure is prepared by Sudharsan Parthasarathy and adapted from Deng *et al*. [85].

(**Figure 4A**), much lower density of negative charge is observed inNcb5or-b5 compared Cyb5A. The number of negatively charged residue may not be the sole factor contributing to difference in surface charge. Other factors like arrangement of charged residue or cluster could also affect the density of surface charge.

In addition to those charged residue, two solvent-exposed residues, Arg^{113} and Trp^{114}, which are near the front edge of the Ncb5or-b5 heme-binding pocket and are adjacent to heme-ligating His^{112}, are identified. Both of these residues are conserved in mammalian Ncb5or, and particularly Trp^{114} is invariant among known Ncb5or orthologs (**Supplemental Figure 2**). In corresponding region of Cyb5A, no amino acid side chains are found to be highly exposed solvent. No positively charged residue in Cyb5A has been identified to mediate interaction with Cyb5R3. We therefore generated the Ncb5or-b5R113A and Ncb5or-b5W114A mutants for comparison with the wild-type protein in inter-domain electron transfer studies (see below).

Inter-domain electron transfer. Although previous steady state kinetics studies with Cyb5A and Cyb5R3 have typically been performed in the presence of air [58,67], we observed that reduction of Ncb5or-b5 by Ncb5or-b5R only occurred at a detectable rate when air was excluded from the system. One likely contributing factor is that the reduction potential of Ncb5or-b5 (-108 mV vs. standard hydrogen electrode or SHE) [2] is much more negative than that of Cyb5A (-9 mV vs. SHE) [66], making its reduced form much more susceptible to auto-oxidation. Consequently, all studies reported herein were performed under an inert atmosphere (see Materials and Methods). For reasons that will become clear below, we also needed to perform comparative kinetics studies at low ionic strength (5 mM sodium phosphate; $\mu = 0.009$ M).

A.

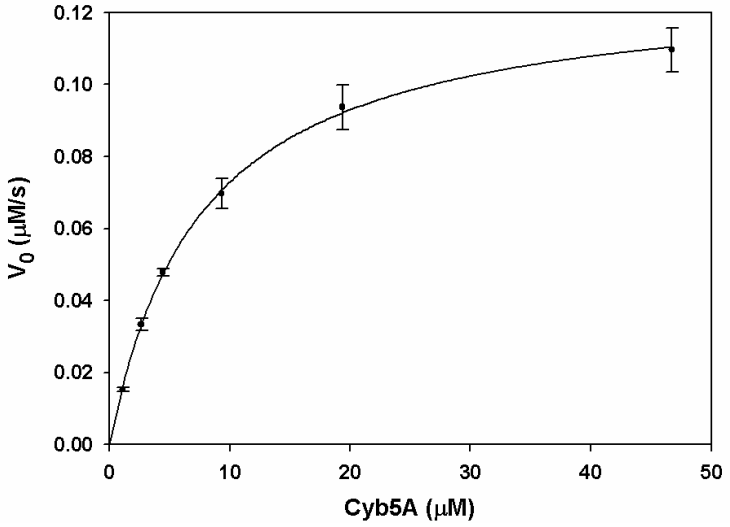

B.

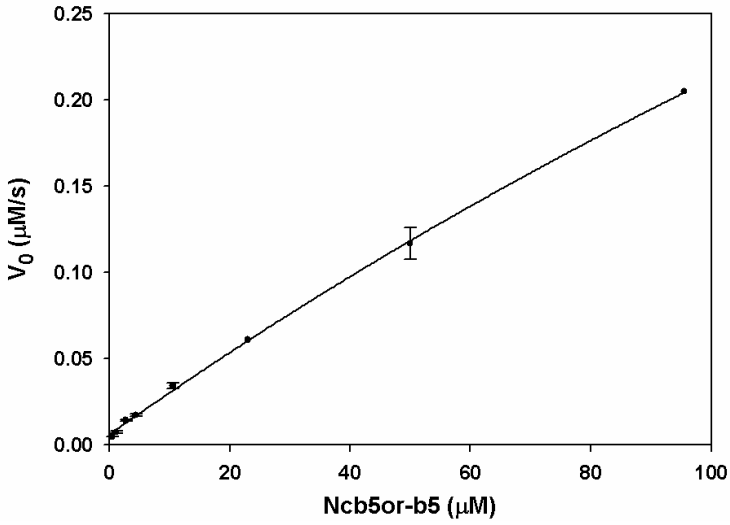

Figure 5. Kinetics of heme reduction of (A) Cyb5A and (B) Ncb5or-b5 under low ionic strength (0.009 M). The initial rate (V_0) is plotted against substrate concentration [S]. Cyb5A (1.4-50 μM) was reduced by Cyb5R3 (0.56 nM), and Ncb5or-b5 (0.7-100 μM) by Ncb5or-b5R (140 nM). Each data point with error bar is averaged from 2 to 4 independent reactions. The substrate is the b5 (Cyb5A or Ncb5or-b5), and the enzyme is the b5R (Cyb5R3 or Ncb5or-b5R). These figures are adapted from Deng *et al*. [85].

Table 1. Kinetic properties of Cyb5A/Cyb5R3 and Ncb5or-b5/Ncb5or-b5R reduction. The raw data of V_0 vs. [S] were fit to the Michaelis-Menten equation to generate K_M and k_{cat} (V_{max}/[E]). The substrate is the b5 (Cyb5A or Ncb5or-b5) and the enzyme is the b5R (Cyb5R3 or Ncb5or-b5R). This table is adapted from Deng *et al*. [85].

Substrate/Enzyme	[E]	K_M （μM）	k_{cat} （s^{-1}）	k_{cat} / K_M （$\mu M^{-1}s^{-1}$）
Cyb5A/Cyb5R3	0.56 nM	7.6±0.3	230±3	30.1
Ncb5or-b5/ Ncb5or-b5R	140 nM	498±129	8.8±1.9	0.018

Consistent with previous studies [67], reduction of Cyb5A by Cyb5R3 obeyed Michaelis-Menten kinetics (**Figure 5A; Table 1**). In contrast, saturation of Ncb5or-b5R by Ncb5or-b5 was not approached even when [Ncb5or-b5] reached 100 μM, the highest concentration we could use in our system (**Figure 5B**). As a consequence of the nearly linear V_0 vs. [S] curve, the k_{cat} and K_M values obtained for the Ncb5or-b5/Ncb5or-b5R pair have relatively high standard errors and should therefore be considered as rough estimates (**Table 1**). Our results reveal a much higher K_M value for the Ncb5or-b5/Ncb5or-b5R pair than for the Cyb5R3/Cyb5A pair (**Table 1**), suggesting a considerably weaker interaction in the former. It should be noted that the b5 domain in intact Ncb5or is reduced instantaneously following addition of excess NADH [1].

The efficiency of Cyb5A reduction by Cyb5R3 decreased 4-fold when the solution ionic strength was increased from 0.009 M (buffer *i*) to 0.108 M (buffer *ii*), as measured by kinetic studies performed at a single substrate concentration (**Table 2**). This is indicative of a strong electrostatic component to docking between the molecules, consistent with previous reports [55,94]. A similar decrease in catalytic efficiency was observed in analogous experiments performed with Ncb5or-b5 and Ncb5or-b5R (**Table 2**), suggesting that electrostatic interactions contribute to docking between this redox pair as well.

In initial rate studies, we observed that Cyb5R3 reduces Cyb5A approximately 70-fold more rapidly than Ncb5or-b5 (**Table 3**). In contrast, Ncb5or-b5R did not exhibit specificity towards its cognate redox partner, instead reducing Cyb5A approximately four-fold more rapidly than Ncb5or-b5. When Ncb5or-b5R was replaced by the Ncb5or-CS/b5R construct, we observed a

Table 2. Observed rate constants (K_{obs}, $min^{-1}\mu M^{-1}$) of inter-domain electron transfer as a function of environmental ionic strength. Ncb5or-b5 or Cyb5A (1.4 μM each) was reduced by Ncb5or-b5R or Cyb5R3, respectively, in the presence of excess NADH (50 μM) in buffer with various ionic strength (pH 7.0, no air). Amount of enzyme used: [a] 0.56 nM; [b] 140 nM. This table is adapted from Deng *et al*. [85].

Buffer	Ionic strength, μ (M)	Cyb5A/Cyb5R3	Ncb5or-b5/Ncb5or-b5R
i	0.009	1400±90 [a]	4.20±0.17 [b]
ii	0.108	331±16 [a]	1.13±0.06 [b]

Table 3. Initial rate (μM/min/μM) of inter-domain electron transfer. Ncb5or-b5 (wild-type, W114A and R113A mutants) or Cyb5A (1.4 μM each) was reduced by Ncb5or-b5R, Ncb5or-CS/b5R or Cyb5R3, in the presence of excess NADH (50 μM) in 5 mM sodium phosphate (pH 7.0, no air). Amount of reductase used: [a] 0.56 nM; [b] 28 nM; [c] 140 nM, [d] 500 nM (All the values in this table were normalized by reductase concentrations). This table is adapted from Deng *et al*. [85].

	Cyb5A	Ncb5or-b5	Ncb5or-b5W114A	Ncb5or-b5R113A
Cyb5R3	1730±63 [a]	24.60±1.73 [b]	11.06±1.23 [b]	24.52±2.27 [b]
Ncb5or-b5R	22.97±1.67 [b]	5.69±0.29 [c]	2.80±0.22 [c]	4.63±0.10 [c]
Ncb5or-CS/b5R	0.24±0.01 [d]	0.69±0.06 [d]	0.17±0.02 [d]	0.42±0.04 [d]

Table 4. Observed rate constants ($min^{-1}\mu M^{-1}$) of cytochrome *c* reduction. Single enzyme or mixture was used to reduce cytochrome c (1.4 μM) in the presence of excess NADH (50 μM) and 5 mM phosphate (pH7.0, no air). An enzyme concentration of 28 nM (each protein) was used in all cases. This table is adapted from Deng *et al*. [85].

	Cyb5R3	Ncb5or-b5R	Ncb5or-CS/b5R	Ncb5or
cytochrome *c* alone	10.39±0.50	9.32±0.36	12.41±0.57	34.70±1.07
+ Ncb5or-b5	14.09±0.64	9.69±0.49	13.27±0.39	N/A

95-fold decrease in the initial rate of Cyb5A reduction while reduction of Ncb5or-b5 was diminished only 8-fold (**Table 3**). Thus, Ncb5or-CS/b5R reduces Ncb5or-b5 nearly three-fold more rapidly than it reduces the non-cognate electron acceptor Cyb5A. Ncb5or-CS/b5R, Ncb5or-b5R and Cyb5R3 all reduce the non-specific substrate cytochrome *c* with essentially identical rate constants (**Table 4**). The fact that Ncb5or-CS/b5R is less efficient than Ncb5or-b5R at reducing Ncb5or-b5 therefore cannot be ascribed to deactivation of the b5R domain by the presence of the CS domain. Indeed, as noted above, Ncb5or-CS/b5R is more stable than Ncb5or-b5R.

As noted above, there are no amino acid side chains directed toward solvent in the segment of Cyb5A corresponding most closely to that containing Arg^{113} and Trp^{114} in Ncb5or. To investigate possible roles of these residues in interactions between the b5 and b5R domains of Ncb5or, we generated and characterized the R113A and W114A mutants of our Ncb5or-b5 construct. The R113A mutant was reduced by Ncb5or-b5R with nearly identical catalytic efficiency (**Table 3**), while the W114A mutation decreased the rate of Ncb5or-b5 reduction by approximately 3-fold. A similar fold-change was observed for both mutants when they were reduced by Ncb5or-CS/b5R (**Table 3**). Neither mutation had a measurable effect on protein stability as determined in thermal denaturation studies (**Supplemental Figure 4**). Small differences in far-UV and Soret-region CD spectra of the WT, R113A and W114A proteins suggest that the mutations may cause subtle alterations in local structure. However, W114A mutant appears to exert a larger effect (**Supplemental Figure 5**).

Discussion

The cytochrome b5 fold was first revealed when Mathews determined the X-ray crystal structure of the lipase fragment of bovine Cyb5A [91,92]. In comparison of the b5 domain between Cyb5A and the two-domain protein yeast flavocytochrome b2, fold of the heme-binding region is similar, especially from α2 to α4. There are variations in orientation and length of α5, and position of heme relative to heme packet. Based on structure above, and a three-dimensional model of tobacco nitrate reductase, and amino acid sequences of multiple other b5 superfamily members, Lederer aptly described the cytochrome b5 fold as an adaptable module [15]. In spite of only 30% sequence identity with Cyb5A (**Figure 1B**), Ncb5or-b5 still follows the adaptable module, eventually resulting in the similar fold to Cyb5A. However, the large difference in primary structure of Ncb5or-b5 compared to Cyb5A also leads to absence of C-terminal α6 in Ncb5or-b5 (**Figure 3A)**, unusual structure in α5 and the loop nearby (**Figure 3A and B**), alteration in heme environment (**Figure 3D**) and decrease on surface charge (**Figure 4).** The difference in sequence eventually leads to difference in the property.

Some of the structural differences described above are almost certainly linked to the divergent functional roles of Cyb5A and Ncb5or. Both proteins have been implicated to function in fatty acid desaturation [34,48], but more studies are needed to delineate their specific roles. We have identified a unique His ligand orientation in Ncb5or. The rings of the two heme-ligating His residues in Ncb5or-b5 is nearly orthogonal to each other, resulting a tetragonally distorted environment corresponding to a HALS EPR spectrum. In contrast, so far as known, in other members of cytochrome b5 superfamily, dihedral angles are no more than 57° (**Supplemental**

Table 2), corresponding to a rhombically distorted heme environment. Actually heme proteins with nearly orthogonal His ligands have been found in the mitochondrial respiratory chain including the cytochrome bc_1 complex (heme b_L) [88,90,95] and in quinol:fumarate reductase (proximal heme b) [96,97]. Similar to Ncb5or, these proteins exhibit HALS EPR spectra; however, the heme is localized in transmembrane region, which is constructed by a four-helix bundle with left-handed twist [89]. Heme is coordinated by two His residues from opposite side of the bundle, making direction of heme plane generally follow the orientation of the four helix bundle. To the best of our knowledge, Ncb5or is the only member of the cytochrome b5 superfamily demonstrated to exhibit a HALS EPR spectrum and/or orthogonal His ligands, and compared to these mitochondrial cytochrome with HALS EPR, Ncb5or is soluble. It differs from other b-type heme proteins in this category in two key ways. First, while available evidence suggests that Ncb5or may be loosely associated with the ER membrane [2], its b5 domain has a high polarity on surface and therefore very likely exposed into solvent. In spite of tendency to form aggregate, Ncb5or-b5R is still soluble in aqueous solution and its electron source, NADH can only exist in aqueous environment. Therefore, a solvent-exposed location would seem to be essential for Ncb5or-b5's role in shuttling electrons from the b5R domain to its downstream partner or partners. Secondly, even though heme is surrounded by a four helices in Ncb5or-b5, the helices are separated by loops and cannot form bundle. Eventually four helices are oriented into different directions. For the two heme-ligating His residue, one is located in a loop while the other is located at C-terminal boundary of helix (followed by a loop).

Perpendicular histidine ligands are clearly not essential for inter-domain electron transfer in

Ncb5or, as evidenced by the fact that Ncb5or-b5R reduces its cognate partner Ncb5or-b5 less efficiently than it reduces Cyb5A. Instead the difference in orientation of His ligands between Ncb5or and Cyb5A may affect the biophysical properties of the two proteins and make them better fit the biological functions. It is likely that the perpendicular His ligands in Ncb5or-b5 contribute to its substantially more negative redox potential (-108 mV vs. SHE) [2] in comparison to Cyb5A (-9 mV vs. SHE) [66]. However, molecular orbital theory suggests that changing from parallel to perpendicular His ligands should be accompanied by a significant positive shift in redox potential [88,97], though many other factors could also play roles in affecting redox potential. Indeed in contrast to Phe^{35} in Cyb5A, Tyr^{85} in Ncb5or-b5 points toward the heme, and likely make the heme exposed in a more polar environment. This may cause the negative shift of redox potential in Ncb5or-b5. Ncb5or-b5 will provide the opportunity to firmly establish the relationship between heme environment and redox potential in bis-histidine ligated heme proteins.

An alternative possibility is that the position of the second His ligand is restricted by the coordination with the heme. Once a shift occurs in Ncb5or-b5 compared to Cyb5A (**Figure 1B**), the location change of the His residue in Ncb5or-b5 can exert the effect on the adjacent region up to helix α5. In this context, it is worth noting that the region encompassing ligand His^{112} through the C-terminus of helix α5 in Ncb5or from vertebrates has a higher degree of conservation than do the other helices in the heme binding pocket (α2-α4; **Supplemental Figure 2**). In contrast, a lower conservation in helix α5 than α2 – α4 in Cyb5A from vertebrates (**Supplemental Figure 1**) is found. This secondary structure difference around α5 and the loop nearby, coupled with

divergence in primary structure, especially distribution of charged residues, results in strikingly different protein surfaces in Cyb5A and Ncb5or-b5 (**Figure 4**).

Studies have shown that Cyb5A/Cyb5R3 recognition is dominated by a strong electrostatic component involving interactions between negatively charged residues on Cyb5A and positively charged residues on Cyb5R3 [56,57,58]. Our ionic strength studies have shown that recognition between the b5 and b5R domains of Ncb5or also involves a significant electrostatic component. In this context, it is noteworthy that there are eleven negatively charged residues in the four-helix bundle surrounding heme in Cyb5A but only eight in the corresponding region of Ncb5or-b5 (**Figure 1B**). Mutagenesis studies have been performed by others to replace ten of the eleven Glu and Asp residues in core 1 of Cyb5A by Ala (**Supplemental Table 3**). Results suggest that only Glu^{43} and Asp^{71} are involved in strong interactions with Cyb5R3 [57,58]. As indicated in **Figure 4B**, both of these residues are located in α2 and α4, at the opening of heme pocket. These locations may bring in Cyb5R3 to the heme propionate group that is thought to be important in Cyb5R3 recognition as well. Notably, the residues in human Ncb5or-b5 corresponding to Glu^{43} and Asp^{71} in Cyb5A are uncharged (Tyr^{88} and Asn^{116}, respectively). Asn^{116} is an invariant residue among all known Ncb5or orthologs, whereas residue 88 is either Tyr or Phe (**Supplemental Figure 2**). As a consequence, there is much lower negative charge density near the front edge of heme in Ncb5or-b5 (**Figure 4B**) than in Cyb5A (**Figure 4A**), the region of each protein likely to undergo the most extensive interactions with the cognate reductase proteins for electron transfer [58,98]. The much larger K_M value obtained in our studies for the Ncb5or-b5/Ncb5or-b5R pair than for the Cyb5A/Cyb5R3 pair may therefore have a major contribution from weaker

electrostatic interactions. Such a large difference in K_M values for these pairs is perhaps not surprising, given that Cyb5A and Cyb5R3 must diffuse through the ER membrane prior to docking, whereas the b5 and b5R domains in intact Ncb5or are held in proximity by the intervening other domains [1]. A low K_M value for the b5 and b5R domains of Ncb5or might reasonably be expected to impair the ability of Ncb5or to deliver electrons to its downstream partner or partners.

On the basis of studies with Cyb5A and Cyb5R3, it can be inferred that residues most likely to be involved in docking of the Ncb5or b5 domain to its b5R domain are located at the front of the four-helix bundle that surrounds heme. A major difference in this region of Ncb5or-b5 in comparison to Cyb5A is the presence of Trp^{114}, which is invariant among all known Ncb5or orthologs in animals, and the adjacent positively charged residue Arg^{113} which is invariant among known mammalian Ncb5or orthologs. Both residues have fully solvent-exposed side chains whereas the corresponding region of Cyb5A is devoid of exposed side chains. Solvent-exposed residues in proteins, if not constrained by structural or functional demand, are more subject to random mutation than buried residues. Our CD and thermal denaturation data indicate that Arg^{113} and Trp^{114} do not play essential structural or stabilizing roles in human Ncb5or. It can therefore reasonably be assumed that they are necessary for function. Our mutagenesis studies strongly suggest that Arg^{113} is not involved in the b5-b5R interaction in Ncb5or. Trp^{114} appears to play little if any role in this interaction either, as the three-fold decrease in electron transfer rate constant observed for the W114A mutant seems insufficiently large to explain the invariance of Trp^{114} among known Ncb5or proteins. These conclusions ultimately need to be verified in rapid

kinetics studies of full-length Ncb5or and its R113A and W114A mutants. Full-length proteins will also be necessary to examine possible roles of Arg^{113}, Trp^{114} and other highly conserved Ncb5or-b5 residues in interactions between Ncb5or and its likely downstream partner SCD. This represents a significant challenge given that SCD is an integral membrane protein. Efforts are underway to develop an *in vivo* reconstitution system with primary hepatocyes from Ncb5or knockout mice for this purpose. We prefer this experimental system over the classical *in vitro* reconstitution for two reasons: (1) The *in vivo* system reflects more accurately the native desaturation pathway, considering two recent papers that show no major phenotype in lipid metabolism of mice lacking Cyb5A in the liver [35] or in the whole body [45], in contrast to the *in vitro* data [34]; (2) The SCD enzyme is an intergral membrane protein which is hard to purify in an active form for biochemical assays.

The physical interaction between the b5 and b5R domains of Ncb5or is clearly different from that in the Cyb5A and Cyb5R3 complex. The CS domain has been shown to be functionally important to allow the electron flow from b5R to b5 domains in the full-length Ncb5or (1). When the individual domains are separated and mixed in vitro, Ncb5or-b5R is able to reduce Ncb5or-b5 at a slow rate. The electron transfer in the Ncb5or-b5/Ncb5or-b5R pair requires complex formation involving electrostatic interaction, which may be weaker than those in the Cyb5A/Cyb5R3 pair. Nc5or-CS/b5R selectively reduces Ncb5or-b5 over Cyb5A, in contrast to Ncb5or-b5R, but the presence of the CS domain also retards reduction of Ncb5or-b5. Coupled with the finding that the CS domain does not affect the rate of cytochrome *c* reduction, this observation leads us to conclude that the role of the CS domain in Ncb5or is more complex than

simply keeping the b5 and b5R domains in close proximity. At the very least, the CS domain appears to play a role in mediating docking of the b5 and b5R domains. We are currently working to determine the three-dimensional structure of full-length Ncb5or in order to address this and other questions related to its functions.

Supplemental Figure 1. Sequence alignment of Cyb5A from vertebrates. Residue numbers and helices of human Cyb5A corresponding to those in Figure 1B are labeled. Conserved amino acid residues in each group are marked by "*" (identical, heme-ligands in red) or "-" (chemically similar). All are annotated from genomic sequences except those from human, mouse, rat, bovine, horse, pig, rabbit, Xenopus and Zebrafish are confirmed by transcript or protein sequences. GenBank accession numbers are: Human (NP_683725), Chimpanzee (XP_001135885), Monkey (XP_001083378), Orangutan (ENSPPYP00000010369), Guinea pig (ENSCPOP00000010893), Mouse (NP_080073), Rat (NP_071581), Bovine (NP_776458), Horse (NP_001153204), Pig (NP_001001770), Goat (ABQ12619), Dog (XP_533373), Rabbit (P00169), Opossum (XP_001373630), Zebrafinch (XP_002195467), Chicken (NP_001001748), Xenopus laevis (NP_001086707), Xenopus tropicalis (NP_001015979), Rice fish (ENSORLT00000004278), Zebrafish (NP_998300), salmon (ACI66502), pufferfish (ENSTNIP00000008519), Fugu (ENSTRUP00000013474), Stickleback (ENSGACP00000002650), C. Armatus (CAE75863), Rainbow smelt (ACO09548). A 92% identity or a 96% similarity is found for human and rat Cyb5A sequences. This figure is adapted from Deng *et al*. [85].

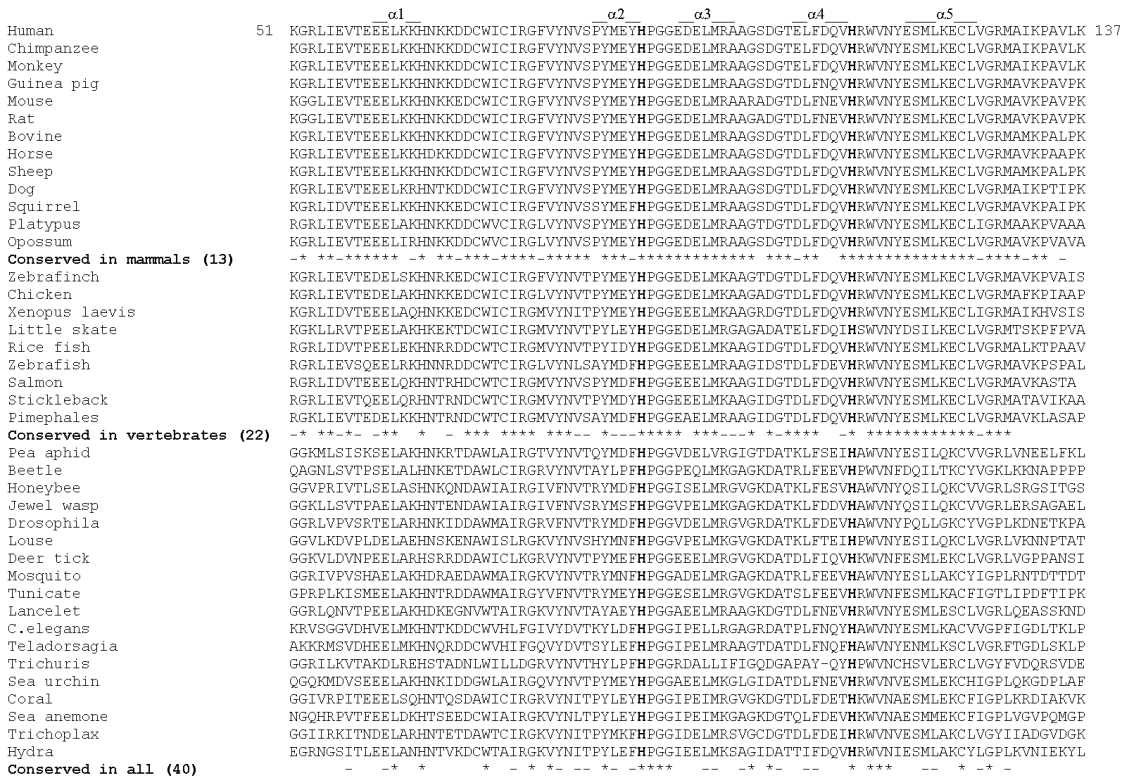

Supplemental Figure 2. Sequence alignment of Ncb5or-b5 core from animals. Residue numbers and helices of human Ncb5or-b5 corresponding to those in Figure 1B are labeled. Conserved amino acid residues in each group are marked by "*" (identical, heme-ligands in red) or "-" (chemically similar). All sequences are annotated from genomic sequences except sequences of human, mouse and rat have been confirmed by cloned cDNAs. Ncb5or is also named Cyb5R3, b5/b5R, and b5+b5R. GenBank accession numbers are: Human (NM_016230), Chimpanzee (XM_518614), Monkey (XM_001085835), Guinea pig (EB369672), Mouse (NM_024195), Rat (NM_133427), Bovine (NM_001038159), Horse (XM_001499913), Sheep (DY519717), Dog (XM_532219), Squirrel (CO734025), Platypus (XM_001512881), Opossum (XM_001375853), Zebrafinch (XM_002188637), Chicken (XM_001233870), Xenopus laevis (NM_001016756), Little skate (CV222314), Rice fish (AM140533), Zebrafish (NM_001020660), Salmon

(DY707237), Stickleback (DN714575), Pimephales (DT192112), Pea aphid (XM_001948299), Beetle (XM_963135), Honeybee (XM_394412), Jewel Wasp (XM_001601866), Drosophila (NM_137575), Louse (XM_002428283), Deer tick (XM_002401084), Mosquito (XM_001650886), Tunicate (XR_053035), Lancelet (XM_002603916), C.elegans (NM_001026613), Teladorsagia (CB038604), Trichuris (BM277379), Sea urchin (CD307914), Coral (EZ038676), Sea anemone (DV081463), Trichoplax (XM_002112883), Hydra (XM_002165807). A 93% identity or a 100% similarity is found for human and rat Ncb5or-b5 sequences. This figure is adapted from Deng *et al*. [85].

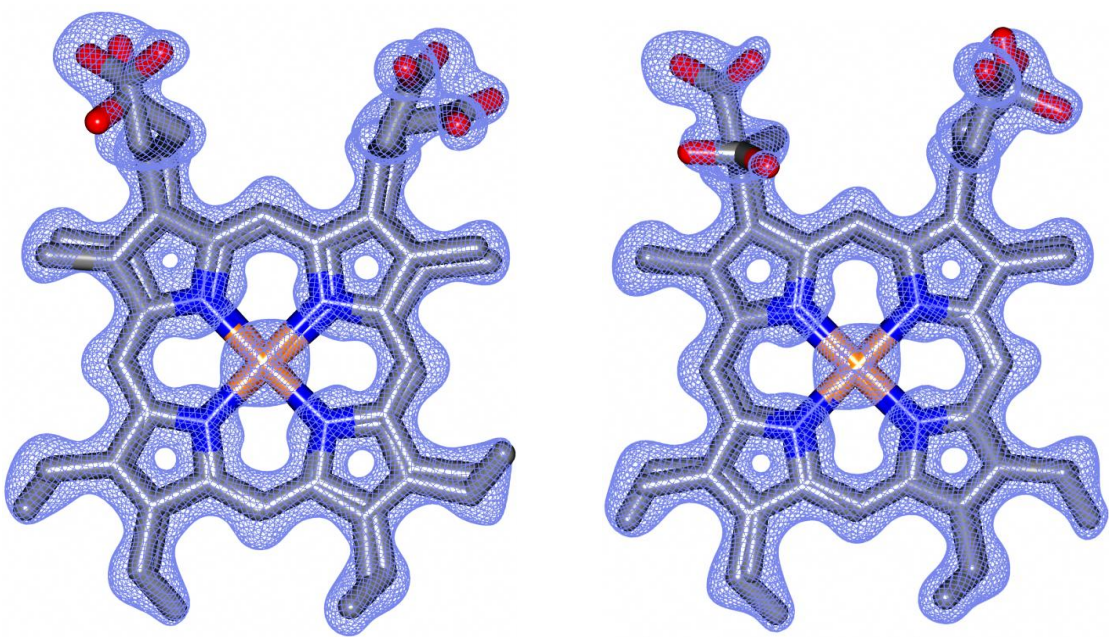

Supplemental Figure 3. 2Fo-Fc electron density map contoured at 1σ showing the two orientations of the heme molecules in Ncb5or-b5 associated with subunit A (left) and subunit B (right). These figures are adapted from Deng *et al*. [85].

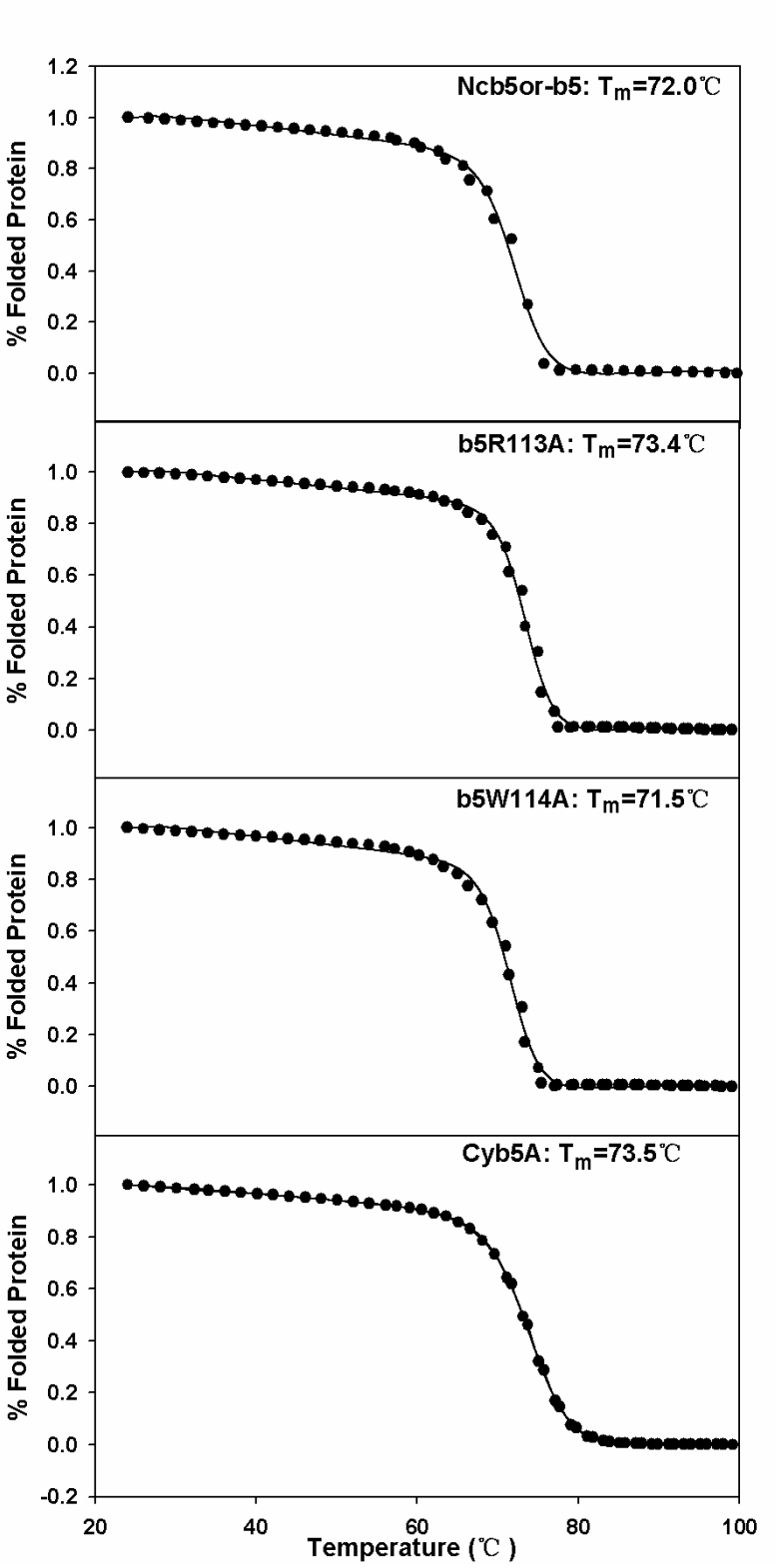

Supplemental Figure 4. Thermostability of wild-type Ncb5or-b5 and its two mutants, b5W114A and b5R113A. The percent of heme loss (Y axis) was monitored by the decrease in

A413 and plotted as a function of temperature. Thermal denaturation experiments were performed on a Varian Carey 100 Bio UV/Visible spectrophotometer equipped with a Peltier-thermostated multiple cell holder and a dedicated temperature probe accessory (± 0.1 °C). Solutions were buffered to pH 7.0 using 50 mM potassium phosphate. Experiments were performed in quartz cuvettes of 1 cm path length and 1 mL sample volume, equipped with tight-fitting PTFE lids. The temperature was increased in increments of 2 °C, and samples were equilibrated for 5 min after reaching each desired temperature. Thermal denaturation midpoints (T_m values) were obtained by fitting plots of absorbance at the Soret band λ_{max} (412 nm) vs. temperature to a previously described equation describing a two-state equilibrium (100). Tm (mid-point temperature) = 72.0 (Ncb5or-b5), 73.4 (Ncb5or-b5R113A), 71.5 (Ncb5or-b5W114A), 73.5 (human Cyb5A). This figure is adapted from Deng *et al*. [85].

A.

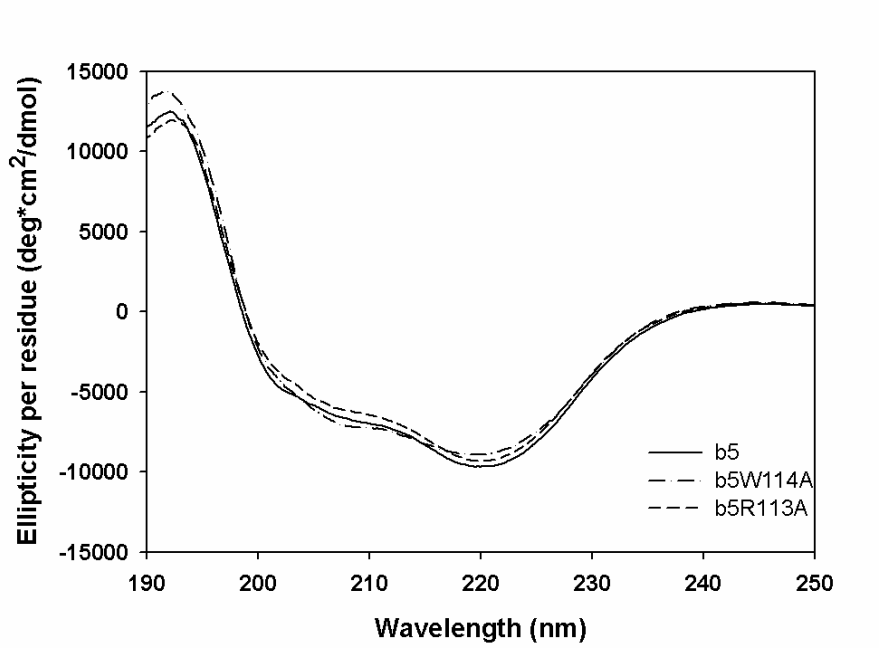

B.

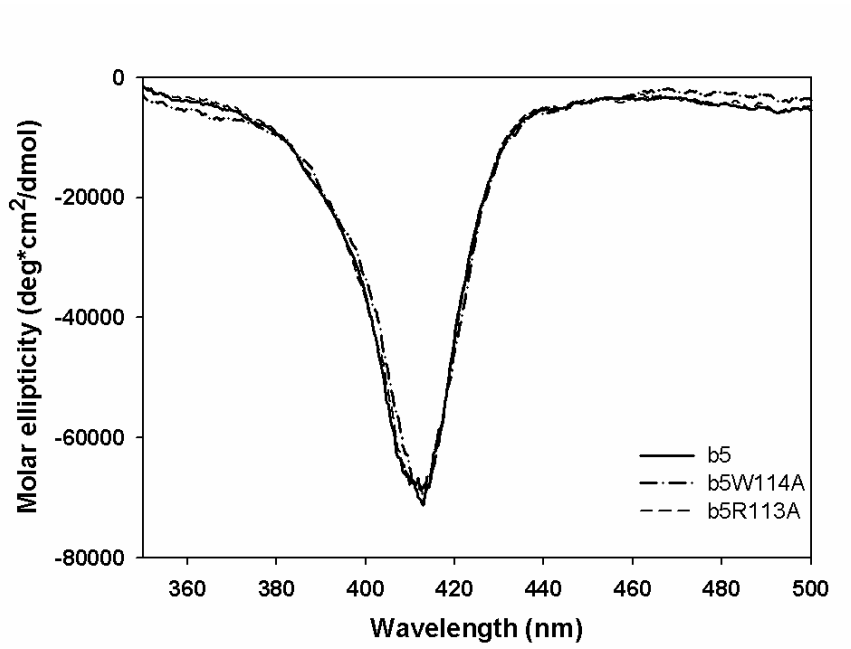

Supplemental Figure 5. Circular dichroism (CD) spectra of human Ncb5or-b5. (A) Far UV (190 – 250 nm) and (B) visible (350 – 500 nm) spectra of wild-type Ncb5or-b5 and its two mutants, b5W114A and b5R113A, monitored at a concentration of 17.4, 14.5, and 15.3 μM heme,

respectively. CD spectra were recorded on a JASCO-815 spectropolarimeter equipped with a Peltier thermostated cell holder (101). Solutions were buffered to pH 7.0 using 10 mM sodium phosphate. All spectra were obtained at 0.1 nm with a response time of 4 sec and a scan rate of 50 nm/min at room temperature. Final spectra represent the average of at least five scans. Background correction was accomplished by subtraction of a spectrum recorded at the same temperature and containing only buffer. Far-UV spectra are reported in terms of mean residue ellipticity ([θ], in $deg \cdot cm^2 \cdot dmol^{-1}$), calculated as $[\theta] = [\theta]_{obs}[MRW/(10lc)]$ where $[\theta]_{obs}$ is the ellipticity measured in millidegrees, MRW is the polypeptide mean residue molecular weight (molecular weight divided by the number of amino acids), c = sample concentration in mg/mL, and l = optical path length of the cell in cm. Near-UV and visible region spectra are reported in terms of molar ellipticity ([θ], in $deg \cdot cm^2 \cdot dmol^{-1}$), calculated as $[\theta]= [\theta]_{obs}[MW/(10lc)]$ where MW is the molecular weight of the polypeptide. These figures are adapted from Deng *et al*. [85].

Supplemental Table 1. Crystallographic data for human Ncb5or-b5 refined to 1.25Å resolution.

Data Collection	
Unit-cell parameters (Å, ^{o})	a = 38.48, b = 56.37, c = 42.56, β = 100.67
Space group	$P2_1$
Resolution (Å)[1]	30.0-1.25 (1.28-1.25)
Wavelength (Å)	1.0000
Temperature (K)	100
Observed reflections	185,062
Unique reflections	49,981
$<I/\sigma (I)>$[1]	13.0 (1.9)
Completeness (%)[1]	99.0 (93.6)
Redundancy[1]	3.8 (3.1)
R_{sym} (%)[1, 2]	5.8 (72.4)
Refinement	
Resolution (Å)	30.0-1.25
Reflections (working/test)	46,492 / 2,489
R_{factor} / R_{free} (%)[3]	14.7 / 17.3
No. of atoms (protein (A:B) / Heme / sulfate /water)	742:743 / 172 / 10 / 145
Model Quality	
R.m.s deviations	
Bond lengths (Å)	0.013
Bond angles (^{o})	1.477
Average B factor (Å^2)	
All Atoms	15.9
Protein (chain A/B)	15.2 / 15.3
Heme	11.0
Sulfate	27.7
Water	28.0
Coordinate error based on R_{free} (Å)	0.043
Ramachandran Plot (chain A/B)	
Most favored (%)	97.1
Additionally allowed (%)	2.9

1) Values in parenthesis are for the highest resolution shell.

2) $R_{sym} = \Sigma_{hkl}\Sigma_i |I_i(hkl) - <I(hkl)>| / \Sigma_{hkl}\Sigma_i I_i(hkl)$, where $I_i(hkl)$ is the intensity measured for the ith reflection and $<I(hkl)>$ is the average intensity of all reflections with indices hkl.

3) $R_{factor} = \Sigma_{hkl} ||F_{obs}(hkl)| - |F_{calc}(hkl)|| / \Sigma_{hkl} |F_{obs}(hkl)|$; Rfree is calculated in an identical manner using 5% of randomly selected reflections that were not included in the refinement.

This table is adapted from Deng *et al*. [85].

Supplemental Table 2. Summary of interplanar dihedral angles and EPR signals of Ncb5or and other members of the cytochrome b5 superfamily. Interplanar dihedral angles of bis-histidine ligands were calculated with Mercury (http://www.ccdc.cam.ac.uk/products/mercury/). N/A: not available. This table is adapted from Deng *et al*. [85].

Protein Name (source)	PDB #	g_{max} or g_z	Interplanar dihedral angles	Reference
Ncb5or (human)	3LF5	3.56	83.2° / 81.3° (His^{89},His^{112})	This study
Ncb5or (rat)	N/A	3.54	N/A	[70]
Cyb5A (human)	N/A	3.09	N/A	This study
Cyb5A (bovine)	1CYO	3.1	21.2° (His^{44},His^{68})	[17,99]
Cyb5A (rat)	N/A	3.05	N/A	[70]
Cyb5B (rat)	1B5M	3.03	11.9° (His^{42},His^{66})	[100,101]
Cytochrome b5 (M. domestica)	2IBJ	3.07	23.8° (His^{39},His^{63})	[102,103]
Cytochrome b5 (A. suum)	1X3X	N/A	46.1° (His^{38},His^{62})	[104]
Cytochrome b558 (E. vacuolata)	1CXY	N/A	43.9° (His^{42},His^{70})	[105]
Sulfite oxidase (chicken)	1SOX	2.93	9.6° (His^{40},His^{65})	[6,7]
Cytochrome b_2 (yeast)	1LTD	2.99	42.3° (His^{43},His^{66})	[106,107]
Nitrate reductase (spinach)	N/A	2.98	N/A	[12]

Supplemental Table 3. Kinetic properties of Cyb5A mutants tested for electrostatic interaction with Cyb5R3. Heme ligands are His^{44} and His^{68} in Cyb5A, corresponding to His^{89} and His^{112} in Ncb5or, respectively. [a]Both k_{cat} and K_M values are the ratio against that of wild-type Cyb5A. [b]N116 is displaced relative to D71 given the difference in local secondary structure, but it is the closest residue spatially and is pointed generally in the same direction. This table is adapted from Deng *et al*. [85].

Cyb5A	k_{cat} [a]	K_M [a]	Helix	Residue in Ncb5or	Ref.
E42A	1.0	1.2	α2	E87	[58]
E43A	1.0	3.1	α2	Y88	[58]
E48A	1.3	1.7	α3	E93	[57]
E49A	0.8	0.6	α3	D94	[57]
E48A/E49A	1.3	1.1	α3	-	[57]
E53A	1.2	1.2	α3	R98	[57]
E61A	1.3	1.4	α4	E106	[57]
E64A	1.0	1.0	α4	D109	[58]
D65A	1.0	1.5	α4	Q110	[57]
D71A	0.7	6.4	α5	N116 [b]	[58]
E74A	1.1	1.8	α5	S119	[58]
E48/E49/E53/E61/D65→A	0.9	1.4	α3,4	-	[57]
E42/E43/E48/E49/E53/D58/E61/E64/D65→A	0.9	6.1	α2,3,4	-	[57]

Chapter Three

Structural and Functional Elucidations of the N-terminal Region in Ncb5or Unveil a Novel Mechanism to Facilitate Inter-domain Electron Transfer

Abstract

NADH cytochrome b5 oxidoreductase (Ncb5or) is a redox enzyme involved in lipid metabolism and prevention of diabetes. Ncb5or contains a novel N-terminal region and three known domains: the b5 domain (Ncb5or-b5), the CS domain and the b5R domain (Ncb5or-b5R) that are homologous to microsomal cytochrome b5 (Cyb5A), heat shock protein 20 (HSP20/p23) and cytochrome b5 reductase (Cyb5R3), respectively. This unique structural arrangement makes Ncb5or a novel model to study inter-domain electron transfer. The weak physical interaction between the individual b5 and b5R domains of Ncb5or is insufficient to mediate inter-domain electron transfer, suggesting critical roles of other domain(s). The CS domain appears to assist specific recognition between the b5 and b5R domains but does not facilitate electron transfer. In this study, we investigate the structure of the N-terminal region and the roles of its specific residues in inter-domain electron transfer, by combining a reductionist approach of domain analyses, serial deletions and mutagenesis with biophysical and biochemical analyses. Our results suggest that the N-terminal region accelerates inter-domain electron transfer though cooperatively interacting with the CS and b5 domains, and that the region between Gly^{22} and Trp^{37} is critical for this function. The invariant Trp^{37} residue is situated in a highly conserved stretch of residues (LMDW). Mutation of Trp^{37} residue disrupts the formation of a tertiary structure that is essential for the function of the N-terminal region. Unlike single-domain structural homologues Cyb5A and Cyb5R3, Ncb5or employs a novel mechanism to facilitate inter-domain electron transfer.

Introduction

NADH cytochrome b5 oxidoreductase (Ncb5or) is found in all animal tissues. It is a natural fusion of a novel N-terminal region and three known domains, namely, b5 (Ncb5or-b5), CHORD and SGT1 (CS), and b5R (Ncb5or-b5R) [1,2]. Ncb5or-b5 and Ncb5or-b5R are homologous to microsomal cytochrome b5 (Cyb5A) and cytochrome b5 reductase (Cyb5R3), respectively, whereas the CS domain is a member of the p23 family [3]. HSP20 (p23) and SGT1 are two other members of the p23 family that function as a co-chaperone of HSP90 to facilitate protein folding and cellular regulation [23] and in innate immunity [24], respectively.

The role of the N-terminal region has remained mysterious since the identification of Ncb5or. This N-terminal region is composed of 50 residues, and the sequence does not have homology with any known proteins. Truncation of the first 34 residues in Ncb5or seems to have no impact on the intracellular localization, but accelerates auto-oxidation of the heme center [2].

The single-domain homologues of Ncb5or, Cyb5A and Cyb5R3, function as electron donors to stearoyl-CoA desaturase (SCD) in fatty acid desaturation, as shown by the reconstitution of fatty acid desaturation system *in vitro* [34]. However, mice with liver-specific or global deletion of Cyb5A are viable and fail to develop significant phenotype associated with lipid metabolism [35,45]. In contrast, mice with global deletion of Ncb5or exhibit diabetes, lipoatrophy and lipotoxicity [48,50,51,52,53], all of which may be associated with impaired SCD desaturation. Ncb5or is localized in the endoplasmic reticulum (ER), as are Cyb5A, CybR3, and SCD, consistent with a role of Ncb5or as an important electron donor in fatty acid desaturation. Characterization of the structural basis of inter-domain electron transfer in Ncb5or remains a key

to our understanding of its biochemical function *in vivo*.

We recently solved the crystal structure of Ncb5or-b5 at 1.25 Å resolution. Ncb5or-b5 has a b5 fold similar to that in Cyb5A with two helix-loop-helix motifs sandwiching the heme [85]. However, the heme environment of Ncb5or is unique among members of the b5 superfamily, namely, the two heme-ligating His side chains are perpendicular to each other [85]. This is a potential contributor to the lower redox potential of the heme center in Ncb5or (-108 mV vs. -9 mV in Cyb5A), which is another unique feature of Ncb5or [2,66,85].

The interaction between Ncb5or-b5 and Ncb5or-b5R is electrostatic in nature [55], but Ncb5or-b5 has fewer surface charged residues than does Cyb5A [85]. Kinetic analyses also reveal a much weaker affinity between the individual Ncb5or-b5 and Ncb5or-b5R domains than in the Cyb5A-Cyb5R3 complex [85]. These findings suggest important contributions from other domains, namely the CS domain and the N-terminal region, to inter-domain recognition and interaction in native Ncb5or to support its function as a redox enzyme.

We report here the role of the N-terminal region of Ncb5or in facilitating inter-domain electron transfer through structural and functional evaluations. Serial deletion of the N-terminal and mutagenesis reveal that residues from Gly^{22} to Trp^{37} are responsible for the formation of tertiary structure in the N-terminal region, which is essential for the acceleration effect in inter-domain electron transfer.

Method and Materials

Molecular Cloning and Site-directed Mutagenesis. The definition of each domain in human

Ncb5or has been described previously [85]. Further nomenclature use here includes Met^{1} through Lys^{137} as Nb5 (the N-terminal region plus Ncb5or-b5), Gly^{22} through Lys^{137} as Nb5G22, Met^{35} through Lys^{137} as Nb5M35, Lys^{51} through Lys^{137} as Ncb5or-b5, Lys^{260} through Ala^{521} as Ncb5or-b5R, and Gly^{164} through Ala^{521} as Ncb5or-CS/b5R (**Figure 1B**). The cDNAs of all constructs except Ncb5or-b5R, Ncb5or-CS/b5R, Ncb5or and D50Ncb5or were cloned into pET22b bacterial expression vector (Novagen) with no histidine or epitope tag. The cDNAs of Ncb5or, D50Ncb5or, Ncb5or-b5R and Ncb5or-CS/b5R were cloned into pET19b vector with six-His tag at the N terminus as previously described [85]. Site-directed mutagenesis was performed to generate missense mutants, Nb5W37A, Nb5LMAA (double mutations of Leu34 and Met35 to Ala residues), and Ncb5orW114A, with the QuikChange mutagenesis kit (Strategene, La Jolla, CA) using wild-type Nb5 and Ncb5or as the templates. All primers for mutagenesis were synthesized by Integrated DNA Technology (Coralville, IA). Primer sequences are available upon request. All constructs are subjected to DNA sequencing to confirm the desired sequences.

Protein preparation. Soluble protein for each construct was expressed in *E.coli* BL21(DE3), similar to that previously described [85]. Purification of Ncb5or-b5 and Nb5M35 is identical to that previously described [85]. Preparation of Nb5 (mutants), and Nb5G22 are similar to that of Ncb5or-b5, whereas a SP HP column was used for purification of Nb5 and Nb5G22 instead of the Q HP column previously used for b5. Preparation of Ncb5or-b5R and Ncb5or-CS/b5R was described previously [85]. Expression of Ncb5or, D50Ncb5or and Ncb5orW114A (the same method was used for these three proteins) was similar to previously described [2] except that 0.5

mM IPTG was added to TB media for induction at 15 ^{o}C. All the following steps of protein purification were performed at 4 ^{o}C or on ice. Cell pellet was resuspended in lysis buffer (50 mM Tris-HCl, pH 8, 300 mM NaCl and 10 mM imidazole) supplemented with tablet protease inhibitor cocktail (Sigma, EDTA free) and 1 mM PMSF , and cells were broken by French press under 1000 psi twice. The supernatant was separated by centrifugation under 15000 g for 45 min, and was supplemented with hemin to constitute holo-protein as described in the preparation of Ncb5or-b5 [85]. The excessive hemin was removed by centrifugation under 20000 g for 2 h, and the supernatant was collected and run through columns following the order of Ni affinity and ionic exchange at a rate of 1 ml/min. 4 ml of Ni-NTA beads (QIAGEN) was used in Ni affinity column connected with a constant pump, and the supernatant was loaded. The beads were washed with 20 column volumes of lysis buffer containing 20 mM imidazole. This resulted in the A_{280} of the flow through being reduced below 0.1. Protein was eluted with 200 mM imidazole, and oranges fractions were pooled and dialyzed against 10 mM Tris-HCl (pH 8) 50 mM NaCl and 0.1 mM EDTA overnight. Dialyzed sample was diluted 5 fold in 10 mM Tris-HCl (pH 8), and loaded on to a 4 ml Q-Sepharose resin. Bound protein was washed with 2 column volumes of 10 mM Tris-HCl (pH 8), and then eluted sequentially with batches of 50, 100, 150, 200 and 250 mM NaCl (all buffered with 10 mM Tris-HCl, pH 8). Fractions with orange color (i.e. absorbance at 413 nm) were pooled. All proteins were concentrated, aliquoted, flash frozen, and stored in -80 ^{o}C until use. SDS-PAGE was used to estimate the purity of each protein. Usually the ratio of A_{413}/A_{280} for purified protein is ≥4 for Ncb5or-b5, ≥3.6 for Nb5, 1 for Ncb5or and 1.1 for D50Ncb5or. The FAD contents of Ncb5or-b5R and Ncb5or-CS/b5R were determined by A_{461} and

used to represent enzyme concentrations. Final yields of purified protein were 8 mg/L for Ncb5or-b5, 5 mg/L for Nb5, 2 mg/L for Ncb5or-b5R, 1 mg/L for Ncb5or-CS/b5R, ≤1 mg/L for Ncb5or and ≤1 mg/L for D50Ncb5or. The solubility is Nb5 > Ncb5or-b5 > Ncb5or > D50Ncb5or > Ncb5or-CS/b5R > Ncb5or-b5R. Ncb5or and D50Ncb5or are vulnerable to non-specific proteolytic cleavage at the border of b5 and CS domains. This can be avoided by including protease inhibitor in all buffers during preparation. Proteins used for spectral analyses are greater than 95% pure (**Supplemental Figure 1**). All polypeptide products have the expected molecular weights by mass spectrometry as detected in the previous study [85] or here (**Supplemental Figure 2**).

Spectroscopy. UV/visible spectra were obtained on Cary 50 Bio or Cary 100 Bio spectrophotometer (Varian). The concentrations of heme and FAD were determined as previously described by the following ε values ($mM^{-1}cm^{-1}$): 130 (413 nm) of oxidized heme for Ncb5or-b5, Nb5/mutants, Nb5G22, Nb5M35, Ncb5or/mutants and D50Ncb5or [2], and 10.5 (461 nm) of FAD for Ncb5or-b5R and Ncb5or-CS/b5R [70].

Circular dichroism (CD) methodology has previously been described [85,102]. The measurement was performed by JASCO-815 spectropolarimeter. Protein concentrations for CD analysis were 8 to 10 μM for Ncb5or-b5 and Nb5/mutants.

Far-UV (190 nm to 250 nm) spectra were reported in terms of ellipticity per residue ([θ], in $deg \cdot cm^2 \cdot dmol^{-1}$), and 1 mm cuvette was used. In near-UV (250 nm to 350 nm) and visible CD (350 nm to 550 nm), 1 cm cuvette was used to hold the sample. The concentrations were 4 μM for Ncb5or, 7 μM for D50Ncb5or, and 8 to 10 μM for Ncb5or-b5 and Nb5/mutants. Near-UV and

visible spectra were reported in terms of molar ellipticity ([θ], in $deg \cdot cm^2 \cdot dmol^{-1}$).

Inter-domain electron transfer between individual domains. The rate of inter-domain electron transfer between individual domains was measured as the initial rate of heme reduction under anaerobic condition as previously described [2,85]. Each assay of single-point kinetics was under excessive NADH (50 μM) in low-salt buffer (5 mM sodium phosphate, pH 7.0) with 1.4 μM Ncb5or-b5 or Nb5/mutants as the substrate and an appropriate amount of Ncb5or-b5R or Ncb5or-CS/b5R as the reductase. To determine Michaelis-Menten parameters, substrate (1.4 μM – 100 μM Ncb5or-b5 or Nb5) was reduced by an appropriate amount of enzyme (Ncb5or-b5R or Ncb5or-CS/b5R) in the presence of excess (100 μM) NADH. Initial rate (V_0) as a function of substrate concentration [S] was fit into the Michaelis-Menten equation to estimate K_m and V_{max} as previously described [85].

Stop-flow kinetics. Inter-domain electron transfer in full-length Ncb5or and variants (D50Ncb5or and Ncb5orW114A) was determined using stop-flow kinetics as previously described [108]. Briefly, 3 μM protein (Ncb5or, D50Ncb5or or Ncb5orW114A) was mixed with 200 μM NADH on BioLogic SFM 400 stop-flow reactor coupled to a MOS 250 spectrophotometer at a rate of 5.5 ml/min in a total volume of 150 μl (5 mM phosphate, pH 7.0, room temperature). Increase in A_{424} was recorded and the data were averaged from 10 individual runs. Approximately 50-60% of heme was reduced within the dead time (1.3 ms). Concentration of reduced heme was calculated with ε_{424} = 120 $mM^{-1}cm^{-1}$. Percentage of reduced heme among total vs. time was fit to the equation:

$$\% \text{ reduction} = y_0 + A_1 * \exp(-k_1 * t) + A_2 * \exp(-k_2 * t)$$

Rate constants (s^{-1}) of fast phase (k_1) and slow phase (k_2) were solved. All stop-flow kinetic runs were carried out under aerobic conditions, because the currently available apparatus deactivated the b5R and CS/b5R construct during the removal of oxygen. Reduction of heme in Ncb5or (>2 nmol/s $\approx 10^{15}$ s^{-1}) appears much faster than auto-oxidation of heme (k_{cat}= 1 s^{-1}) [2], therefore we concluded that existence of air does not affect the reactions, especially the fast phase.

^{1}H nuclear magnetic resonance (NMR). NMR spectra were recorded for Ncb5or-b5 (778 μM heme) and Nb5 (719 μM) in 100 mM phosphate with 10% D_2O at 25 °C on a 500 MHz Bruker DRX spectrometer equipped TXI probe with tri-axis gradients. RF pre-saturation was used to suppress the water signal.

Results

Novel features of the N-terminal region. We define the N-terminal region of Ncb5or as Met^1 through Leu^{50}. No proteins homologous to the N-terminal region can be found in the current database of non-redundant protein sequences by BLAST searches. Visual inspection of sequences of Ncb5or entries (**Figure 1A**) revealed the following features of the N-terminal region: (a) the first 21 residues are variable among Ncb5or from all animals, in contrast to well conserved sequences in the rest of the N-terminal region; (b) a well conserved core ($L^{34}MDW^{37}$) exists within a long stretch rich in Arg and Lys residues and thus with a high isoelectric point (pI). It is worth noting that Trp^{37} residue is invariant in all Ncb5or orthologs.

These distinctive features in the primary structure of the N-terminal region reflect its special structural and functional properties that are characterized below through a series of biophysical

studies. Electron transfer assays with mixtures of various domains were performed to identify the role of the N-terminal region, whereas stop-flow kinetics was used for full-length Ncb5or with or without the N-terminal region. CD analyses were used to detect the presence of secondary structure (far-UV signals) and tertiary structure (near-UV signals from aromatic residues) of the N-terminal region. The impact of N-terminal region on the heme center was investigated by CD (Soret signals) and NMR spectral analyses.

The N-terminal region facilitates inter-domain electron transfer. Serendipitously, we discovered the role of the N-terminal region in facilitating inter-domain electron transfer. When purified in the absence of protease inhibitor, Ncb5or is vulnerable to non-specific proteolytic cleavage at the border of the b5 and CS domains, which results in two fragments. The small fragment is generally equivalent to Nb5 (the N-terminal region + Ncb5or-b5). The big fragment is generally equivalent to Ncb5or-CS/b5R. In experiments with samples containing these fragments, we observed nearly 100% reduction of the b5 fragment following addition of NADH in the presence of air. In contrast, less than 50% reduction is observed in analogous experiments performed with Ncb5or-b5 and Ncb5or-b5R. This suggested a major function for the N-terminal region in inter-domain electron transfer (data not shown).

In order to determine the rate of inter-domain electron transfer, we performed Michaelis-Menten kinetics for various combinations of substrate and enzyme (**Figure 1B, 2** and **Table 1**): Ncb5or-b5 + Ncb5or-b5R, Nb5 + Ncb5or-b5R (Nb5: the N-terminal region+Ncb5or-b5), Ncb5or-b5 + Ncb5or-CS/b5R (Ncb5or-CS/b5R: the CS domain+Ncb5or-b5R) and Nb5 + Ncb5or-CS/b5R. In each combination, the construct containing

the b5 domain (Ncb5or-b5 or Nb5) was an electron acceptor, and thus was considered as a substrate. The electron donor (Ncb5or-b5R or Ncb5or-CS/b5R) was considered as an enzyme or reductase. Comparisons among these four cases (with or without the N-terminal region; with or without the CS domain) enabled us to identify effects of the N-terminal region and of the CS domain in inter-domain electron transfer. All of the assays in the study, except stop-flow kinetics, were done under anaerobic conditions to exclude complications from auto-oxidation of heme. In our recent study, we observed little or no complex formation in studies with Ncb5or-b5 and Ncb5or-b5R (**Figure 2A**), as indicated by the linear relation between the substrate concentration [S] and initial rate (V_0). In contrast, replacing Ncb5or-b5 with Nb5 (**Figure 2B**) resulted in a lower K_m (higher affinity), as indicated by the curvature in the V_0-[S] plot. Similar findings were observed for the interaction with Ncb5or-CS/b5R **(Figure 2C, D**, respectively), suggesting that the N-terminal region facilitates the interaction between the b5 and b5R domains.

Our previous study suggested that the CS domain facilitated the recognition between Ncb5or-b5 and Ncb5or-b5R, but slowed down inter-domain electron transfer for unknown reasons [85]. In comparison to the Ncb5or-b5 + Ncb5or-b5R pair, the addition of the CS domain, i.e. the replacement of Ncb5or-b5R by Ncb5or-CS/b5R, decreased the rate of electron transfer (k_{cat}/K_m) by 5-fold. Similarly, the addition of the N-terminal region, i.e. the replacement of Ncb5or-b5 by Nb5, increased the rate of electron transfer (k_{cat}/K_m) by 3-fold **(Table 1**). Additions of both the N-terminal region and the CS domain (in the case of Nb5 + Ncb5or-CS/b5R) resulted in a 7-fold increase in the rate of electron transfer (k_{cat}/K_m) compared to that of the Ncb5or-b5 + Ncb5or-b5R pair and more than a 30-fold increase compared to Ncb5or-b5 + Ncb5or-CS/b5R

A.

```
                          * ** ** * ********** ** ** **
MLNVPSQSFPAPRSQQRVASG     GRSKVPLKQGRSLMDWIRLTK SGKDLTGL human
MLNVPSQAFPAPGSQQRVSSQ     GRSKVPLKQGRSLMDWIRLTK SGKDLTGL mouse
MLNVPSQAFPAPGSQQRVASQ     GRSKVPLKQGRSLMDWFRLTK SGKDFTGL rat
MLNVPSQSFPGPSSQQRVASG     GRSKVPLKQGRSLMDWIRLTK SGKDLTGL cow
MLNVPPQAFPAPGSQQRVAAG     GRTKVPLKPGRSLMDWIRLTK SGKDLTGL chicken
MLNVPSQSFPAPSSQQRVAAI     GRSKVPLKPGRSLMDWIRLTK SGKDLTGL Xenopus
MLNVPAQSFPASGSQQRVASSGA   GRNKVVLKPGHSLMDWIRFAK SGKDLTGL rice fish
MLNIPTQSFPSPSSQQRVSPSGQS GRSKVALKPGHSLMDWIRFSK SGKDLTGL Zebrafish
MLNVPSQAFPAAGSQQRVAPAGQS  RSKVVLKPGHSLLDWIRLTK SGQDLTGL Zebrafish.Singapore
   MSKELFPAANSAQRLGVPAPVLNTTKVPLQRGRSLMDWIRLSK SNVDLRGT tunicate
LQLPVTAPQKLNSNGSSASGSATGNPRNKCALKPGYSLMNWIRLCN SGADLSGT Drosophila
MNSPQRAGGSSSLSVPSGSS       SRIKAALKPGRSLMDWVRLGKQQGKKLNGV sea urchin
SVNGSSNGLFAKPTIG RSEY     GRVKVALAPGKGFMDWLRLT  TNKHLAKR C.elegans
 MLLNLPTLTAKPPIG RSEY     GRVKVALLPGKGLMDWVRLA  SGKVLA K Teladorsagia
```

B.

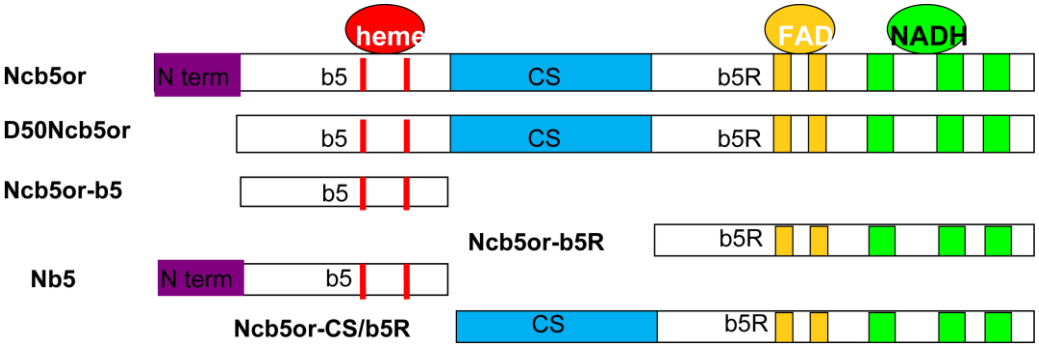

C.

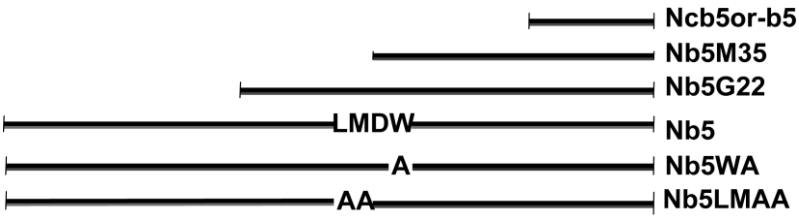

Figure 1. (A) Sequence alignment of the N-terminal region of Ncb5or from human to worms. (B) Ncb5or constructs with various combination of individual domains that are used in the current study. Ncb5or and D50Ncb5or are subjected to stop-flow analyses to identify the N-terminal role in the context of the full-length protein (see Figure 3). Other constructs allow analyses to identify the N-terminal role in the context of the separate domains (see Figure 2). (C) Serial deletions of the N-terminal region and point mutations of conserved residues in the hydrophobic core.

(Table 1). Therefore, the Nb5 and Ncb5or-CS/b5R combination results in the highest catalytic efficiency (affinity and rate) among all four combinations.

Instead of slowing down electron transfer to Ncb5or-b5, the addition of the CS domain greatly accelerates inter-domain electron transfer in the presence of the N-terminal region. These data suggest that the N-terminal region facilitates electron transfer from Ncb5or-b5R to Ncb5or-b5 through cooperative interaction with the CS domain. The maximum substrate concentration that could be used in the kinetic experiments was 100 μM, as higher concentrations generated readings beyond the linear response of the spectrophotometer. Even at this relatively high concentration, the initial rate (V_0) does not approach a maximum. The K_m and k_{cat} (**Table 1**) can therefore only be considered as estimates. The estimated k_{cat}/K_m values are relatively more accurate since they only require the early phase in the V_0 vs. [S] plot. Initial rates at single substrate concentrations show a similar trend of change as observed in k_{cat}/K_m measurements (**Table 1**) and therefore were used in the assays of Nb5 mutants described below.

So far, we investigated the role of the N-terminal region with mixtures of separated domains. Now we investigate its role in full-length Ncb5or by stop-flow kinetics. In wild-type Ncb5or, two phases, fast phase and slow phase were observed. Within the dead time of 1.3 ms, 50%-60% of heme was reduced. Data from all forms of Ncb5or can be fit by the equation (see Method and Materials) to solve rate constants for the fast phase ((k_1) and the slow phase (k_2). Compared to wild-type Ncb5or, truncation of the N-terminal region (to give D50Ncb5or) caused a 2.5-fold drop in the fast-phase rate constant (k_1) (**Figure 3A** and **Table 2**), in agreement with the result of assays using the individual domains in **Table 1**. This supports a critical role of the N-terminal

region in inter-domain electron transfer. In the Nb5 + Ncb5or-CS/b5R pair (**Table 1**), in which the linkage between the b5 domain and the CS domain is disrupted, removal of the N-terminal region (i.e., Ncb5or-b5 + Ncb5or-CS/b5R) caused a 30-fold decrease of rate constant. In contrast, truncation of the N-terminal region from Ncb5or, in which the linkage between the b5 domain and the CS domain is intact, caused only a 2.5-fold drop in the rate constant (**Table 2**). This suggests a significant contribution of the b5-CS linkage to the inter-domain electron transfer.

Trp^{114} is an invariant surface residue in Ncb5or-b5. It was shown that the W114A mutation caused a 2-fold decrease in the rate constant for electron transfer [85] when a mixture of seperated domains was used. In the case of full-length Ncb5or, however, the W114A mutation only led to a 1.2-fold drop in the rate constant of the fast phase (**Figure 3B** and **Table 2**), suggesting that Trp^{114} does not contribute significantly to the inter-domain electron transfer.

Structural elucidation of the N-terminal region. Next, we explore the structural feature of the N-terminal region since it is functionally important in electron transfer. On the basis of the Ncb5or amino acid sequence (**Figure 1A**), the N-terminal region was predicted to be disordered by PONDR VL-XT [59,60,61]. However, the highly conserved $L^{34}MDW^{37}$ sequence was predicted to potentially form a helix by PROF [109,110].

Far-UV CD spectra show that Ncb5or-b5 contains a mixture of helices and sheets, consistent with five helices and the five-strand β-sheet in the crystal structure of Ncb5or-b5 obtained previously [85] (**Figure 4A**). The presence of the N-terminal region (Nb5) enhances the negative ellipticity in the vicinity of 200 nm, suggesting that the N-terminal region is rich in random coils.

A.

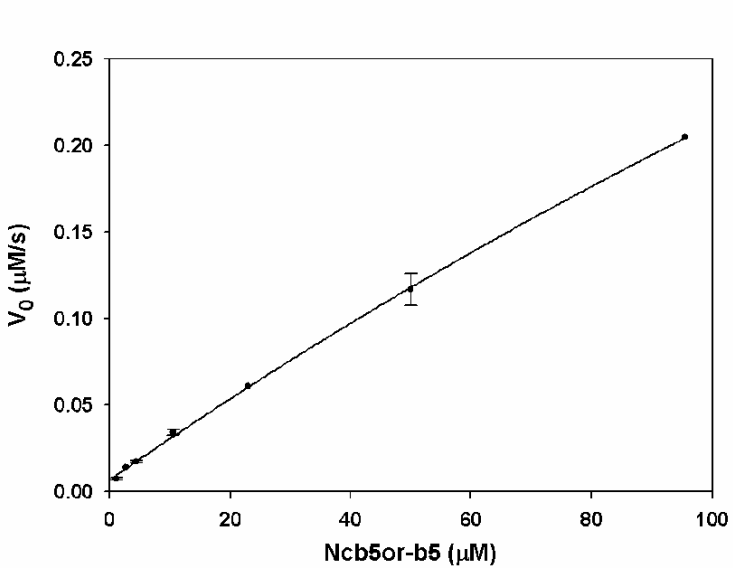
0.25
0.20
0.15
0.10
0.05
0.00
V_0 (μM/s)
0
20
40
60
80
100
Ncb5or-b5 (μM)

B.

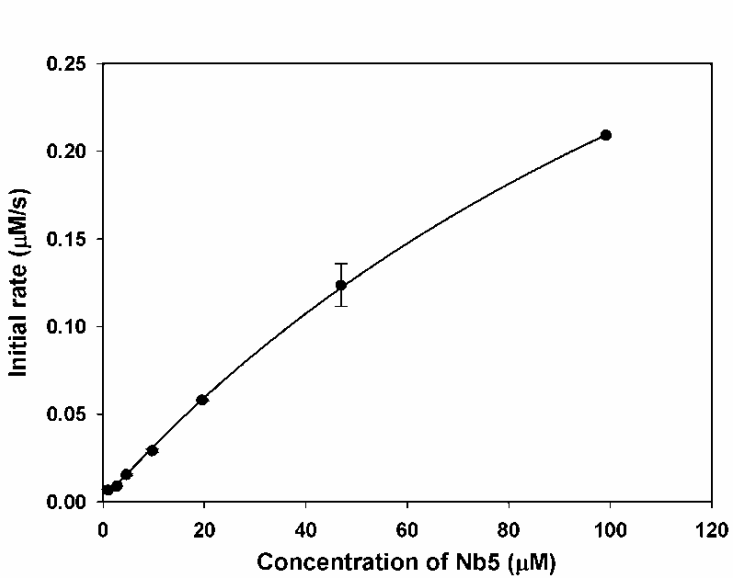
0.25
0.20
0.15
0.10
0.05
0.00
Initial rate (μM/s)
0
20
40
60
80
100
120
Concentration of Nb5 (μM)

C.

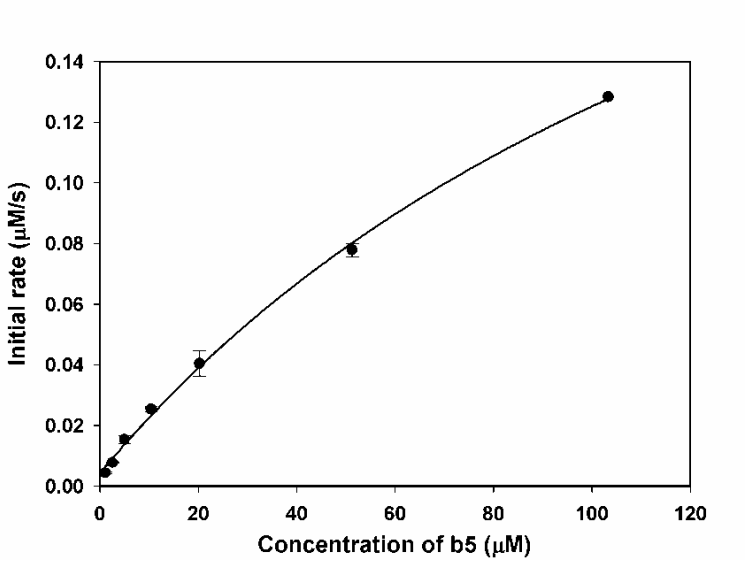

D.

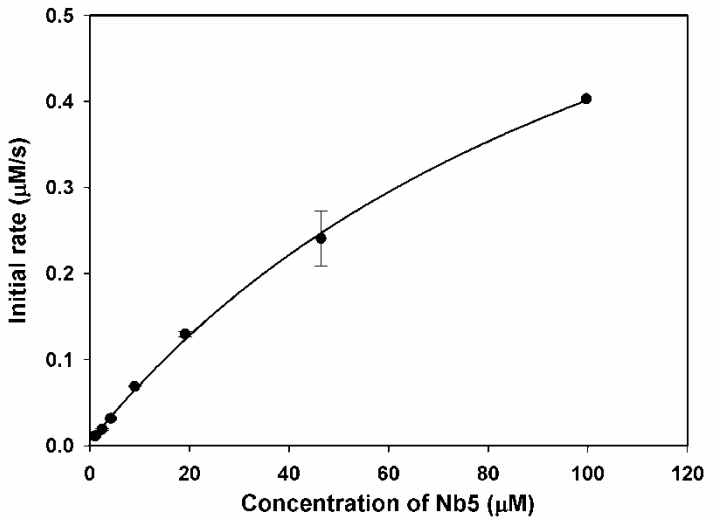

Figure 2. Electron transfer from Ncb5or-b5R to Ncb5or-b5 (A), Ncb5or-b5R to Nb5 (B), Ncb5or-CS/b5R to Ncb5or-b5 (C), and Ncb5or-CS/b5R to Nb5 (D). Data in (A) were published previously (109). The Michaelis-Menten parameters are shown in **Table 1**.

Table 1. Initial rate and Michaelis-Menten kinetic parameters of electron transfer in various heme and reductase combinations. Amount of reductase used: 140 nM Ncb5or-b5R for Ncb5or-b5; 56 nM Ncb5or-b5R for Nb5; 500 nM Ncb5or-CS/b5R for Ncb5or-b5; 56 nM Ncb5or-CS/b5R for Nb5. Initial rate was normalized by the concentration of reductase. ± standard error.

Substrate/Enzyme	Initial rate (μM/min/μM)	K_m (μM)	k_{cat} (s^{-1})	k_{cat}/K_m ($\mu M^{-1}s^{-1}$)
Ncb5or-b5/ Ncb5or-b5R	3.65±0.16	498±129	8.8±1.9	0.018
Nb5/Ncb5or-b5R	7.06±0.23	182±19	10.5±0.7	0.058
Ncb5or-b5/Ncb5or-CS/b5R	0.69±0.06	166±35	0.6±0.1	0.0039
Nb5/Ncb5or-CS/b5R	12.02±0.31	123±16	15.8±1.2	0.13

The difference spectrum representing the N-terminal region, (Nb5 minus Ncb5or-b5), shows a strong negative absorbance around 200 nm, confirming that the N-terminal region is generally disordered. However, the absorbance at both 190 and 220 nm, which represents helix signals [111], suggests that part of the N-terminal region is structured. Therefore the N-terminal region is a mixture of random coils and helix. An interesting possibility is that the structure in this region of the polypeptide arises as a consequence of cooperative interactions with the b5 core.

Side chains of aromatic residues that are located in highly asymmetric (i.e. well-structured) regions of proteins can give signals in both far-UV and near-UV CD spectra. Near-UV CD spectra are particularly useful for identifying the type of side chain giving rise to particular signals. For example, Trp side chains in well-structured regions of proteins typically have signals centered near 290 nm [111]. Nb5 contains three invariant Trp residues: one in the N-terminal region (Trp^{37}) and two in Ncb5or-b5 (Trp^{72} and Trp^{114}). The spectrum of Ncb5or-b5 in **Figure 4B** reveals only weak signals in the vicinity of 290 nm, suggesting that the Trp^{72} and Trp^{114} side chains are not in highly asymmetric environments. Indeed, both side chains are located at the protein surface in contact with the solvent [85]. In contrast, Nb5 exhibits a broad absorbance band with a peak close to 290 nm, suggesting Trp^{37} in the N-terminal region is likely the source of this signal.

This is confirmed by the loss of the Trp signal in Nb5W37A mutant (**Figure 6C**). The signal of Trp residue indicates that it is situated in a well packed environment. In this context, it is worth noting that a signal with positive ellipticity is observed near 230 nm in the far-UV difference CD spectrum of the N-terminal region.

A.

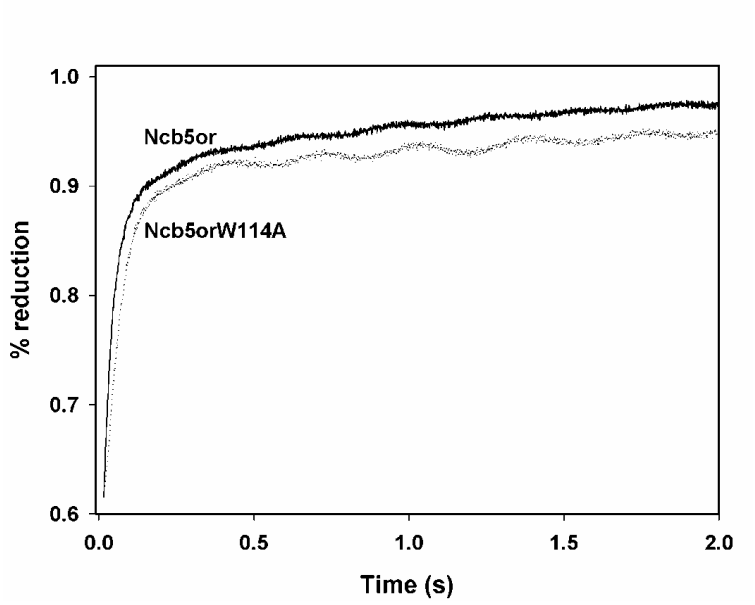

B.

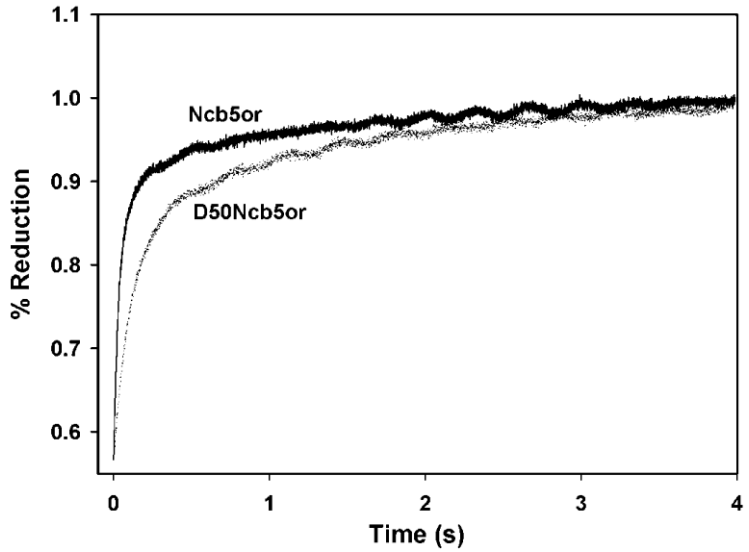

Figure 3. Stop-flow kinetics of inter-domain electron transfer in Ncb5or, Ncb5orW114A and D50Ncb5or. The *y* axle represents the percentage of heme reduction, which is an indicator of inter-domain electron transfer. The curves can be fit into double-exponential equation as described in Method and Materials.

Table 2. Rate constants of electron transfer by stop-flow kinetics. Final concentration of 1.5 μM of each protein was used for the assay. Data were obtained from 10 independent reactions for each run, and the average was fit into double-exponential equation to solve rate constants for fast phase (k_1) and slow phase (k_2). ± stands for standard error.

	k_1 (s^{-1})	k_2 (s^{-1})
Ncb5or	20.94±0.11	0.77±0.01
W114A	16.61±0.06	0.31±0.00
D50Ncb5or	8.71±0.05	0.74±0.01

Impact of the N-terminal region on the heme center. CD spectra in the Soret region have been used to investigate heme environment in heme-containing proteins [112]. As shown by CD spectra (**Figure 4B**), addition of the N-terminal region to the b5 domain alters the CD Soret band spectrum, suggestive of an altered heme environment.

Further evidence that the presence of the N-terminal domain affects the heme environment was obtained in a comparison of NMR spectra of Ncb5or-b5 and Nb5 (**Figure 5**). In comparison to Ncb5or-b5, Nb5 shows shift of peaks in the far downfield region (27 to 10 ppm) and far upfield region (0 to -6 ppm), both of which represent signals of heme protons. This is consistent with a change in the heme environment elicited by the addition of the N-terminal region through Soret CD spectra (**Figure 4B**). It is unlikely that the orientation of the two heme-ligating His residues is altered, because it is mainly determined by the backbone of Ncb5or-b5 domain.

Critical residues in the N-terminal region. Next, an attempt was made to identify the parts/residues in the N-terminal region that are essential for inter-domain electron transfer, by serial truncation of Nb5 at the N-terminal region (**Figure 1C**).

We performed kinetic assays by mixing separated domains under anaerobic condition. When Ncb5or-CS/b5R is the reductase, truncation of the N-terminal 21 residues prior to Gly^{22} (Nb5G22) results in the same (fast) rate of electron transfer that is observed when using Nb5. However, subsequent deletion of Gly^{22}-Leu^{34} (Nb5M35) decreases the rate by 20-fold. In fact, the rate for reduction of Nb5M35 is virtually the same as that caused by Ncb5or-b5 (**Table 3**). This suggests that residues from Gly^{22} to Leu^{34} are essential for the function of the N-terminal region in facilitating electron transfer.

A.

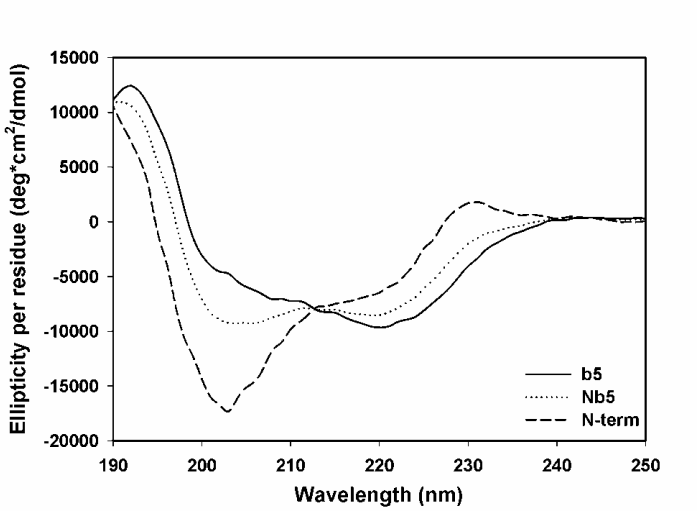

B.

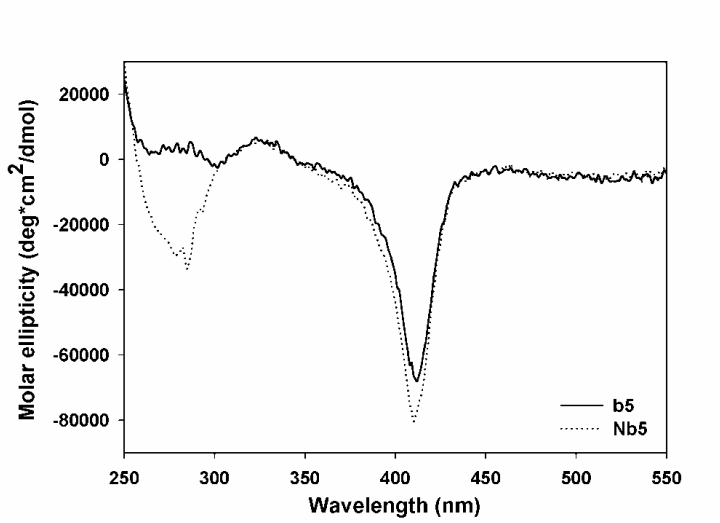

Figure 4. (A) Far UV CD spectra of Nb5, Ncb5or-b5, and the N-terminal region. The spectrum of the N-terminal region was obtained by subtracting spectra of Ncb5or-b5 from Nb5 (both in units of molar ellipticity) and then dividing by the residue number to convert the spectrum to units of mean residue ellipticity (B) Near UV and visible CD spectra of Nb5 and Ncb5or-b5. Nb5 and Ncb5or-b5 (b5) were scanned in near UV region (250 to 350 nm) to detect the environment of aromatic residue, and in the Soret region (around 413 nm) to detect the environment of heme.

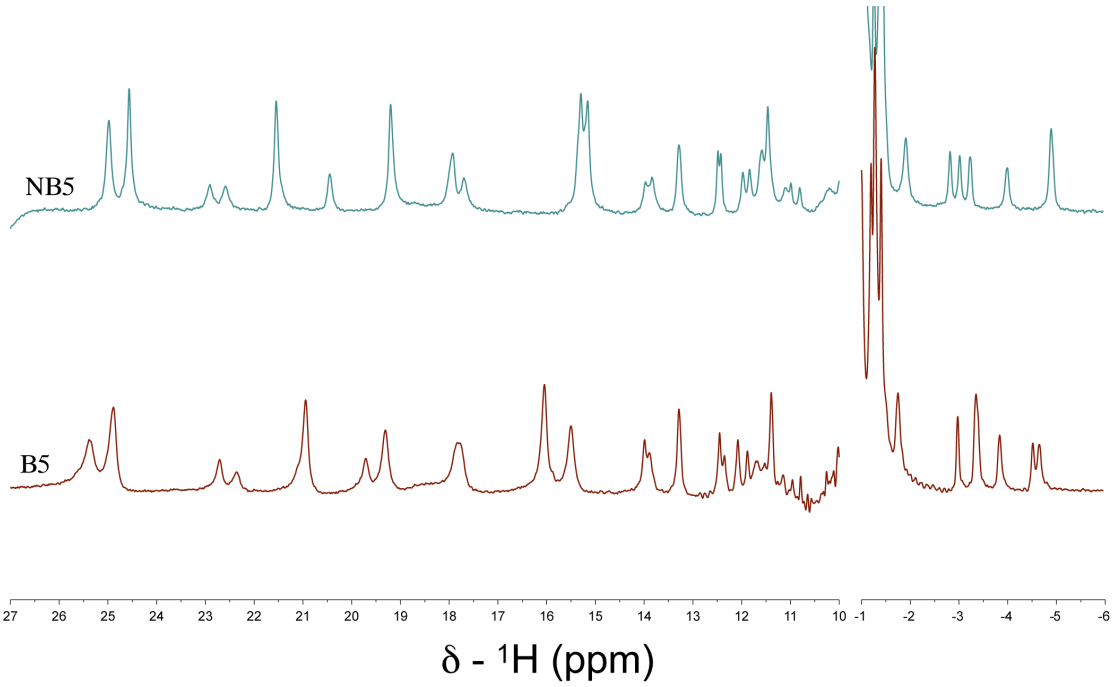

Figure 5. ^{1}H NMR spectra of Nb5 and Ncb5or-b5. Far downfield region (27 to 10 ppm) and far upfield region (0 to -6 ppm), which are associated with heme protons, were shown here. Nb5 (NB5) and Ncb5or-b5 (B5) have different heme proton signals. Dr. Justin Douglas (Department of Chemistry, KU) collected the data and prepared this figure.

A similar but smaller effect was observed for residues Gly^{22} - Leu^{34}, when Ncb5or-b5R was the reductase (**Table 3**). Deletion of residues Gly^{22} - Leu^{34} only resulted in a 3-fold decrease in the rate of electron transfer. The larger effect of residues Gly^{22} - Leu^{34} by Ncb5or-CS/b5R as the reductase than Ncb5or-b5R as the reductase is consistent with the highest efficiency of electron transfer in Nb5 + Ncb5or-CS/b5R (**Table 1**). This evidence suggests that this essential region of the N terminus facilitates inter-domain electron transfer through cooperating with the CS domain.

The near-UV and Soret CD spectra of Nb5G22 are nearly identical to those of Nb5 (**Figure 6A**), suggesting that residues from Met^{1} to Gly^{21} neither contribute to the tertiary structure involving the N-terminal domain, nor exert an impact on the heme center. The kinetic assays described above also showed that these residues do not play a role in inter-domain electron transfer (**Table 3**).

Deletion of downstream residues from Gly^{22} to Leu^{34} in the Nb5M35 mutant altered the signal near 290 nm and the CD Soret signal. The Soret signal of this mutant is identical to that of Ncb5or-b5, indicating that its heme center is identical. This suggests that residues Gly^{22}-Leu^{34} contribute to the complete formation of the tertiary structure, and that they also cooperatively interact with the heme or with residues near the heme. Furthermore formation of the tertiary structure may be correlated to the impact on the heme center. Residues Gly^{22}-Leu^{34} have been shown to play an essential role in inter-domain electron transfer (**Table 3**). Hereby we speculate that the formation of the tertiary structure and the association between the N-terminal region and Ncb5or-b5 contribute to inter-domain electron transfer.

We further tested whether Trp^{37} is responsible for the near-UV CD signal near 290 nm

(**Figure 4B**), and the presence of secondary structure in the N-terminal region (**Figure 4A**). We confirmed that the W37A mutation not only caused the disappearance of the near-UV signal (290-nm peak) in this mutant (**Figure 6C**) but also caused the disappearance of the helix signal at 190 and 220 nm (**Figure 6B**). In addition, the CD signal of Nb5W37A in the Soret region (**Figure 6C**) is identical to that of Ncb5or-b5 (**Figure 6A**), suggesting that the mutant N-terminal region cannot cooperatively interact with the heme center once the N-terminal structure is disrupted.

In parallel, we observed that, with Ncb5or-CS/b5R as the reductase, the W37A mutation caused a 90% decrease in the rate of electron transfer (**Table 3**). These findings suggest that Trp^{37} governs the formation of tertiary structure in the N-terminal region, and the N terminal tertiary fold is essential for its cooperative interaction with the heme center and its acceleration in inter-domain electron transfer.

We also tested the role of two neighboring residues of Trp^{37} in the LMDW sequence by changing both Leu^{34} and Met^{35} to alanine (LMAA). We observed a subtle change in secondary structure but no change in the signal around 290 nm. Surprisingly, the CD Soret band of this mutant is identical to that of Ncb5or-b5 and Nb5WA (**Figure 6C**), suggesting that the N-terminal region in this mutant cannot cooperatively interact with the heme center. Accordingly, the LMAA mutation also causes a more than 70% decrease in the rate of electron transfer when Ncb5or-CS/b5R is the reductase, indicating that cooperative interaction between this region and the heme center is important for electron transfer. It is noteworthy that the LM to AA mutation may retain helicity in the region of AADW, since Ala is a strong helix forming residue [113].

Table 3. The initial rate (μM/min/μM) of electron transfer from a reductase (Ncb5or-b5R or Ncb5or-CS/b5R) to Nb5 or its variant. For each reaction, 1.4 μM Nb5 or its mutant was reduced by proper amount of reductase: [a]140 μM, [b]56 μM, [c]500 μM, [d]300 μM. Results are mean ± standard error (n= 3-4).

	Ncb5or-b5R	Ncb5or-CS/b5R
Ncb5or-b5	3.65±0.16[a]	0.69±0.06[c]
Nb5M35	3.16±0.13[a]	0.69±0.06[c]
Nb5G22	9.51±0.37[b]	13.09±0.44[b]
Nb5	7.06±0.23[b]	12.02±0.31[b]
Nb5W37A	3.30±0.25[a]	1.51±0.08[d]
Nb5LMAA	4.92±0.15[a]	3.32±0.03[d]

A.

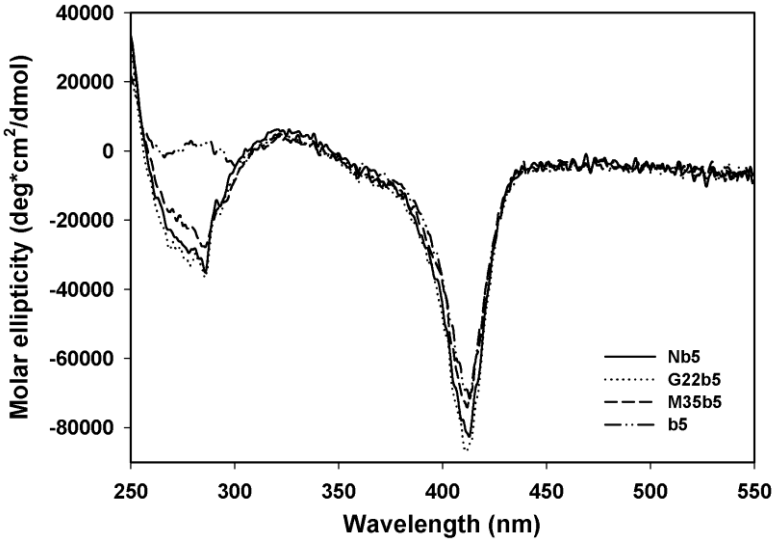
40000
20000
0
-20000
-40000
-60000
-80000
Molar ellipticity (deg*cm2/dmol)
250
300
350
400
450
500
550
Wavelength (nm)
Nb5
G22b5
M35b5
b5

B.

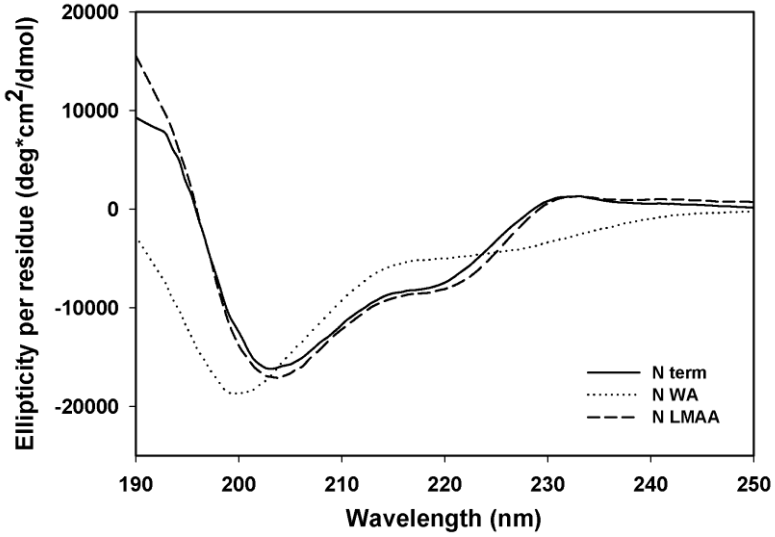
20000
10000
0
-10000
-20000
Ellipticity per residue (deg*cm2/dmol)
190
200
210
220
230
240
250
Wavelength (nm)
N term
N WA
N LMAA

C.

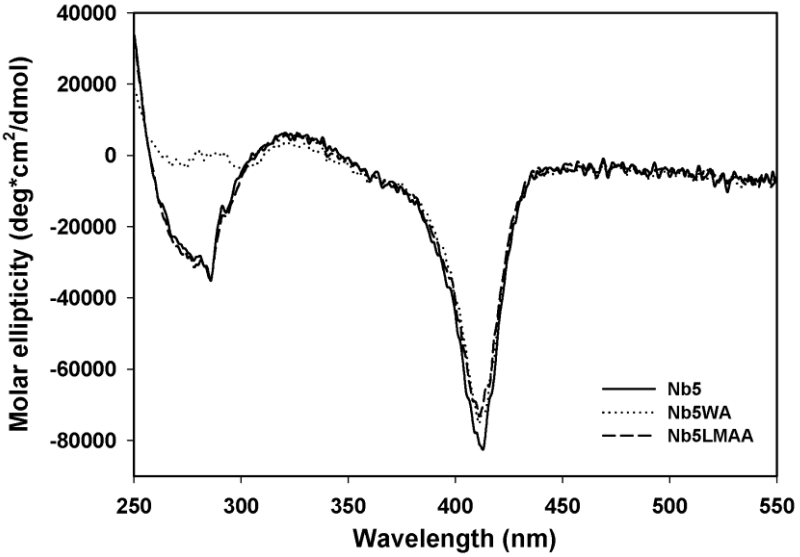

Figure 6. (A) CD spectra of Nb5 and its mutants with different length of the N-terminal region in near-UV and Soret region. (B) Far UV CD spectra of the N-terminal region and its mutants. Signals of N-terminal mutants (N WA: Nb5W37A-b5; N LMAA: Nb5LMAA-b5) were obtained by difference spectra, similar to that of the "N term" in Figure 4A. Each curve was smoothed by the negative exponential program in SigmaPlot 10 by using raw data in Supplemental Figure 3. (C) CD spectra of Nb5 and its mutants in near-UV region and Soret region.

Table 4. Signature CD signals in wild-type Nb5 and its variants. Helix in the N-terminal region: far-UV (Figure 6B). Molar ellipticity values were listed based on near-UV signals (286 nm) and Soret signals (413 nm) in Figures 6A and 6C to compare difference among different forms of Nb5. There are three categories of signals at 286 nm: (a) Ellipticity around -35000 represents complete formation of the N-terminal tertiary structure; (b) Ellipticity around -27000 represents incomplete formation of the N-terminal tertiary structure; (c) Ellipticity around 0 represents no N-terminal tertiary structure. There are two categories of signals at 413 nm: (a) Ellipticity above -80000 represents the heme center with the N-terminal impact; (b) Ellipticity around -70000 represents the heme center without the N-terminal impact. N/A: not applicable.

	Helix formation	Molar ellipticity (deg*cm^2/dmol) at 286 nm	Molar ellipticity (deg*cm^2/dmol) at 413 nm
Nb5	Yes	-35041	-82501
Nb5W37A	No	-346	-72577
Nb5LMAA	Yes	-34688	-69546
Nb5G22	N/A	-36453	-84650
Nb5M35	N/A	-27727	-70516
Ncb5or-b5	N/A	2262	-71620

Therefore, we speculate that the change from LMDW to AADW diminishes cooperative interactions of the N-terminal region with the heme center by decreasing its hydrophobicity.

The LMAA mutation retained the negative band around 290 nm while diminishing the cooperative interaction between the N-terminal region and Ncb5or-b5 (**Figure 6C**). This suggests that the signal around 290 nm is independent of the cooperative interaction between N-terminal and Ncb5or-b5 domains. W37A mutation, however, abolished the signal around 290 nm, suggesting that Trp^{37} is the major residue contributing to the negative band around 290 nm.

Discussion

Our current study shows that the N-terminal region of Ncb5or fulfills a novel function in facilitating inter-domain electron transfer through cooperatively interacting with the CS domain and the heme center in Ncb5or. The functional importance of the N-terminal region is supported by studies *in vivo* in which transgenic expression of truncated Ncb5or lacking the first 34 residues in Ncb5or-null mouse fails to rescue its diabetes phenotype (personal communication, H. Franklin Bunn).

On the basis of results from our structural (**Table 4**) and functional analyses (**Table 3**), we propose the following model of how the N-terminal region facilitates inter-domain electron transfer in Ncb5or. The invariant residues $^{34}LMDW^{37}$ form a hydrophobic core, in which Trp^{37} organizes the formation of tertiary structure in concert with the adjacent 15 residues upstream. This folded structure allows the N-terminal region to cooperatively interact with the b5 domain and the CS domain, thereby accelerating inter-domain electron transfer.

Our data indicate that the N-terminal region facilitates inter-domain electron transfer through its cooperative interaction with the heme center. The supporting evidence includes: (a) In the previous study [2], the presence of the N-terminal region inhibits auto-oxidation of heme potentially through blocking the opening of the heme pocket; (b) The presence of the N-terminal region alters the CD Soret band signal (**Figure 4B**); (c) The presence of the N-terminal region causes changes in heme proton signals in NMR spectra (**Figure 5**); (d) Disruption of helical structure in the W37A mutant also abolishes the impact of the N-terminal region on the heme center (**Figures 6B** and **C**). (e) Loss of the N-terminal impact on the heme center in the Nb5W37A, Nb5LMAA (**Figure 6C**) and Nb5M35 (**Figure 6A**) mutants results in a drastic drop in the rate of electron transfer from Ncb5or-CS/b5R (**Table 3**). All three mutants mentioned above have nearly identical Soret signal to Ncb5or-b5 that is without the N terminal impact.

Points (a-c) support a conclusion that the N-terminal region exerts its impact on the heme center. Point (d) indicates that the structural formation in the N terminal region is critical to its interaction with the heme center. Point (e) demonstrates that loss of the N-terminal impact on the heme abolishes the N-terminal function in facilitating inter-domain electron transfer.

The structural basis of disruption of cooperation between the N-terminal region and the heme center is, however, different in these variants. The Nb5W37A mutant has disrupted helical structure. Mutant Nb5LMAA maintains the helical structure but its core (AADW) has decreased hydrophobicity. Mutant Nb5M35 has an incomplete N-terminal structure. In all three cases, the loss of N-terminal impact on the heme correlates to a striking decrease in the rate of electron transfer, suggesting the cooperative interaction between the N terminal region and the heme

center is essential for its function to facilitate electron transfer.

Our data also suggest that residues G^{22}RSKVPLKQGRSLMDW^{37} are critical to the function of the N-terminal region. These residues are well conserved in all Ncb5or orthologs. Removal of the residues from Gly^{22} to Leu^{34} (Nb5M35) results in partial loss of the Trp^{37} signal, indicating incomplete formation of the tertiary structure. In this case, there is no complete tertiary structure in the N-terminal region to cooperatively interact with the heme center. Consequently, the N-terminal region loses its function. This strongly suggests that at least part of this critical region is present in the tertiary structure, which determines the function of the N terminal region.

The effect of Trp residues on CD spectra have been documented in barnase [114] and human carbonic anhydrase II [115]. In both cases, Trp signals contribute to a broad spectrum ranging from near-UV to far-UV region. Trp37 is invariant in all known members of Ncb5or family and is localized in a well conserved sequence, LMDW. Trp signals include a negative band at 286 nm and a positive feature at 230 nm, and the W37A mutation causes the disappearance of both signals (**Figures 6B** and **C**). The signal of Trp^{37} in the near-UV region resembles that of the Trp residue buried in human carbonic anhydrase II [115]. Thus we speculate that Trp^{37} is generally buried and is essential to the organization of the N-terminal tertiary fold. The W37A mutation causes intrinsic disruption of structure in the N-terminal region (**Figure 6B**), leading to an approximately 90% drop in electron transfer rate **(Table 3**). Residues such as Trp, Arg and Tyr are hot spots in protein-protein interaction interfaces, as demonstrated by the change in free energy upon binding [116].

Trp^{37} is not directly involved in the interaction with the heme center, as indicated by the

following: (a) The Nb5LMAA mutation only causes a subtle change in secondary structure (**Figure 6B**) with no significant change in the environment of Trp^{37} (**Figure 6C**, near-UV), but abolishes the N-terminal impact on the heme center (**Figure 6C**, Soret); (b) Deleting residues Gly^{22} to Leu^{34} but keeping Trp^{37} prevents the N-terminal region from cooperatively interacting with the heme center (**Figure 6A**, Soret). In (a), the environment of Trp^{37} is not altered significantly after mutation of LM to AA (**Figure 6C**, near-UV) while the N-terminal region fails to alter the heme environment (**Figure 6C**, Soret). In (b), Trp^{37} is kept in the truncated N-terminal region but the N-terminal region cannot cooperatively interact with the heme center (**Figure 6A**, Soret). Deletion of residues Gly^{22} to Leu^{34} abolishes the N-terminal impact on the heme, suggesting that certain residues between Gly^{22} and Leu^{34} are responsible for the effect on the heme pocket.

Visual inspection reveals potential hot spot residues, such as Arg^{23} and Arg^{39}, in this region. More detailed NMR studies are underway to identify these residues. Efforts are also undertaken to compare CD signals of the individual N-terminal region (residues 1-50 of Ncb5or by themselves) with those of the N-terminal signal in the context of Nb5 (difference spectra), in order to determine if the N-terminal region has any intrinsic structural preferences or if it only adopts structure via cooperative interaction with the b5 core.

Visual inspection of the CS domain reveals a few conserved charged residues and aromatic residues (**Supplemental Figure 4**). In contrast to a high pK value in the N-terminal region, the CS domain has a relatively low pK value due to abundant Glu and Asp residues. These features suggest that the CS domain likely interacts with the N-terminal region through an electrostatic

interaction. Accordingly the N-terminal region exerts its maximal effect on inter-domain electron transfer in the presence of the CS domain (**Tables 1 and 3**). We have chosen to generate the reductase including the CS domain, named Ncb5or-CS/b5R, to study electron transfer as in our previous report [85] for the following reasons: (a) The non-specific cleavage of Ncb5or occurs at the border between the b5 domain and the CS domain; (b) Sequence alignment suggests that the region between Ncb5or-b5 and the CS domain is more flexible than the one between the CS domain and Ncb5or-b5R, making the former more susceptible for the cleavage. (c) Electron transfer remains active between the cleaved products. In this study, deletion of the N-terminal region caused a larger fold decrease in the rate of electron transfer in the Nb5 + Ncb5or-CS/b5R pair (**Table 1**) than in the intact form of Ncb5or (**Table 2**). This strongly suggests a key role of the b5-CS linkage in mediating inter-domain electron transfer.

On the basis of the data presented in **Table 4** and **Figure 6**, the fold of the N-terminal region of Ncb5or can be described as a mixture of random coils and helix. Mammalian proteins contain a higher percentage of disordered regions than counterparts in lower animals and these regions are often involved in protein-protein interactions, DNA or RNA binding, substrate binding, modification, in many different protein groups [93,117]. The invariant surface residues that are not involved in inter-domain electron transfer may play a role in interacting with the physiological partner(s) of Ncb5or. For example, Trp^{114}, an invariant solvent-exposed residue, does not significantly affect inter-domain electron transfer in this study, but may play a role in mediating inter-protein electron transfer. A better understanding of the inter-domain electron transfer in Ncb5or, especially the cooperation between the N-terminal and the CS domains, will

provide insight into the action of other multi-domain protein or multi-step electron transfer.

Single-domain structural homologs of Ncb5or, namely, Cyb5A and Cyb5R3, contain considerable numbers of surface-charged residues. Inter-protein electron transfer is mainly mediated by strong electrostatic interaction [55], which mediates recognition on the ER membrane. Mutagenesis and cross-linking studies identified the residues as Asp and Glu at the opening of the heme pocket in Cyb5A and Lys at the FAD side in Cyb5R3 [56,57,58], suggesting that electron transfer from Cyb5R3 to Cyb5A is achieved by close proximity between flavin and heme. In contrast, Ncb5or-b5 and Ncb5or-b5R domains contain fewer surface-charged residues, resulting in weaker electrostatic interaction and less efficient electron transfer when individual redox domains are mixed [85]. The presence of the CS domain (Ncb5or-CS/b5R) appears to increase the specific recognition and at the same time to hinder their access to each other, resulting in a 5-fold drop in rate, k_{cat}/K_m (**Table 1**). Our results suggest that the N-terminal region of Ncb5or serves as a mediator or an adaptor with the CS domain to maintain appropriate orientation of redox domains for electron transfer. Meanwhile, the N-terminal region cooperatively interacts with the heme center to potentially facilitate the electron delivery. The model of electron transfer in Ncb5or will provide insight into studies of other multi-domain protein or multi-step electron transfer.

A.

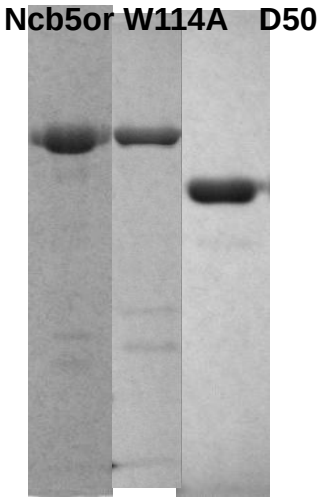

B.

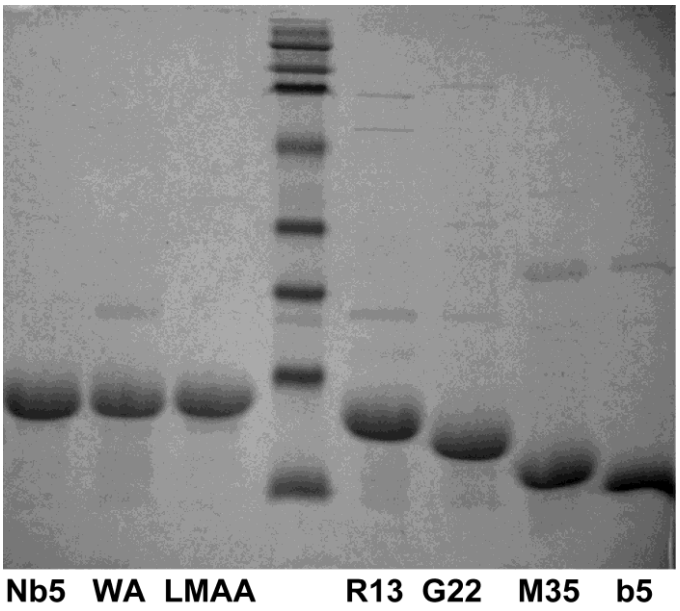

Supplemental Figure 1. (A) Purifications of Ncb5or and its mutants. Left lane: Ncb5or (60.5 kD); middle lane: Ncb5orW114A (60.5 kD); right lane: D50Ncb5or (55.2 kD) (B) Purifications of Nb5 and its mutants. The size for Nb5, Nb5W37A and Nb5LMAA is about 15.6 kD. The size of Nb5R13, Nb5G22, Nb5M35 and Ncb5or-b5 is 14.4 kD, 13.5 kD, 11.9 kD and 10.2 kD, respectively.

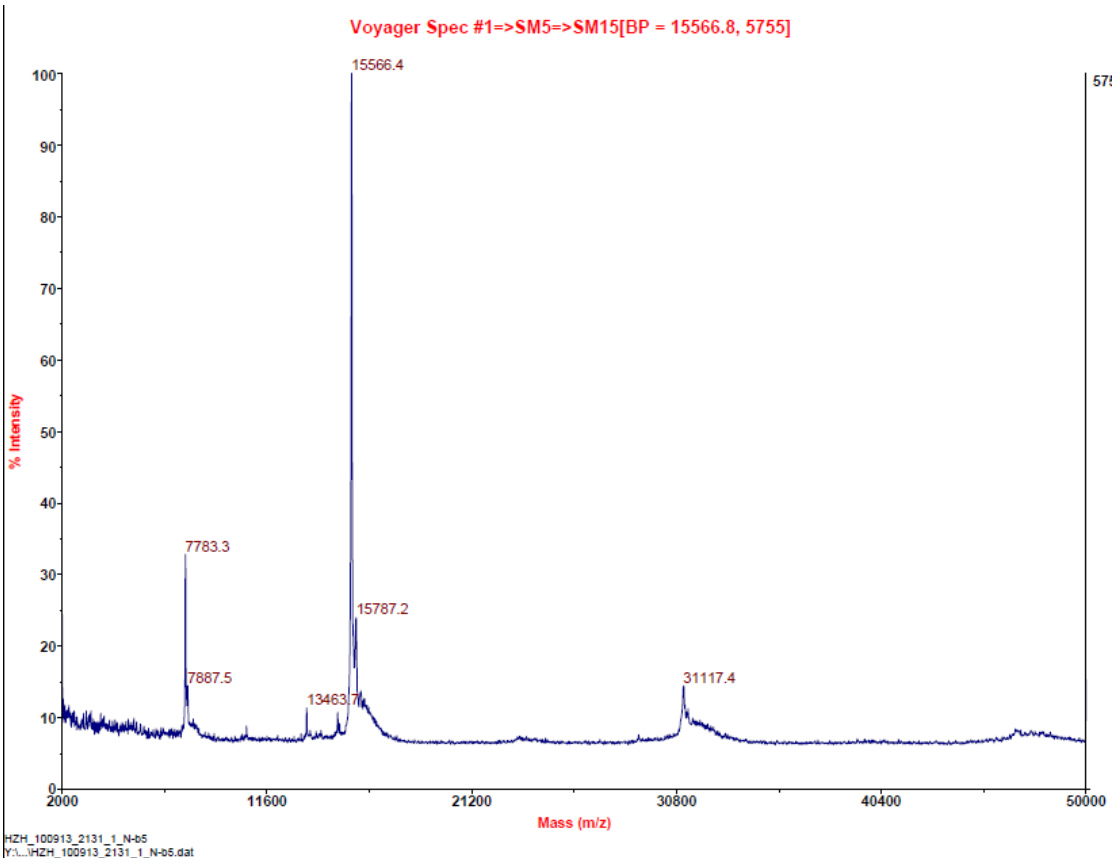

Supplemental Figure 2. MALDI mass spectra of Nb5. The expected size of Nb5 is 15567, and purified Nb5 has 15566.4. The peak with m/z of 7783.3 represents two-charge form of Nb5.

A.

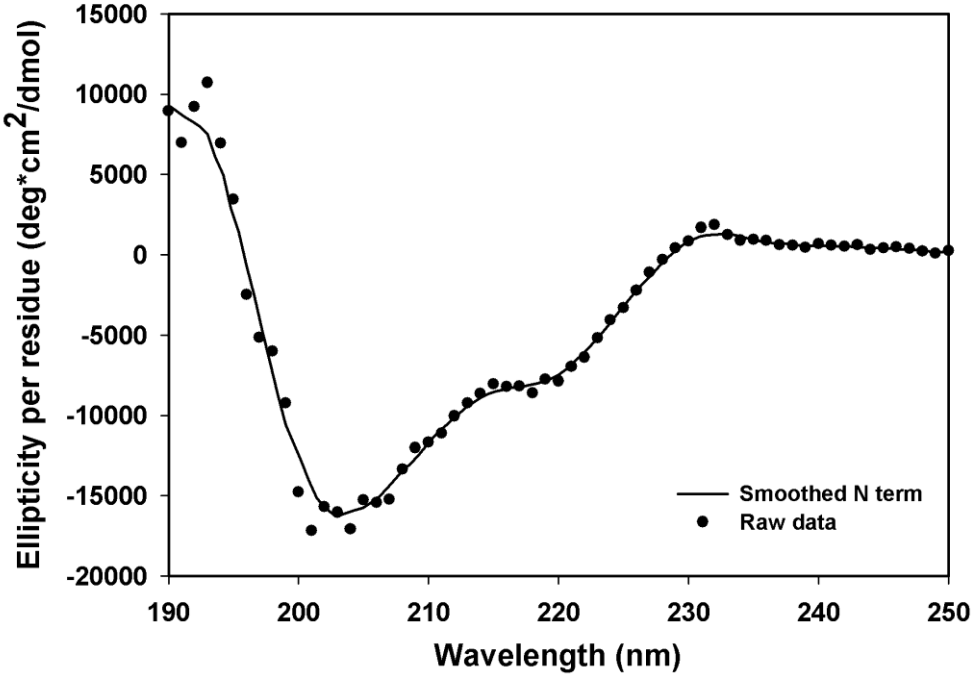
Ellipticity per residue (deg*cm2/dmol)
15000
10000
5000
0
-5000
-10000
-15000
-20000
190
200
210
220
230
240
250
Wavelength (nm)
Smoothed N term
Raw data

B.

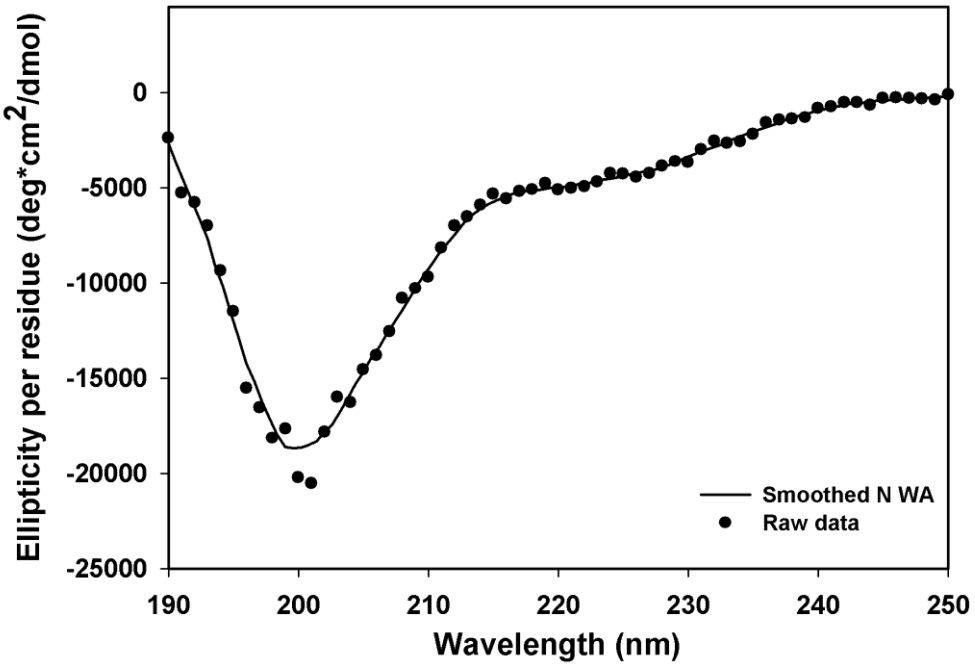
Ellipticity per residue (deg*cm2/dmol)
0
-5000
-10000
-15000
-20000
-25000
190
200
210
220
230
240
250
Wavelength (nm)
Smoothed N WA
Raw data

C.

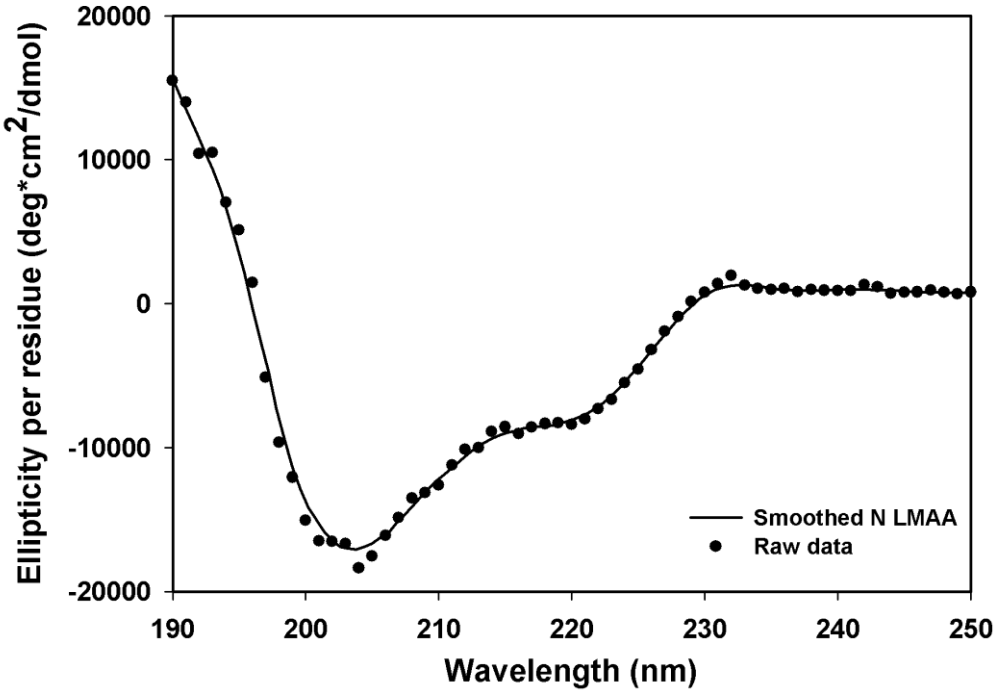

Supplemental Figure 3. Far UV spectra of the N-terminal region (A), N WA (B) and N LMAA (C). Signals of N terminal mutants (N WA: Nb5W37A-b5; N LMAA: Nb5LMAA-b5) were obtained by difference spectra. For each form of the N-terminal region, both raw data and the smoothed line were plotted. The smoothed line was obtained by applying negative exponential in SigmaPlot 10.0.

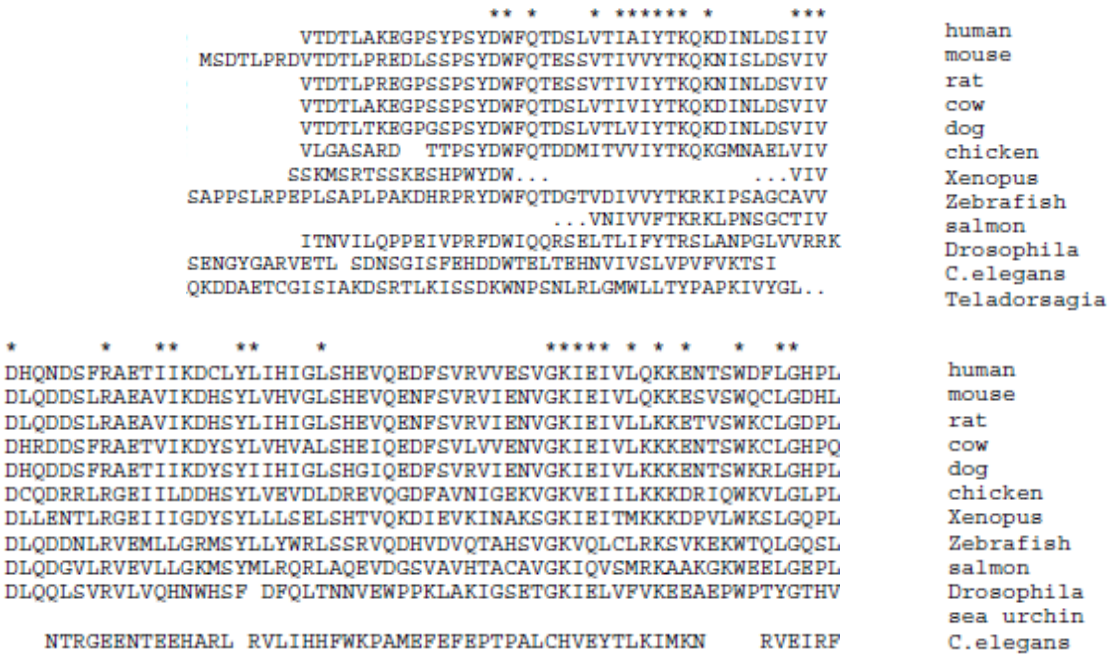

Supplemental Figure 4. Sequence alignment of the CS domain of Ncb5or in invertebrates and vertebrates. * represents conserved residue.

Chapter Four

Summary and Future Direction

Findings from *in vivo* studies of Ncb5or null mice suggest that Ncb5or potentially functions with SCD in fatty acid metabolism. However, physiological or redox partner(s) of Ncb5or are yet to be determined with *in vivo* studies or *in vitro* enzymatic assays. The latter relies on a better understanding of mechanism of the inter-domain or inter-protein electron transfer.

This study focuses on the structural features of Ncb5or that are important for inter-domain electron transfer. Our findings have shed light on the structure and function of each domain of Ncb5or (**Table 1**). The N-terminal region contains both random coils and helix. The latter dominates the formation of a tertiary structure, which is essential for the N terminal region to cooperatively interact with the CS domain and the heme and to facilitate electron transfer between the b5 and the b5R domains.

Ncb5or-b5 shows a b5 fold similar to that of Cyb5A. In the heme-binding region, both Ncb5or-b5 and Cyb5A have two helix-loop-helix motifs with heme sandwiched between two His residues. However, Ncb5or has a tetragonally distorted heme environment, which is unique in the cytochrome b5 superfamily. Ncb5or-b5 accepts electrons from Ncb5or-b5R and donates to downstream partner(s). Ncb5or-b5R is predicted to have a similar backbone to that of Cyb5R3 [21], and this domain functions as an electron donor for Ncb5or-b5.

The CS domain between Ncb5or-b5 and Ncb5or-b5R is predicted to contain seven β sheets plus turns [3,21]. This domain has been shown to mediate inter-domain electron transfer with the N-terminal region. Since the CS domain is homologous to chaperon-like protein, it may have similar function in protein-protein interaction, but more studies are needed for further characterization.

Our study has also shed light on the function of two invariant Trp residues in Ncb5or (**Table 2**). Trp^{114} is a surface residue, which is expected to have high rates of mutations during evolution if not functionally important. Trp^{114} plays a minor role in the inter-domain electron transfer, therefore is likely to mediate inter-protein electron transfer. Trp^{37} plays an essential role in organizing the tertiary fold in the N-terminal region, which is important in electron transfer. Through studies on these residues, the mechanism of electron transfer in Ncb5or becomes clear. Although many studies have been carried out on docking between Cyb5A and Cyb5R3, no clear interface has been found. Thus, Ncb5or provides a novel model to study inter-domain and inter-protein electron transfer.

There are several potential directions in the future: 1) Effect of the known missense mutations in human patients. D371Y and L424M have been identified in breast cancer. Our well-established methodologies, such as stop-flow and Michaelis-Menten kinetics and thermal denaturation, will enable us to identify functional or structural consequences of these mutations, i.e. electron transfer or stability. 2) Structure-function relation of the CS domain. The CS domain has homology with p23 family members like p23 and Sgt1, which are involved in protein-protein interactions. It is important to determine structure of the CS domain and identify protein bound to this domain. It would be equally meaningful to identify residues in the N-terminal domain that are responsible for its cooperative interaction with the CS domain through NMR analyses. 3) Search of inhibitors or activators through targeting inter-domain or inter-protein electron transfer. The knowledge on these processes will make it feasible to screen for or design small molecules that specifically target Ncb5or for both research and therapeutic purposes.

Table 1. Structure and function of individual domains in Ncb5or

Protein	Structure	Function
N-terminal region	Random coils and helix	Inter-domain electron transfer
b5 domain	Conserved b5 fold; unique heme center	Receives electrons from Ncb5or-b5R and donates them to partners
CS domain	Similar to HSP20 (prediction)	Inter-domain electron transfer; partners?
b5R domain	Similar to Cyb5R3 (prediction)	Donor of electrons to Ncb5or-b5

Table 2. Important Trp residues in Ncb5or

Residue	Domain	Function
W37	N-terminal region	Organization of structure in inter-domain electron transfer
W114	b5	Not involved in inter-domain electron transfer; inter-protein electron transfer?

REFERENCES

[1] H. Zhu, H. Qiu, H.W. Yoon, S. Huang, H.F. Bunn, Identification of a cytochrome b-type NAD(P)H oxidoreductase ubiquitously expressed in human cells, Proc Natl Acad Sci U S A 96 (1999) 14742-14747.

[2] H. Zhu, K. Larade, T.A. Jackson, J. Xie, A. Ladoux, H. Acker, U. Berchner-Pfannschmidt, J. Fandrey, A.R. Cross, G.S. Lukat-Rodgers, K.R. Rodgers, H.F. Bunn, NCB5OR is a novel soluble NAD(P)H reductase localized in the endoplasmic reticulum, J Biol Chem 279 (2004) 30316-30325.

[3] J.A. Garcia-Ranea, G. Mirey, J. Camonis, A. Valencia, p23 and HSP20/alpha-crystallin proteins define a conserved sequence domain present in other eukaryotic protein families, FEBS Lett 529 (2002) 162-167.

[4] H.P. Cho, M. Nakamura, S.D. Clarke, Cloning, expression, and fatty acid regulation of the human delta-5 desaturase, J Biol Chem 274 (1999) 37335-37339.

[5] H.P. Cho, M.T. Nakamura, S.D. Clarke, Cloning, expression, and nutritional regulation of the mammalian Delta-6 desaturase, J Biol Chem 274 (1999) 471-477.

[6] D.L. Kessler, K.V. Rajagopalan, Purification and properties of sulfite oxidase from chicken liver. Presence of molybdenum in sulfite oxidase from diverse sources, J Biol Chem 247 (1972) 6566-6573.

[7] C. Kisker, H. Schindelin, A. Pacheco, W.A. Wehbi, R.M. Garrett, K.V. Rajagopalan, J.H. Enemark, D.C. Rees, Molecular basis of sulfite oxidase deficiency from the structure of sulfite oxidase, Cell 91 (1997) 973-983.

[8] M.J. Rudolph, J.L. Johnson, K.V. Rajagopalan, C. Kisker, The 1.2 A structure of the human sulfite oxidase cytochrome b(5) domain, Acta Crystallogr D Biol Crystallogr 59 (2003) 1183-1191.

[9] Z.X. Xia, N. Shamala, P.H. Bethge, L.W. Lim, H.D. Bellamy, N.H. Xuong, F. Lederer, F.S. Mathews, Three-dimensional structure of flavocytochrome b2 from baker's yeast at 3.0-A resolution, Proc Natl Acad Sci U S A 84 (1987) 2629-2633.

[10] A.C. Cannons, M.J. Barber, L.P. Solomonson, Expression and characterization of the heme-binding domain of Chlorella nitrate reductase, J Biol Chem 268 (1993) 3268-3271.

[11] G.E. Hyde, N.M. Crawford, W.H. Campbell, The sequence of squash NADH:nitrate reductase and its relationship to the sequences of other flavoprotein oxidoreductases. A family of flavoprotein pyridine nucleotide cytochrome reductases, J Biol Chem 266 (1991) 23542-23547.

[12] M.J. Barber, S.K. Desai, C.C. Marohnic, H.H. Hernandez, V.V. Pollock, Synthesis and bacterial expression of a gene encoding the heme domain of assimilatory nitrate reductase, Arch Biochem Biophys 402 (2002) 38-50.

[13] P.A. Karplus, M.J. Daniels, J.R. Herriott, Atomic structure of ferredoxin-NADP+ reductase: prototype for a structurally novel flavoenzyme family, Science 251 (1991) 60-66.

[14] C.C. Correll, M.L. Ludwig, C.M. Bruns, P.A. Karplus, Structural prototypes for an extended family of flavoprotein reductases: comparison of phthalate dioxygenase reductase with ferredoxin reductase and ferredoxin, Protein Sci 2 (1993) 2112-2133.

[15] F. Lederer, The cytochrome b5-fold: an adaptable module, Biochimie 76 (1994) 674-692.

[16] M.A. Baker, A. Krutskikh, B.J. Curry, L. Hetherington, R.J. Aitken, Identification of cytochrome-b5 reductase as the enzyme responsible for NADH-dependent lucigenin chemiluminescence in human spermatozoa, Biol Reprod 73 (2005) 334-342.

[17] R.C. Durley, F.S. Mathews, Refinement and structural analysis of bovine cytochrome b5 at 1.5 A resolution, Acta Crystallogr D Biol Crystallogr 52 (1996) 65-76.

[18] S. Parthasarathy, A. Altuve, S. Terzyan, X. Zhang, K. Kuczera, M. Rivera, D.R. Benson, Accommodating a Nonconservative Internal Mutation by Water-Mediated Hydrogen Bonding between beta-Sheet Strands: A Comparison of Human and Rat Type B (Mitochondrial) Cytochrome b(5), Biochemistry 50 (2011) 5544-5554.

[19] Z.X. Xia, F.S. Mathews, Molecular structure of flavocytochrome b2 at 2.4 A resolution, J Mol Biol 212 (1990) 837-863.

[20] S. Bando, T. Takano, T. Yubisui, K. Shirabe, M. Takeshita, A. Nakagawa, Structure of human erythrocyte NADH-cytochrome b5 reductase, Acta Crystallogr D Biol Crystallogr 60 (2004) 1929-1934.

[21] Y. Zhang, I-TASSER server for protein 3D structure prediction, BMC Bioinformatics 9 (2008) 40.

[22] T. Sjoblom, S. Jones, L.D. Wood, D.W. Parsons, J. Lin, T.D. Barber, D. Mandelker, R.J. Leary, J. Ptak, N. Silliman, S. Szabo, P. Buckhaults, C. Farrell, P. Meeh, S.D. Markowitz, J. Willis, D. Dawson, J.K. Willson, A.F. Gazdar, J. Hartigan, L. Wu, C. Liu, G. Parmigiani, B.H. Park, K.E. Bachman, N. Papadopoulos, B. Vogelstein, K.W. Kinzler, V.E. Velculescu, The consensus coding sequences of human breast and colorectal cancers,

Science 314 (2006) 268-274.

[23] J. Buchner, Hsp90 & Co. - a holding for folding, Trends Biochem Sci 24 (1999) 136-141.

[24] A. Mayor, F. Martinon, T. De Smedt, V. Petrilli, J. Tschopp, A crucial function of SGT1 and HSP90 in inflammasome activity links mammalian and plant innate immune responses, Nat Immunol 8 (2007) 497-503.

[25] M. Zhang, Y. Kadota, C. Prodromou, K. Shirasu, L.H. Pearl, Structural basis for assembly of Hsp90-Sgt1-CHORD protein complexes: implications for chaperoning of NLR innate immunity receptors, Mol Cell 39 (2010) 269-281.

[26] M. Zhang, M. Boter, K. Li, Y. Kadota, B. Panaretou, C. Prodromou, K. Shirasu, L.H. Pearl, Structural and functional coupling of Hsp90- and Sgt1-centred multi-protein complexes, EMBO J 27 (2008) 2789-2798.

[27] A.J. Weaver, W.P. Sullivan, S.J. Felts, B.A. Owen, D.O. Toft, Crystal structure and activity of human p23, a heat shock protein 90 co-chaperone, J Biol Chem 275 (2000) 23045-23052.

[28] G. Andersen, L. Wegner, C.S. Rose, J. Xie, H. Zhu, K. Larade, A. Johansen, J. Ek, J. Lauenborg, T. Drivsholm, K. Borch-Johnsen, P. Damm, T. Hansen, H.F. Bunn, O. Pedersen, Variation in NCB5OR: studies of relationships to type 2 diabetes, maturity-onset diabetes of the young, and gestational diabetes mellitus, Diabetes 53 (2004) 2992-2997.

[29] F. Lederer, R. Ghrir, B. Guiard, S. Cortial, A. Ito, Two homologous cytochromes b5 in a single cell, Eur J Biochem 132 (1983) 95-102.

[30] J. Mitoma, A. Ito, The carboxy-terminal 10 amino acid residues of cytochrome b5 are necessary for its targeting to the endoplasmic reticulum, EMBO J 11 (1992) 4197-4203.

[31] N. Borgese, R. Longhi, Both the outer mitochondrial membrane and the microsomal forms of cytochrome b5 reductase contain covalently bound myristic acid. Quantitative analysis on the polyvinylidene difluoride-immobilized proteins, Biochem J 266 (1990) 341-347.

[32] N. Borgese, D. Aggujaro, P. Carrera, G. Pietrini, M. Bassetti, A role for N-myristoylation in protein targeting: NADH-cytochrome b5 reductase requires myristic acid for association with outer mitochondrial but not ER membranes, J Cell Biol 135 (1996) 1501-1513.

[33] J. Ozols, S.A. Carr, P. Strittmatter, Identification of the NH2-terminal blocking group of NADH-cytochrome b5 reductase as myristic acid and the complete amino acid sequence of the membrane-binding domain, J Biol Chem 259 (1984) 13349-13354.

[34] P. Strittmatter, L. Spatz, D. Corcoran, M.J. Rogers, B. Setlow, R. Redline, Purification and properties of rat liver microsomal stearyl coenzyme A desaturase, Proc Natl Acad Sci U S A 71 (1974) 4565-4569.

[35] R.D. Finn, L.A. McLaughlin, S. Ronseaux, I. Rosewell, J.B. Houston, C.J. Henderson, C.R. Wolf, Defining the in Vivo Role for cytochrome b5 in cytochrome P450 function through the conditional hepatic deletion of microsomal cytochrome b5, J Biol Chem 283 (2008) 31385-31393.

[36] M.A. Peyronneau, J.P. Renaud, G. Truan, P. Urban, D. Pompon, D. Mansuy, Optimization of yeast-expressed human liver cytochrome P450 3A4 catalytic activities by coexpressing NADPH-cytochrome P450 reductase and cytochrome b5, Eur J Biochem 207 (1992)

109-116.

[37] V.V. Reddy, D. Kupfer, E. Caspi, Mechanism of C-5 double bond introduction in the biosynthesis of cholesterol by rat liver microsomes, J Biol Chem 252 (1977) 2797-2801.

[38] W.E. Rainey, Y. Nakamura, Regulation of the adrenal androgen biosynthesis, J Steroid Biochem Mol Biol 108 (2008) 281-286.

[39] T. Ogishima, J.Y. Kinoshita, F. Mitani, M. Suematsu, A. Ito, Identification of outer mitochondrial membrane cytochrome b5 as a modulator for androgen synthesis in Leydig cells, J Biol Chem 278 (2003) 21204-21211.

[40] D.E. Hultquist, P.G. Passon, Catalysis of methaemoglobin reduction by erythrocyte cytochrome B5 and cytochrome B5 reductase, Nat New Biol 229 (1971) 252-254.

[41] M.J. Percy, T.R. Lappin, Recessive congenital methaemoglobinaemia: cytochrome b(5) reductase deficiency, Br J Haematol 141 (2008) 298-308.

[42] Congenital methemoglobinemia with cytochrome b5 deficiency, N Engl J Med 315 (1986) 893-894.

[43] J.W. DePierre, L. Ernster, Enzyme topology of intracellular membranes, Annu Rev Biochem 46 (1977) 201-262.

[44] M.R. Prasad, K. Sreekrishna, V.C. Joshi, Topology of the delta 9 terminal desaturase in chicken liver microsomes and artificial micelles. Inhibition of the enzyme activity by the antibody and susceptibility of the enzyme to proteolysis, J Biol Chem 255 (1980) 2583-2589.

[45] L.A. McLaughlin, S. Ronseaux, R.D. Finn, C.J. Henderson, C. Roland Wolf, Deletion of

microsomal cytochrome b5 profoundly affects hepatic and extrahepatic drug metabolism, Mol Pharmacol 78 (2010) 269-278.

[46] R.D. Finn, L.A. McLaughlin, C. Hughes, C. Song, C.J. Henderson, C. Roland Wolf, Cytochrome b (5) null mouse: a new model for studying inherited skin disorders and the role of unsaturated fatty acids in normal homeostasis, Transgenic Res 20 (2011) 491-502.

[47] J.K. Yee, C.S. Mao, H.S. Hummel, S. Lim, S. Sugano, V.K. Rehan, G. Xiao, W.N. Lee, Compartmentalization of stearoyl-coenzyme A desaturase 1 activity in HepG2 cells, J Lipid Res 49 (2008) 2124-2134.

[48] K. Larade, Z. Jiang, Y. Zhang, W. Wang, S. Bonner-Weir, H. Zhu, H.F. Bunn, Loss of Ncb5or results in impaired fatty acid desaturation, lipoatrophy, and diabetes, J Biol Chem 283 (2008) 29285-29291.

[49] B. Rost, PHD: predicting one-dimensional protein structure by profile-based neural networks, Methods Enzymol 266 (1996) 525-539.

[50] J. Xie, H. Zhu, K. Larade, A. Ladoux, A. Seguritan, M. Chu, S. Ito, R.T. Bronson, E.H. Leiter, C.Y. Zhang, E.D. Rosen, H.F. Bunn, Absence of a reductase, NCB5OR, causes insulin-deficient diabetes, Proc Natl Acad Sci U S A 101 (2004) 10750-10755.

[51] W. Wang, Y. Guo, M. Xu, H.H. Huang, L. Novikova, K. Larade, Z.G. Jiang, T.C. Thayer, J.R. Frontera, D. Aires, H. Ding, J. Turk, C.E. Mathews, H.F. Bunn, L. Stehno-Bittel, H. Zhu, Development of diabetes in lean Ncb5or-null mice is associated with manifestations of endoplasmic reticulum and oxidative stress in beta cells, Biochim Biophys Acta (2011).

[52] M. Xu, W. Wang, J.R. Frontera, M.C. Neely, J. Lu, D. Aires, F.F. Hsu, J. Turk, R.H.

Swerdlow, S.E. Carlson, H. Zhu, Ncb5or deficiency increases fatty acid catabolism and oxidative stress, J Biol Chem 286 (2011) 11141-11154.

[53] Y. Zhang, K. Larade, Z.G. Jiang, S. Ito, W. Wang, H. Zhu, H.F. Bunn, The flavoheme reductase Ncb5or protects cells against endoplasmic reticulum stress-induced lipotoxicity, J Lipid Res 51 (2010) 53-62.

[54] J.M. Ntambi, M. Miyazaki, J.P. Stoehr, H. Lan, C.M. Kendziorski, B.S. Yandell, Y. Song, P. Cohen, J.M. Friedman, A.D. Attie, Loss of stearoyl-CoA desaturase-1 function protects mice against adiposity, Proc Natl Acad Sci U S A 99 (2002) 11482-11486.

[55] T.E. Meyer, K. Shirabe, T. Yubisui, M. Takeshita, M.T. Bes, M.A. Cusanovich, G. Tollin, Transient kinetics of intracomplex electron transfer in the human cytochrome b5 reductase-cytochrome b5 system: NAD+ modulates protein-protein binding and electron transfer, Arch Biochem Biophys 318 (1995) 457-464.

[56] P. Strittmatter, C.S. Hackett, G. Korza, J. Ozols, Characterization of the covalent cross-links of the active sites of amidinated cytochrome b5 and NADH:cytochrome b5 reductase, J Biol Chem 265 (1990) 21709-21713.

[57] K. Shirabe, T. Nagai, T. Yubisui, M. Takeshita, Electrostatic interaction between NADH-cytochrome b5 reductase and cytochrome b5 studied by site-directed mutagenesis, Biochim Biophys Acta 1384 (1998) 16-22.

[58] M. Kawano, K. Shirabe, T. Nagai, M. Takeshita, Role of carboxyl residues surrounding heme of human cytochrome b5 in the electrostatic interaction with NADH-cytochrome b5 reductase, Biochem Biophys Res Commun 245 (1998) 666-669.

[59] X. Li, P. Romero, M. Rani, A.K. Dunker, Z. Obradovic, Predicting Protein Disorder for N-, C-, and Internal Regions, Genome Inform Ser Workshop Genome Inform 10 (1999) 30-40.

[60] Romero, Obradovic, K. Dunker, Sequence Data Analysis for Long Disordered Regions Prediction in the Calcineurin Family, Genome Inform Ser Workshop Genome Inform 8 (1997) 110-124.

[61] P. Romero, Z. Obradovic, X. Li, E.C. Garner, C.J. Brown, A.K. Dunker, Sequence complexity of disordered protein, Proteins 42 (2001) 38-48.

[62] A.G. Mitchell, C.E. Martin, A novel cytochrome b5-like domain is linked to the carboxyl terminus of the Saccharomyces cerevisiae delta-9 fatty acid desaturase, J Biol Chem 270 (1995) 29766-29772.

[63] F.S. Mathews, E.W. Gerwinsky, P. Argos, The X-ray crystallographic structure of calf liver cytochrome b5, in The Porphyrins (Dolphin, D. ed.), Academic Press, New York (1979) 107-147.

[64] T. Yubisui, Y. Naitoh, S. Zenno, M. Tamura, M. Takeshita, Y. Sakaki, Molecular cloning of cDNAs of human liver and placenta NADH-cytochrome b5 reductase, Proc Natl Acad Sci U S A 84 (1987) 3609-3613.

[65] G. Pietrini, P. Carrera, N. Borgese, Two transcripts encode rat cytochrome b5 reductase, Proc Natl Acad Sci U S A 85 (1988) 7246-7250.

[66] E. Lloyd, J.C. Ferrer, W.D. Funk, M.R. Mauk, A.G. Mauk, Recombinant human erythrocyte cytochrome b5, Biochemistry 33 (1994) 11432-11437.

[67] G.W. Roma, L.J. Crowley, M.J. Barber, Expression and characterization of a functional canine variant of cytochrome b5 reductase, Arch Biochem Biophys 452 (2006) 69-82.

[68] C.J. Falzone, M.R. Mayer, E.L. Whiteman, C.D. Moore, J.T. Lecomte, Design challenges for hemoproteins: the solution structure of apocytochrome b5, Biochemistry 35 (1996) 6519-6526.

[69] A.B. Cowley, M. Rivera, D.R. Benson, Stabilizing roles of residual structure in the empty heme binding pockets and unfolded states of microsomal and mitochondrial apocytochrome b5, Protein Sci 13 (2004) 2316-2329.

[70] C.A. Davis, I.K. Dhawan, M.K. Johnson, M.J. Barber, Heterologous expression of an endogenous rat cytochrome b(5)/cytochrome b(5) reductase fusion protein: identification of histidines 62 and 85 as the heme axial ligands, Arch Biochem Biophys 400 (2002) 63-75.

[71] B.W. Matthews, Solvent content of protein crystals, J Mol Biol 33 (1968) 491-497.

[72] F. Long, A.A. Vagin, P. Young, G.N. Murshudov, BALBES: a molecular-replacement pipeline, Acta Crystallogr D Biol Crystallogr 64 (2008) 125-132.

[73] M. Wirtz, V. Oganesyan, X. Zhang, J. Studer, M. Rivera, Modulation of redox potential in electron transfer proteins: effects of complex formation on the active site microenvironment of cytochrome b5, Faraday Discuss (2000) 221-234; discussion 257-268.

[74] K. Cowtan, The Buccaneer software for automated model building. 1. Tracing protein chains, Acta Crystallogr D Biol Crystallogr 62 (2006) 1002-1011.

[75] W. Kabsch, Automatic indexing of rotation diffraction patterns, J Applied Crystallography 21 (1988) 67-72.

[76] A. Vagin, A. Teplyakov, MOLREP: an automated program for molecular replacement, J Applied Crystallography 30 (1997) 1022-1025.

[77] G.N. Murshudov, A.A. Vagin, E.J. Dodson, Refinement of macromolecular structures by the maximum-likelihood method, Acta Crystallogr D Biol Crystallogr 53 (1997) 240-255.

[78] P. Emsley, K. Cowtan, Coot: model-building tools for molecular graphics, Acta Crystallogr D Biol Crystallogr 60 (2004) 2126-2132.

[79] S.C. Lovell, I.W. Davis, W.B. Arendall, 3rd, P.I. de Bakker, J.M. Word, M.G. Prisant, J.S. Richardson, D.C. Richardson, Structure validation by Calpha geometry: phi,psi and Cbeta deviation, Proteins 50 (2003) 437-450.

[80] M. Carson, Ribbons, Methods Enzymol 277 (1997) 493-505.

[81] L. Potterton, S. McNicholas, E. Krissinel, J. Gruber, K. Cowtan, P. Emsley, G.N. Murshudov, S. Cohen, A. Perrakis, M. Noble, Developments in the CCP4 molecular-graphics project, Acta Crystallogr D Biol Crystallogr 60 (2004) 2288-2294.

[82] N.A. Baker, D. Sept, S. Joseph, M.J. Holst, J.A. McCammon, Electrostatics of nanosystems: application to microtubules and the ribosome, Proc Natl Acad Sci U S A 98 (2001) 10037-10041.

[83] T.J. Dolinsky, J.E. Nielsen, J.A. McCammon, N.A. Baker, PDB2PQR: an automated pipeline for the setup of Poisson-Boltzmann electrostatics calculations, Nucleic Acids Res 32 (2004) W665-667.

[84] D.C. Bas, D.M. Rogers, J.H. Jensen, Very fast prediction and rationalization of pKa values for protein-ligand complexes, Proteins 73 (2008) 765-783.

[85] B. Deng, S. Parthasarathy, W. Wang, B.R. Gibney, K.P. Battaile, S. Lovell, D.R. Benson, H. Zhu, Study of the individual cytochrome b5 and cytochrome b5 reductase domains of Ncb5or reveals a unique heme pocket and a possible role of the CS domain, J Biol Chem 285 (2010) 30181-30191.

[86] L.A. Yatsunyk, A. Dawson, M.D. Carducci, G.S. Nichol, F.A. Walker, Models of the cytochromes: crystal structures and EPR spectral characterization of low-spin bis-imidazole complexes of (OETPP)Fe(III) having intermediate ligand plane dihedral angles, Inorg Chem 45 (2006) 5417-5428.

[87] C.T. Migita, K. Migita, M. Iwaizumi, Electron paramagnetic resonance studies of highly anisotropic low-spin states of ferrimyoglobin derivatives, Biochim Biophys Acta 743 (1983) 290-298.

[88] J.C. Salerno, Cytochrome electron spin resonance line shapes, ligand fields, and components stoichiometry in ubiquinol-cytochrome c oxidoreductase, J Biol Chem 259 (1984) 2331-2336.

[89] E.A. Berry, F.A. Walker, Bis-histidine-coordinated hemes in four-helix bundles: how the geometry of the bundle controls the axial imidazole plane orientations in transmembrane cytochromes of mitochondrial complexes II and III and related proteins, J Biol Inorg Chem 13 (2008) 481-498.

[90] G. Zoppellaro, K.L. Bren, A.A. Ensign, E. Harbitz, R. Kaur, H.P. Hersleth, U. Ryde, L.

Hederstedt, K.K. Andersson, Review: studies of ferric heme proteins with highly anisotropic/highly axial low spin (S = 1/2) electron paramagnetic resonance signals with bis-histidine and histidine-methionine axial iron coordination, Biopolymers 91 (2009) 1064-1082.

[91] F.S. Mathews, M. Levine, P. Argos, Three-dimensional Fourier synthesis of calf liver cytochrome b 5 at 2-8 A resolution, J Mol Biol 64 (1972) 449-464.

[92] F.S. Mathews, M. Levine, P. Argos, The structure of calf liver cytochrome b 5 at 2.8 A resolution, Nat New Biol 233 (1971) 15-16.

[93] H.J. Dyson, P.E. Wright, Intrinsically unstructured proteins and their functions, Nat Rev Mol Cell Biol 6 (2005) 197-208.

[94] A.V. Yantsevich, A.A. Gilep, S.A. Usanov, Mechanism of electron transfer in fusion protein cytochrome b5-NADH-cytochrome b5 reductase, Biochemistry (Mosc) 73 (2008) 1096-1107.

[95] S. Iwata, J.W. Lee, K. Okada, J.K. Lee, M. Iwata, B. Rasmussen, T.A. Link, S. Ramaswamy, B.K. Jap, Complete structure of the 11-subunit bovine mitochondrial cytochrome bc1 complex, Science 281 (1998) 64-71.

[96] C.R. Lancaster, A. Kroger, M. Auer, H. Michel, Structure of fumarate reductase from Wolinella succinogenes at 2.2 A resolution, Nature 402 (1999) 377-385.

[97] M.G. Madej, H.R. Nasiri, N.S. Hilgendorff, H. Schwalbe, C.R. Lancaster, Evidence for transmembrane proton transfer in a dihaem-containing membrane protein complex, EMBO J 25 (2006) 4963-4970.

[98] H. Nishida, K. Miki, Electrostatic properties deduced from refined structures of NADH-cytochrome b5 reductase and the other flavin-dependent reductases: pyridine nucleotide-binding and interaction with an electron-transfer partner, Proteins 26 (1996) 32-41.

[99] R. Davydov, B.M. Hoffman, EPR and ENDOR studies of Fe(II) hemoproteins reduced and oxidized at 77 K, J Biol Inorg Chem 13 (2008) 357-369.

[100] M.J. Rodriguez-Maranon, F. Qiu, R.E. Stark, S.P. White, X. Zhang, S.I. Foundling, V. Rodriguez, C.L. Schilling, 3rd, R.A. Bunce, M. Rivera, 13C NMR spectroscopic and X-ray crystallographic study of the role played by mitochondrial cytochrome b5 heme propionates in the electrostatic binding to cytochrome c, Biochemistry 35 (1996) 16378-16390.

[101] M. Rivera, C. Barillas-Mury, K.A. Christensen, J.W. Little, M.A. Wells, F.A. Walker, Gene synthesis, bacterial expression, and 1H NMR spectroscopic studies of the rat outer mitochondrial membrane cytochrome b5, Biochemistry 31 (1992) 12233-12240.

[102] L. Wang, A.B. Cowley, S. Terzyan, X. Zhang, D.R. Benson, Comparison of cytochromes b5 from insects and vertebrates, Proteins 67 (2007) 293-304.

[103] V.M. Guzov, H.L. Houston, M.B. Murataliev, F.A. Walker, R. Feyereisen, Molecular cloning, overexpression in Escherichia coli, structural and functional characterization of house fly cytochrome b5, J Biol Chem 271 (1996) 26637-26645.

[104] T. Yokota, Y. Nakajima, F. Yamakura, S. Sugio, M. Hashimoto, S. Takamiya, Unique structure of Ascaris suum b5-type cytochrome: an additional alpha-helix and positively

charged residues on the surface domain interact with redox partners, Biochem J 394 (2006) 437-447.

[105] V. Kostanjevecki, D. Leys, G. Van Driessche, T.E. Meyer, M.A. Cusanovich, U. Fischer, Y. Guisez, J. Van Beeumen, Structure and characterization of Ectothiorhodospira vacuolata cytochrome b(558), a prokaryotic homologue of cytochrome b(5), J Biol Chem 274 (1999) 35614-35620.

[106] C.G. Mowat, C.S. Miles, A.W. Munro, M.R. Cheesman, L.G. Quaroni, G.A. Reid, S.K. Chapman, Changing the heme ligation in flavocytochrome b2: substitution of histidine-66 by cysteine, J Biol Inorg Chem 5 (2000) 584-592.

[107] M. Tegoni, C. Cambillau, The 2.6-A refined structure of the Escherichia coli recombinant Saccharomyces cerevisiae flavocytochrome b2-sulfite complex, Protein Sci 3 (1994) 303-313.

[108] B.J. Smagghe, G. Sarath, E. Ross, J.L. Hilbert, M.S. Hargrove, Slow ligand binding kinetics dominate ferrous hexacoordinate hemoglobin reactivities and reveal differences between plants and other species, Biochemistry 45 (2006) 561-570.

[109] B. Rost, P. Fariselli, R. Casadio, Topology prediction for helical transmembrane proteins at 86% accuracy, Protein Sci 5 (1996) 1704-1718.

[110] B. Rost, C. Sander, Prediction of protein secondary structure at better than 70% accuracy, J Mol Biol 232 (1993) 584-599.

[111] S.M. Kelly, T.J. Jess, N.C. Price, How to study proteins by circular dichroism, Biochim Biophys Acta 1751 (2005) 119-139.

[112] L.A. Andersson, J.A. Peterson, Active-site analysis of ferric P450 enzymes: hydrogen-bonding effects on the circular dichroism spectra, Biochem Biophys Res Commun 211 (1995) 389-395.

[113] C.N. Pace, J.M. Scholtz, A helix propensity scale based on experimental studies of peptides and proteins, Biophys J 75 (1998) 422-427.

[114] S. Vuilleumier, J. Sancho, R. Loewenthal, A.R. Fersht, Circular dichroism studies of barnase and its mutants: characterization of the contribution of aromatic side chains, Biochemistry 32 (1993) 10303-10313.

[115] P.O. Freskgard, L.G. Martensson, P. Jonasson, B.H. Jonsson, U. Carlsson, Assignment of the contribution of the tryptophan residues to the circular dichroism spectrum of human carbonic anhydrase II, Biochemistry 33 (1994) 14281-14288.

[116] A.A. Bogan, K.S. Thorn, Anatomy of hot spots in protein interfaces, J Mol Biol 280 (1998) 1-9.

[117] A.K. Dunker, C.J. Brown, J.D. Lawson, L.M. Iakoucheva, Z. Obradovic, Intrinsic disorder and protein function, Biochemistry 41 (2002) 6573-6582.

APPENDICES

Section A: Lipid Technology

Lipid Extraction and Assays

1. 50 mg liver or 5 mg WAT are grinded in 1ml buffer (18 mM Tris-HCl, 300 mM mannitol, 50 mM EGTA, pH=7) for at least 10 stroke until getting homogenous.
2. Pipette 4mL of methanol + BHT (0.05%) into extraction tubes. Add 8 mL Chloroform and vortex overnight.
3. Transfer contents through a funnel lined with filter paper (Whatman #1) into a clean extraction tube.
4. Add 1.6mL KCl and vortex for 10 seconds. Centrifuge for 5 minutes at 750 r.p.m. and transfer bottom phase into a spotting tube with Pasteur pipette. Evaporate solvent in a water bath at 35°C under nitrogen.
5. After the lipids are dry, add 2 ml solvent (10% Triton-X100 in isopropanol). Resuspend the lipids well and incubate in 37 ^{o}C overnight to dissolve all the lipids.
6. Triglyceride concentration can be determined by Triglyceride Kit from Sigma according to the kit instruction. Five μl solution will be used for each assay. The TG amount from liver or WAT will be normalized by tissue weight.
7. Fatty acid can be quantified by Wako NEFA kit.

Isolation of Lipid

Reagents:

0.15M NaCl + 1mM EDTA

0.15 M KCl

Methanol

Methanol + butylated hydroxytoluene (BHT) (0.05% v/v)

Chloroform

Chloroform/Methanol + BHT (C:M; 2:1; v/v)

Internal Standard-phosphatidylcholine (PC) 17:0 (52µg/100µL)

Chloroform/Methanol (1:1; v/v) + 2,5-bis-(5'-tert-butylbenz-oxazolyl-[2'])thiopene (BBOT) (0.1g/L)

Glass distilled water

Pentane

Hexane

Diethyl ether

Benzene

Transesterification (methylation)-reagent: boron trifluoride-methanol or BF_3-M (14% w/w)

Developing solvent for total phospholipids and neutral lipids (hexane : diethyl ether : acetic acid= 80:20:1; v/v/v). For individual phospholipids: chloroform/methanol/acetic acid/water- (60:30: 8.4:4.6; v/v/v/v)

Fatty methyl ester standards-individual standards; PUFA-1 Marine and PUFA-2 Animal-Matreya,

Inc. #1093 and #1081; and NHI-C, NIH-D, and NIH-F – Supelco 0-8256, 0-8381, and 0-8631 quantitative standards

Neutral lipid standards (triglyceride and cholesterol ester)

Phospholipid standards (phosphatidylcholine, phosphatidylethanolamine, phosphatidylserine, sphingomyelin, phosphatidylinositol, phosphatidylglycerol)

Equipment and Supplies:

Extraction tubes

Spotting tubes

Varian 2mL screw top vials (clear vials, black caps, PTFE/Silicon liners, 12x32mm)

200µL, 12x32mm, flat bottom glass inserts

Filter paper (Whatman #1: 15cm circles and 46x57 sheets)

Glass funnels

Pasteur pipettes

Automatic pipettes in range of volumes

Centrifuges: MSE Mistral 3000i and IEC HN-FII

Nitrogen evaporator with water bath that can be temperature controlled

GC (gas chromatograph)

Developing tank

Heating block (dry bath)

Hamilton syringes (100µL for spotting and concentrating FAME's and 10µL for injecting into

GC)

Ice bucket, UV light, vortex

Extraction:

1. Pipette 4mL of methanol + BHT into extraction tubes.
2. For KUDOS add 500µL RBC or Plasma and vortex. For Compliancy study add 1mL RBC or Plasma and vortex. Because the RBC's are sticky, plan to put only 3mL of methanol in each tube and rinse the pipette tip with 1mL methanol (from a separate beaker)
3. For KUDOS add 100µL internal standard (17:0) and vortex. For Compliancy study add 200µL internal standard (17:0) and vortex.
4. Add 8mL Chloroform and vortex.
5. Vortex RBC extract for 15 min. Vortex Plasma for 10 min. (Use the multi-tube vortexer).
6. Transfer contents through a funnel lined with filter paper (Whatman #1) into a clean extraction tube.
7. Add 1.6mL KCl and vortex for 10 seconds.
8. Centrifuge for 5 minutes at 750 r.p.m. and transfer bottom phase into a spotting tube with Pasteur pipette.
9. Evaporate solvent in a water bath at 35°C under nitrogen.
10. [Add 1-2mL benzene and re-evaporate if small amounts of water remain in sample].

Separation of neutral lipids and total or individual phospholipids:

11. When extract is completely dry, dissolve in 100µL cold dichloromethane. Spot all 100µL for analysis of total phospholipids. For compliancy study if separating PE, PC, and Total lipids dissolve in 150µL cold dichloromethane. Spot 100µL for analysis of PE, PC, and PL. Dry remaining 50 µL in water bath at 35°C under nitrogen. Pipette 1mL BF_3 into dry tube to collect Total lipids.
12. Place the spotted plate in a TLC chamber. If separating **total phospholipids** use TLC chamber containing 80:20:1 Hexane: Ether: Acetic Acid and that has been lined with filter paper (Whatman #1 sheets). If separating **partial phospholipids** use TLC chamber containing 60:30:8.4:4.6 Chloroform: methanol: acetic acid: water.
13. Allow the solvent front to run to the top of the plate, dry the plate under Nitrogen and spray with C:M + BBOT.
14. Identify the lipid to be analyzed using appropriate standard runs. Mark the separated lipids under an UV-light and remove the gel containing the lipid fraction of interest with a single edge razor blade onto weighing paper. Carefully transfer the gel to a 15mL Pyrex tube. Make sure that tubes are not cracked or chipped and a cap lined with Teflon is used.

Transmethylation:

15. Immediately add BF_3 (volumes specified in Table 1), layer each tube with Nitrogen. Tighten caps very tight and place in dry bath at 100°C for the time intervals as specified in Table 1.

Table 1

Parameter	BF_3 (mL)	Benzene (mL)	Methanol (mL)	Time (min)
Total Phospholipids	1.0	--	--	20
Individual Phospholipids: PC, PS, PI, PEA	1.0	--	--	10
SM	1.0	--	--	90
Triglycerides (TG)	0.50	0.40	1.10	30
Cholesterol ester (CE)	0.70	0.60	0.70	45

16. After 1-2 min. retighten caps as they tend to loosen during heating.

17. After transmethylation is complete, immediately place tubes on ice. When tubes are very cool, open and add the amounts of H_2O and pentane shown in Table 2.

Table 2

Parameter	Dist. H_2O (mL)	Pentane (mL)
Total phospholipids (TPL)	1.0	2.0
Individual Phospholipids: PC, PS, PI, PEA (each)	1.0	2.0
SM	1.0	2.0
Triglycerides (TG)	2.0	4.0
Cholesterol ester (CE)	2.0	4.0

18. Vortex for 1-2 min. to extract fatty acid methyl esters (FAME) into the pentane phase, then centrifuge for 5 min. at 800 r.p.m.

19. Transfer the upper phase (pentane) with a Pasteur pipette to a Varian 2mL vial with a Teflon-lined cap.
20. Concentrate the FAME under a stream of nitrogen.
21. When completely dry, add 60μL of dichloromethane to vial. Swirl tube and then transfer with syringe to sleeve. Place sleeve inside of 2 mL vial and cover vial with a Teflon-lined cap.
22. Place sample in autosampler tray to inject.

Section B: Molecular Biology

Isolation of RNA

I. For Mouse Tissues (step 3-7 are the same as those for cultured cells)

1. Collect mouse tissues as fast as possible and keep in liquid N2 / -80C or process immediately in Trizol (use > 3-fold volume of each tissue) for homogenization.

2. Grind frozen tissue in liquid N2 and mix with sufficient Trizol or homogenize tissues in Trizol with tissue grinder (at medium speed, such as setting 5).

   Divide each Trizol – sample mixture in 1 ml aliquots in sterile 1.5 ml tube.

II. For Cultured Adherent Cells (steps 1 -2 are different from above)

1. Aspirate off medium as much as possible.

2. Add Trizol to each plate: 1 ml for each 10-cm plate or each 6-cm plate for induced L1.

3. Let Trizol – sample mixture sit at Room Temperature (RT) for 10 minutes.

4. Add choloform to each mixture (0.2 ml per each ml Trizol) and invert tube 20 times to mix.

   For viscous mixtures, vortex briefly and gently to mix, e.g., 2 seconds at setting 5.

5. Let Trizol – choloform mixture sit at Room Temperature (RT) for 15-30 minutes for a good phase separation.

   Spin at 12000g for 10' at 4 ^{o}C to completely separate phases.

6. Keep each clear supernatant in a new sterile 1.5 tube (it's OK to stop here by keeping at -80C).

7. Add isopropanol to the above supernatant (0.5 ml per 1 ml Trizol) to precipitate RNA.

   Inverting tube to mix and let it sit at R.T. for 10' (it's OK to stop here by keeping at -20C).

8. Spin at 12000g for 10' at 4 ^{o}C to collect RNA pellet.

   Pour out the supernatant and wash the pellet with 70% EtOH (made up with DEPC-H2O, 0.5 – 1.0 ml per tube). Spin briefly (9000 rpm / 5') to keep pellet in place.

9. Remove ***all*** liquid (first with sterile 1 ml pipet-tip, brief spin, and then with 200 μl sterile tip to remove the last bit of liquid by touching the pellet).

10. Air-dry the pellet at R.T. for 5 minutes or until the edge of pellet starts to become transparent (over drying will make the pellet hard to dissolve).

11. Resuspend each pellet with formamide at an appropriate volume (20 - 100 μl).

    DEPC-H2O can be used to resuspend RNA, but it is more susceptible to degradation.

12. Determine RNA concentration with spectrophotometer by diluting each sample ~ 300-fold (add 1 μl sample to 299 μl H2O).

    Calculate by following: 1 OD260 unit = 0.04 μg/μl RNA.

Molecular Cloning

PCR reaction by Phusion High-Fidelity PCR Kit:

1. Set up the appropriate reactions in final volume of 25 μl on ice and follow the order from top to bottom:

Component	25 μl	Final concentration
Nuclease-free water	To 25 μl	
5×Phusion HF	5 μl	1×
10 mM dNTPs	0.5 μl	200 μM
10 uM primer each	1.25 μl	0.5 μM
Template DNA (plasmid)		100 ng
Phusion DNA Polymerase	0.25 μl	0.5 unit

Note: In all steps, it is better to use autoclaved tubes and tips. For PCR tube, it is fine to use non-autoclaved ones but tubes need to be clean.

2. Mix well by using pipette and spin down the spilling

3. Start reactions using parameter as follow:

Step	Cycles	Temperature	Time
Initial denaturation	1	98 ^{o}C	30 s
Denaturation	30	98 ^{o}C	7 s
Annealing		55 ^{o}C (5 ^{o}C < Tm)	30 s

Extension		72 ^{o}C	20 s
Final extension	1	72 ^{o}C	10 min
Hold	1	4 ^{o}C	forever

4. Run product in agarose gel (1.5 % for size<500 bp; 1% for 2 kb>size>500 bp). Cut right band in UV and try to shorten the time in UV to avoid mutations. Use gel purification kit to extract the PCR product. Usually Qiagen kit gives high yield.

Enzymatic digestion:

5. Set up restriction enzyme reactions for both PCR product and vector as below:

	PCR product	Vector plasmid
Amount of DNA	~500 ng	1 μg
10×buffer (check enzyme information for double digestion)	3 μl	4 μl
Nuclease-free water	to 30 μl	to 40 μl
BSA if necessary	1 μl	1 μl
Enzyme 1 (10 units/ul)	1 μl	1 μl
Enzyme 2 (10 units/ul)	1 μl	1 μl

6. Mix well by gently pipetting and incubate to right temperature in water bath (usually 37 ^{o}C) for 2 hour.

   Note: Check the manual for time and temperature. Usually 2 hour is required. Shorter time may give low yield of cut insert; long time digestion can cause star activity. Restriction enzymes can have decreased activity after sitting in -20 ^{o}C for long. Usually enzymes from NEB are stable.

7. Add 0.5 μl calf intestinal alkaline phosphatase (CIAP) to the digestion mixture of vector and incubate at 37 ^{o}C for 15 min; add 0.5 μl CIAP again and incubate for another 15 min.

   Note: CIAP is very useful to prevent self ligation of vector plasmid even in the case of double digestion. Self ligation will cause false negative colonies, whose plasmid does not contain insert. Do not treat insert with CIAP; otherwise no ligation will be obtained.

8. Run mixture of vector into agarose gel in longer time to well separate digested vector. Cut the band with right size for vector in UV. Try to avoid any other bands.

Ligation and transformation:

9. Follow the manual of ligation kit. Usually 50 ng vector is used. Insert is added to a **molar** ratio of 3:1 (3 for insert and 1 for vector). Mix them well by pipetting. For ligation, kit from NEB, Promega and Takara is good.

10. Follow the manual of competent cells (*E.coli* DH5α). Volume of ligation mixture should be within 10% of competent cell volume. For example, 5 μl ligation mixture for 50 μl competent cells. After transformation, the mixture is sprayed onto agarose plate containing

100 μg/ml ampicillin or other antibiotics for selection under germ-free condition.

11. After 16 hours of incubation in 37 ^{o}C oven, usually more than 50 colonies will be obtained. Pick two colonies to inoculate in two tubes of media (each 3 ml) supplemented with 100 μg/ml ampicillin or other antibiotics and let it shake at 225 rpm at 37 ^{o}C overnight.
12. Extract plasmid by following the manual of kit. Use about 1/3 for enzymatic digestion as shown in step 5 and 6 to verify the right insert. Send the plasmid with right insert for sequencing.

    Note: Save 700 μl of *E.coli* culture and add 300 μl of autoclaved 50% glycerol to make glycerol stock. Mix the stock well and keep it at -80 ^{o}C.

Mutagenesis

PCR reaction:

1. Mutagenesis is performed by QuikChange Multi Site-Directed Mutagenesis Kit. Use plasmid containing wild-type sequence as template. The whole plasmid is amplified by using two primers which introduce site mutation. Two primers are matched to each other with Tm>75 ^{o}C.

   Tm = 81.5 + 0.41(%GC)-675/N- % mismatch

   N is the primer length in bases

   Usually one primer contains 40-45 bases to make Tm above 75 ^{o}C. No PAGE purification for primer is required if N<45. Generally two mismatched bases (mutation of one amino acid) can give decent yield; four mismatched bases (mutations of two amino acids) give low yield.

2. Set up reaction on the ice as following order:

10×QuikChange Multi reaction buffer	2.5 μl
Nuclease-free water	to 25 μl
Plasmid	100 ng
Primers: 100 ng each	
dNTP	1 μl
QuikChange Multi enzyme blend	1 μl

Note: Increase of plasmid and primer amount can help if yield is too low.

3. Mix them well by pipetting up and down gently. Use the following parameters for PCR:

Segment	Cycles	Temperature	Time
1	1	95 ^{o}C	1 min
2	30	95 ^{o}C 55 ^{o}C 65 ^{o}C	1 min 1 min 2 min/kb
3	1	4 ^{o}C	forever

Note: After PCR is done, if next step can not be done, the mixture needs to be frozen at -20 ^{o}C.

Dpn I digestion of the amplification products:

4. Add 1 μl of *Dpn* I restriction enzyme (10 U/μl-20 U/μl) directly to each amplification reaction. Gently and thoroughly mix each reaction mixture by pipetting the solution up and down several times. Spin down the reaction mixtures, and then immediately incubate each reaction at 37 °C for 2 hour to digest the parental (non-mutated) plasmid.
5. Add 1 μl of *Dpn* I again to further digest the parental plasmid at 37 °C for another 2 hour.

   Note: The efficiency of amplification is not very high; 1 hour of digestion as suggested in the manual is not enough to remove the parental plasmid.
6. After digestion, add 2 μl products into 50 μl competent cells and follow the manual to finish transformation. Pick up two colonies for plasmid extraction. Send at the plasmid from two colonies for sequencing. Usually one of them will be mutated.

Section C: Protein Preparation

Preparation of Ncb5or-b5, Nb5M35 and Cyb5A

Protein expressions:

1. Ncb5or-b5 (the b5 domain of Ncb5or), Ncb5or-b5R113A, Ncb5or-b5W114A, Nb5M35 (the N-terminal region from M35 +Ncb5or-b5) and Cyb5A contain heme and have similarly low pI. Method for preparation of the proteins is identical.
2. Grow 10 ml culture (in LB media) of *E.coli* BL21(DE3) that harbors pET22bNcb5or-b5 at 37 ^{o}C overnight with a shaking speed of 225 rpm.

   Note: Scratch the surface of glycerol stock with autoclaved tips and dip the tip into media containing 100 μg/ml ampicillin. Glycerol stock is very convenient. Try to do this quickly to avoid thawing of glycerol stock.
3. 10 ml culture is inoculated into 2 L LB media, supplemented with 100 μg/ml ampicillin. Shake the 2 L of culture at 37 ^{o}C at a speed of 225 rpm until OD600 is between 0.7 and 0.8. Usually it takes about 3 hour.

   Note: Choose flask with right size for media. The media should be stirred once put into the shaker.
4. Cool the culture to room temperature. Add IPTG to the culture with final concentration of 1 mM. Shake it at 25 ^{o}C with a speed of 150 rpm for 6 hour.

   Note: IPTG and ampicillin can be made as stock of 1 M and 100 mg/ml, respectively, with autoclaved water. Stocks need to be filtered (0.2 um) and aliquot, and can be stored in -20 ^{o}C.
5. Once the induction is done, cool the culture to 4 ^{o}C. Pellet the cells down by centrifugation at

4 ^{o}C at 5000 g for 15 min. Remove the supernatant.

Note: Each centrifuge bottle can hold about 400 ml. It is fine to keep adding more culture after removing the supernatant each time.

6. Freeze cell pellet in mixture of dry ice and ethanol. Store it at -80 ^{o}C until process.

Heme titration:

7. Resuspend the cell pellet with 40 ml lysis buffer (50 mM Tris-HCl, pH 8, 30 mM NaCl, 1 mM EDTA, half tablet of protease inhibitor cocktail from Sigma) by pipetting up and down. Try to avoid air bubble and make resuspension homogenous.

   Note: Protease inhibitor cocktail is not necessary if the following steps are not delayed. For Nb5M35, no NaCl needs to be included in the lysis buffer, since the binding to Q column is not very tight.

8. Break cells by sonication. Right before sonication, add PMSF to the resuspension to the concentration of 1 mM and mix well by invert tube several times. Parameters for sonication are different by disruptors. For disruptor by Fisher which equipped with a big probe, the parameters are:

Sonication	5 s at 70% of maximal magnitude
Rest	45 s

Repeat the cycle above for 20 times

The sample tube should be buried into ice. Dip the probe of sonicator into the sample until close to the bottom of tube. Do not touch the bottom. The lysate is usually pink.

9. Load the lysate into centrifuge tubes (each can hold 30 ml maximal). Spin the lysate at 4 ^{o}C at 15000 g for 45 min. Save the supernatant for the next step.

10. Ncb5or-b5, Nb5M35 and Cyb5A are expressed as apo-protein (little heme bound to protein). To generate functional holo-protein, heme needs to be added. The first step is heme titration to determine amount of heme added to the sample. Take 200 μl from supernatant and dilute it 10 fold with the lysis buffer. The final volume is 2 ml and is held in a wide cuvette. Drop a small stir bar to the bottom of cuvette and let it rotate at grade 7 so that the whole volume can be stirred. Scan the cuvette from 600 nm to 300 nm. Usually the reading at 413 nm is about 0.2-0.3. **Slowly** add 5 μl of 0.5 mg hemin solution (dissolved in DMSO) and let stir bar rotate for **2 min**. Scan the cuvette again in the same range and check the reading at 413 nm. Usually there is increase of 0.2. Repeat adding of heme and scanning until increase of reading at 413 nm is within 0.1. Add 5 μl of 0.5 mg hemin solution again. If the increase at 413 nm is still within 0.1, stop the heme titration. Calculate total volume of hemin added.

    Note: For titration of Cyb5A, supernatant can be diluted more than 20 fold because of the high yield. Keep the stir bar rotate to avoid heme aggregate. After each adding, stirring of 2 min is necessary.

11. Based the result of titration, calculate how much of 5 mg hemin solution (dissolved) to be added to the supernatant. Adding of 5 mg hemin should be divided into at least 4 times. There is an interval of 5 min between two adding. Before the first adding, the sample (supernatant) needs to be warmed to close to room temperature and the pH needs to be adjusted to 8 with 1 M Tris base. In each adding, keep the stir bar rotate. Put the end of tip into sample, **slowly**

push pipette and **gently** release hemin into the sample. Now hemin should diffuse due to stir bar. Gently tilt the tube several times to make hemin homogenous. Wait for 5 min before next adding. When it is finished, the sample should change from pink to red.

Note: Heme adding is the only step to be done at room temperature during sample process and purification. This is to avoid precipitation of DMSO. Slow adding and efficient stirring are important to prevent heme aggregate which crashes protein.

12. Centrifuge the sample titrated with heme at 4 ^{o}C at 20000 rpm for 2 hour. Save supernatant and filter it with 0.45 μm syringe filter.

Protein purification at 4 ^{o}C:

13. Dilute the sample 3 fold with buffer A (20 mM Tris-HCl, pH 8). Diluted sample is loaded to HiTrap Q HP column (10 ml) by ÄKTAxpress purification system (GE Healthcare Life Sciences) at 4 ^{o}C. The flow rate for all steps is 1 ml/min. The program is:

    Inlet A: linked to buffer A (20 mM Tris-HCl, pH 8)

    Inlet B: linked to buffer B (20 mM Tris-HCl, 1M NaCl, pH 8)

    Inlet S: linked to sample

    Column equilibrium: 5 column volumes (CV) of buffer A

    Completion of loading: 2 CV of buffer A

    Washing: 30 ml buffer A

    Gradient elution: linear increase of salt concentration from 0 to 1 M NaCl in 20 CV

    Auto collection: 2 ml of each fraction in 96-well plate

Note: Buffer A and B need to be filtered with 0.2 um filter. Before starting, pump wash of inlet A, B and S is necessary. Pressure limit is set to 0.5 MPa to avoid damage of system. Targeted protein is usually eluted around 200 mM to 300 mM NaCl.

14. Choose red fractions within the dominant peak of UV. The peak does not have any shoulder. Pool them together and add NaCl to 1 M.
15. Resultant sample is loaded to HiTrap Phenyl HP column (10 ml) by ÄKTAxpress purification system. The flow rate for all steps is 1 ml/min. Before starting, perform pump wash for inlet A, B and S. The program is

    Inlet A: linked to buffer B (20 mM Tris-HCl, 1M NaCl, pH 8)

    Inlet B: linked to buffer A (20 mM Tris-HCl, pH 8)

    Inlet S: pooled sample with 1 M NaCl

    Column equilibrium: 5 column volumes (CV) of buffer B

    Completion of loading: 2 CV of buffer B

    Washing: 30 ml buffer B

    Gradient elution: linear decrease of salt concentration from 1M NaCl to 0 M NaCl in 20 CV

    Auto collection: 2 ml of each fraction in 96-well plate.

    Flow through is collected with red color. Try to avoid taking much colorless buffer. Concentrate flow through down to less than 1.5 ml by using a concentrator with selection size of 3 kD or 5 kD.

16. The concentrated sample is injected into sample loop with syringe and loaded to Superdex 200 column (120 ml) by FPLC system (GE Healthcare Life Sciences). Before loading the column is equilibrated with 1.1 column volume of running buffer. The running buffer is 20 mM Tris-HCl, pH 7. The flow rate is 0.5 ml/min. Collect and pool the red fractions within the dominant UV peak.
17. Concentrate protein to 1 ml, dilute with 20 mM Tris-HCl, pH 7 and concentrate to 1 ml again.
18. Aliquot the concentrated protein, freeze them with liquid nitrogen, and store them in -80 ^{o}C. Purified holo Ncb5or-b5 has ratio of A413/A280 about 4. Purified holo Nb5M35 has ratio of A413/A280 about 3.5. Purified holo Cyb5A has a ratio of A413/A280 about 6.4. The yield is 8 mg/L for Ncb5or-b5 and Nb5M35, 20 mg/ml for Cyb5A.

SDS-PAGE and Native PAGE:

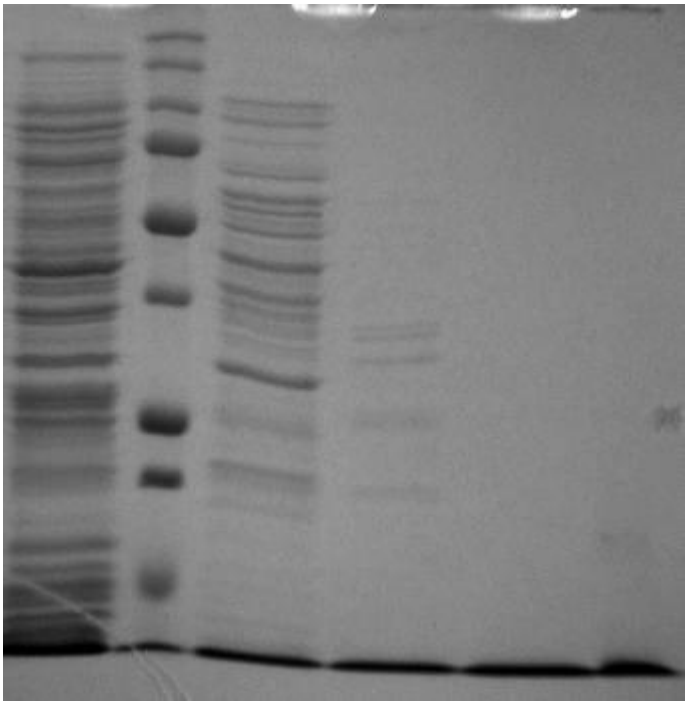

1 2 3 4 5 6

SDS-PAGE of Ncb5or-b5: 1. supernatant; 2. marker; 3. minor peak in ionic exchange (IE); 4.after IE; 5: after Superdex 200; 6. after Superdex 200 without BME. Ncb5or-b5 is at 10 kD mark level.

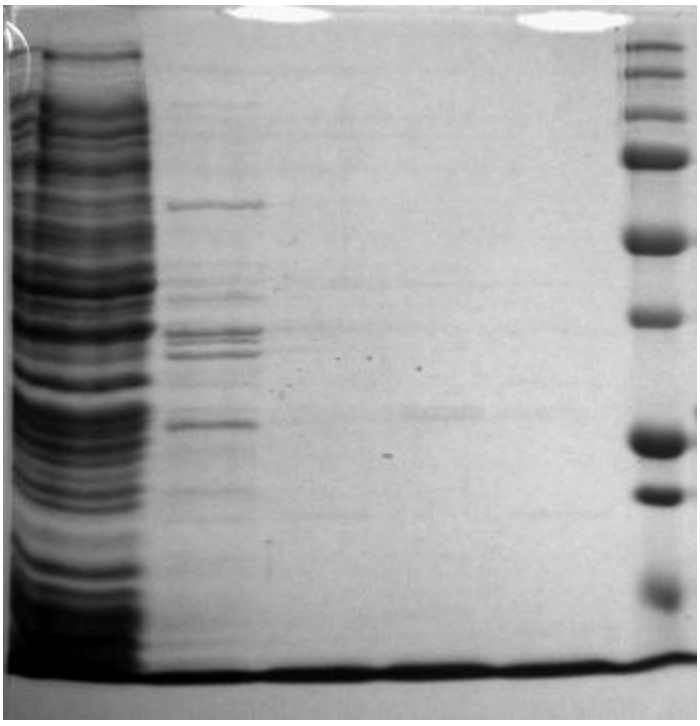

1 2 3 4 5 6

SDS-PAGE of Ncb5or-b5, b5R113 and b5W114A: 1. b5R113 supernatant; 2. b5R113A after phenyl HP column; 3. purified Ncb5or-b5; 4. purified b5W114A; 5. purified b5R113A; 6. marker

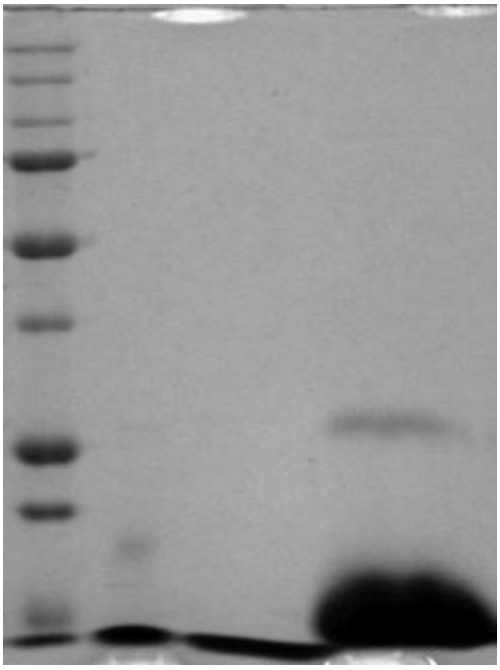

1 2 3 4

SDS-PAGE of Ncb5or-b5 and Cyb5A: 1. marker; 2. Ncb5or-b5 no BME; 3. Ncb5or-b5; 4. Cyb5A

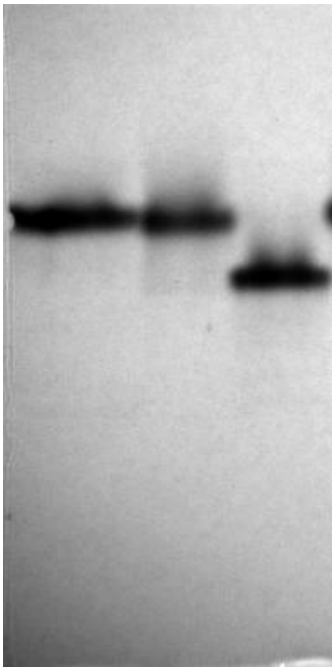

1 2 3

Native gel of Ncb5or-b5, b5W114A and b5R113A: 1. Ncb5or-b5; 2. b5W114A; 3. b5R113A.

1 2

Native gel of Ncb5or-b5 and Nb5M35: 1. Nb5M35; 2. Ncb5or-b5.

Native gel of Cyb5A.

Mass spectra:

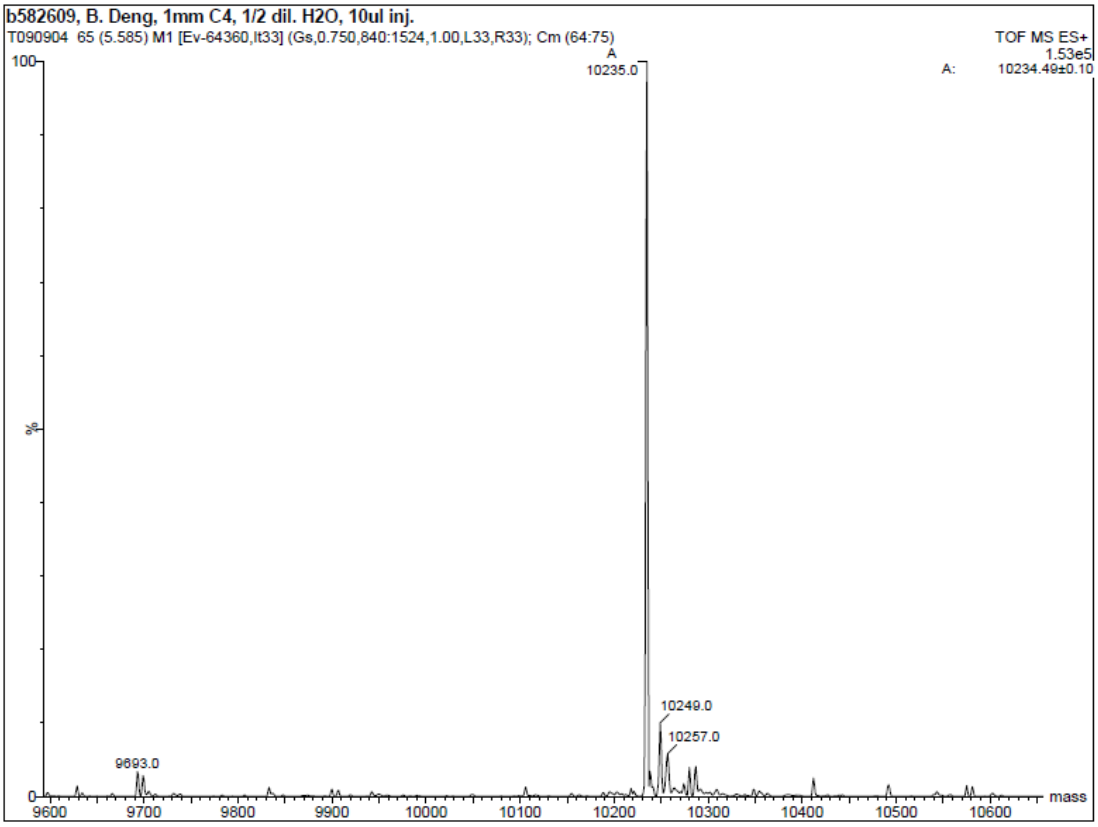

Positive ESI of Ncb5or-b5: the expected size of Ncb5or-b5 is 10234.8.

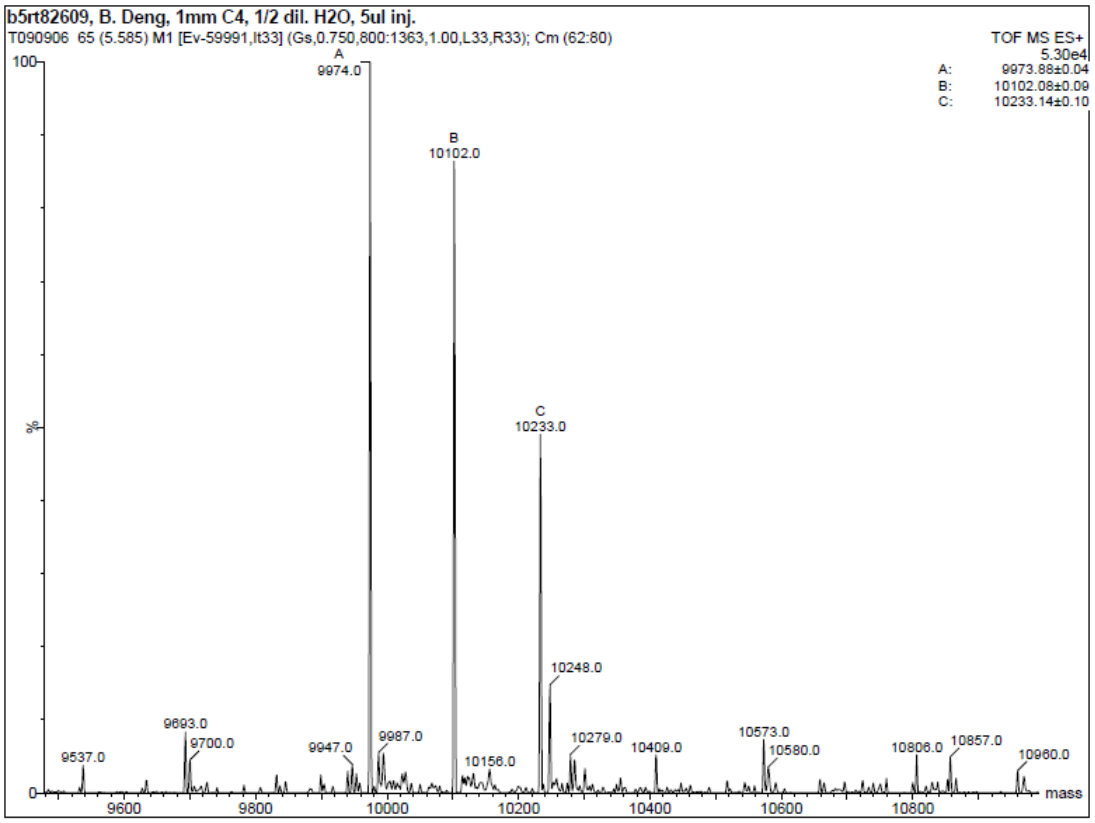

Degrade Ncb5or-b5: After sitting at room temperature for one week, Ncb5or-b5 will be cleaved.

At 4 ^{o}C, Ncb5or-b5 can be stable for more than one week.

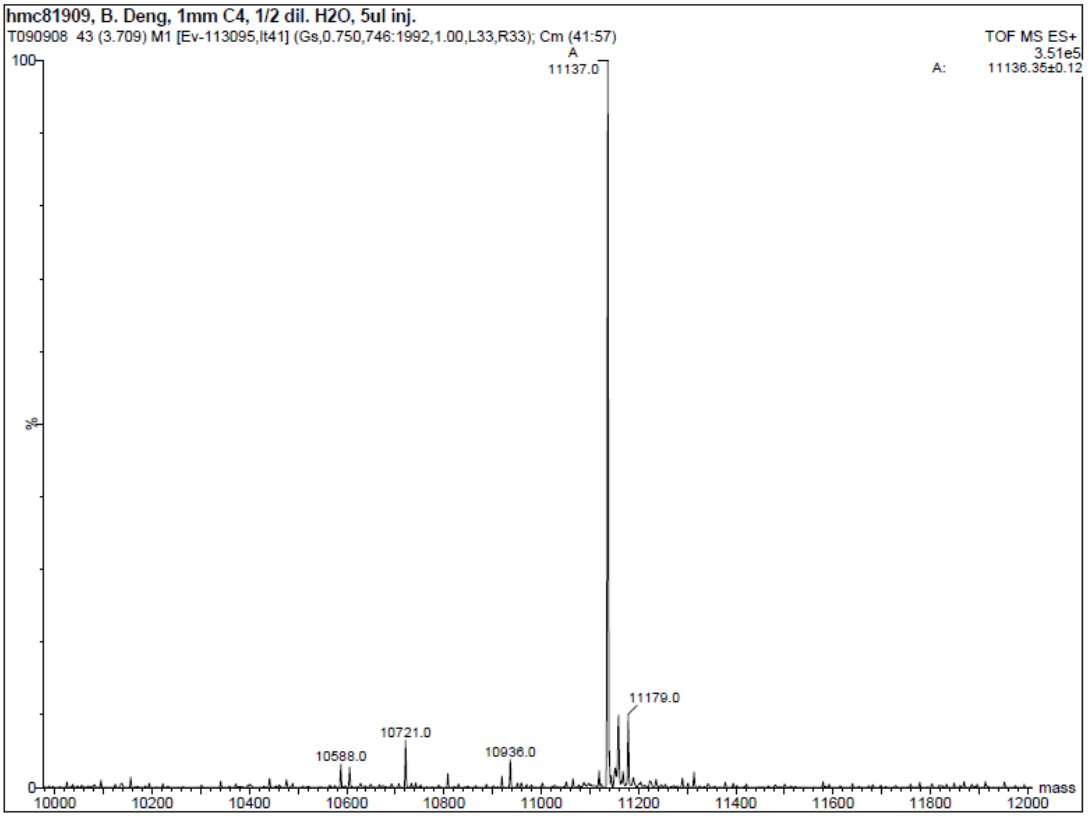

Positive ESI of Cyb5A: expected size for Cyb5A is 11268.4. The difference of 131 is due to cleavage of the initial Met residue.

Sequence of Ncb5or-b5 (in pET22b):

MKGRLIEVTEEELKKHNKKDDCWICIRGFVYNVSPYMEYHPGGEDELMRAAGSDGTEL

FDQVHRWVNYESMLKECLVGRMAIKPAVLK

Sequence of Nb5M35 (in pET22b):

MDWIRLTKSGKDLTGLKGRLIEVTEEELKKHNKKDDCWICIRGFVYNVSPYMEYHPGGE

DELMRAAGSDGTELFDQVHRWVNYESMLKECLVGRMAIKPAVLK

Sequence of Cyb5A (in pET22b):

MAEQSDEAVK YYTLEEIQKH NHSKSTWLIL HHKVYDLTKF LEEHPGGEEV

LREQAGGDATENFEDVGHST DAREMSKTFI IGELHPDDRP KLNKPPEP

Preparation of Nb5, Nb5R13 and Nb5G22

Protein expressions:

1. Nb5 (the N-terminal region + Ncb5or-b5), Nb5R13 (the N-terminal region from R13+Ncb5or-b5), Nb5G22 (the N-terminal region from G22 +Ncb5or-b5), Nb5W37A and Nb5LMAA contain heme and have similarly high pI. Method for preparation of the proteins is identical.
2. 10 ml culture (in LB media) of *E.coli* BL21(DE3) which harbor the plasmid are grown at 37 ^{o}C overnight with a shaking speed of 225 rpm.

   Note: Scratch the surface of glycerol stock with autoclaved tips and dip the tip into media containing 100 μg/ml ampicillin. Glycerol stock is very convenient. Try to do this quickly to avoid thawing of glycerol stock.
3. 10 ml culture is inoculated into 2 L LB media, supplemented with 100 μg/ml ampicillin. Shake the 2 L of culture at 37 ^{o}C at a speed of 225 rpm until OD600 is between 0.7 and 0.8. Usually it takes about 3 hour.

   Note: Choose flask with right size for media. The media should be stirred once put into the shaker.
4. Cool the culture to room temperature. Add IPTG to the culture with final concentration of 0.5 mM. Shake it at 25 ^{o}C with a speed of 150 rpm for 6 hour.

   Note: IPTG and ampicillin can be made as stock of 1 M and 100 mg/ml, respectively, with autoclaved water. Stocks need to be filtered (0.2 um) and aliquot, and can be stored in -20 ^{o}C.
5. Once the induction is done, cool the culture to 4 ^{o}C. Pellet the cells down by centrifugation at

4 ^{o}C at 5000 g for 15 min. Remove the supernatant.

Note: Each centrifuge bottle can hold about 400 ml. It is fine to keep adding more culture after removing the supernatant each time.

6. Freeze cell pellet in mixture of dry ice and ethanol. Store it at -80 ^{o}C until process.

Heme titration:

7. Resuspend the cell pellet with 40 ml lysis buffer (50 mM Tris-HCl, pH 7, 30 mM NaCl, 1 mM EDTA, half tablet of protease inhibitor cocktail from Sigma) by pipetting up and down. Try to avoid air bubble and make resuspension homogenous.

   Note: For Nb5G22, no NaCl needs to be included in the lysis buffer, since the binding to SP column is not very tight.

8. Break cells by sonication. Right before sonication, add PMSF to the resuspension to the concentration of 1 mM and mix well by invert tube several times. Parameters for sonication are different by disruptors. For disruptor by Fish which equipped with a big probe, the parameters are:

Sonication	5 s at 70% of maximal magnitude
Rest	45 s

Repeat the cycle above for 20 times

The sample tube should be buried into ice. Dip the probe of sonicator into the sample until close to the bottom of tube. Do not touch the bottom. The lysate is usually pink.

9. Load the lysate into centrifuge tubes (each can hold 30 ml maximal). Spin the lysate at 4 ^{o}C at

15000 g for 45 min. Save the supernatant for the next step.

10. The protein is expressed as apo-protein (little heme bound to protein). To generate functional holo-protein, heme needs to be added. The first step is heme titration to determine amount of heme added to the sample. Take 400 μl from supernatant and dilute it 5 fold with the lysis buffer. The final volume is 2 ml and is held in a wide cuvette. Drop a small stir bar to the bottom of cuvette and let it rotate at grade 7 so that the whole volume can be stirred. Scan the cuvette from 600 nm to 300 nm. Usually the reading at 413 nm is about 0.2-0.3. **Slowly** add 5 μl of 0.5 mg hemin solution (dissolved in DMSO) and let stir bar rotate for **2 min**. Scan the cuvette again in the same range and check the reading at 413 nm. Usually there is increase of 0.2. Repeat adding of heme and scanning until increase of reading at 413 nm is within 0.1. Add 5 μl of 0.5 mg hemin solution again. If the increase at 413 nm is still within 0.1, stop the heme titration. Calculate total volume of hemin added.

    Note: Keep the stir bar rotate to avoid heme aggregate. After each adding, stirring of 2 min is necessary.

11. Based the result of titration, calculate how much of 5 mg hemin solution (dissolved) to be added to the supernatant. Adding of 5 mg hemin should be divided into at least 4 times. There is an interval of 5 min between two adding. Before the first adding, the sample (supernatant) needs to be warmed to close to room temperature. In each adding, keep the stir bar rotate. Put the end of tip into sample, **slowly** push pipette and **gently** release hemin into the sample. Now hemin should diffuse due to stir bar. Gently tilt the tube several times to make hemin homogenous. Wait for 5 min before next adding. When it is finished, the sample should

change from pink to red.

Note: Heme adding is the only step to be done at room temperature during sample process and purification. This is to avoid precipitation of DMSO. Slow adding and efficient stirring are important to prevent heme aggregate which crashes protein.

12. Centrifuge the sample titrated with heme at 4 ^{o}C at 20000 rpm for 2 hour. Save supernatant and filter it with 0.45 um syringe filter.

Protein purification at 4 ^{o}C:

13. Dilute the sample 3 fold with buffer A (20 mM Tris-HCl, pH 8). Diluted sample is loaded to HiTrap SP HP column (10 ml) by ÄKTAxpress purification system (GE Healthcare Life Sciences) at 4 ^{o}C. The flow rate for all steps is 1 ml/min. The program is:

    Inlet A: linked to buffer A (20 mM Tris-HCl, pH 7)

    Inlet B: linked to buffer B (20 mM Tris-HCl, 1M NaCl, pH 7)

    Inlet S: linked to sample

    Column equilibrium: 5 column volumes (CV) of buffer A

    Completion of loading: 2 CV of buffer A

    Washing: 30 ml buffer A

    Gradient elution: linear increase of salt concentration from 0 to 1 M NaCl in 20 CV

    Auto collection: 2 ml of each fraction in 96-well plate

Note: Buffer A and B need to be filtered with 0.2 um filter. Before starting, pump wash of inlet A, B and S is necessary. Pressure limit is set to 0.5 MPa to avoid damage of

system. Targeted protein is usually eluted around 200 mM to 300 mM NaCl.

14. Choose red fractions within the dominant peak of UV. The peak does not have any shoulder. Pool them together and add NaCl to 1 M.
15. Resultant sample is loaded to HiTrap Phenyl HP column (10 ml) by ÄKTAxpress purification system. The flow rate for all steps is 1 ml/min. Before starting, perform pump wash for inlet A, B and S. The program is

    Inlet A: linked to buffer B (20 mM Tris-HCl, 1M NaCl, pH 7)

    Inlet B: linked to buffer A (20 mM Tris-HCl, pH 7)

    Inlet S: pooled sample with 1 M NaCl

    Column equilibrium: 5 column volumes (CV) of buffer B

    Completion of loading: 2 CV of buffer B

    Washing: 30 ml buffer B

    Gradient elution: linear decrease of salt concentration from 1M NaCl to 0 in 20 CV

    Auto collection: 2 ml of each fraction in 96-well plate.

    Flow through is collected with red color. Try to avoid taking much colorless buffer. Concentrate flow through down to less than 1.5 ml **with 1 mM PMSF** by using a concentrator with selection size of 3 kD or 5 kD.
16. The concentrated sample is injected into sample loop with syringe and loaded to Superdex 200 column (120 ml) by FPLC system (GE Healthcare Life Sciences). Before loading, the column is equilibrated with 1.1 column volume of running buffer. The running buffer is 20 mM Tris-HCl, pH 7. The flow rate is 0.5 ml/min. Collect and pool the red fractions within the

dominant UV peak.

Note: Peak has shoulders.

17. Concentrate protein down to 1 ml, dilute with 20 mM Tris-HCl, pH 7 and concentrate to 1 ml again.

18. Aliquot the concentrated protein, freeze them with liquid nitrogen, and store them in -80 ^{o}C. Purified holo Nb5, Nb5R13, Nb5G22 and Nb5LMAA have ratio of A413/A280 about 3.5. Purified holo Nb5W37A has ratio of A413/A280 about 4. The yield is about 3-5 mg/L for each.

SDS-PAGE and Native gel

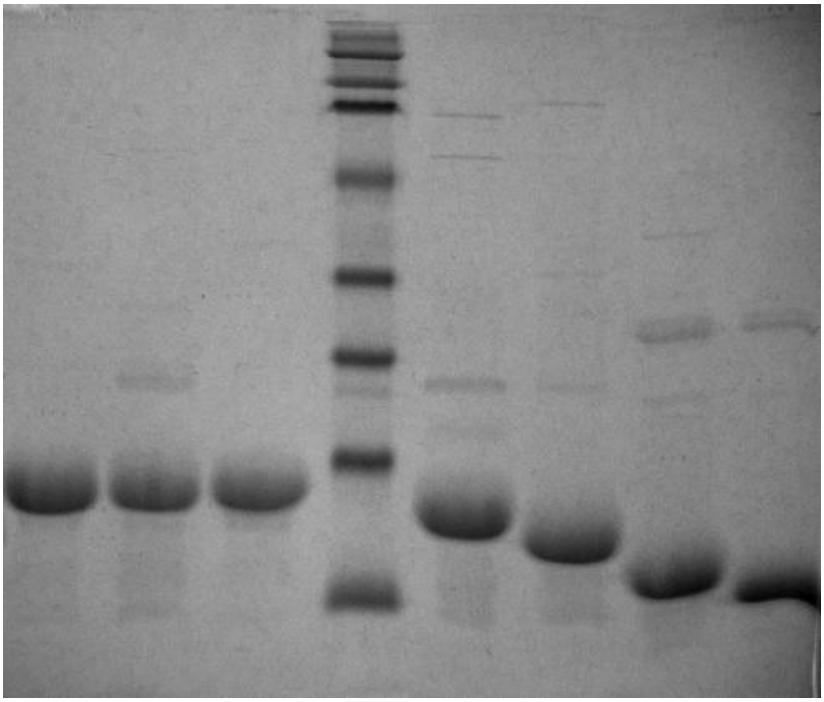

1 2 3 4 5 6 7 8

SDS-PAGE of different Nb5: 1. Nb5; 2. Nb5W37A; 3. Nb5LMAA; 4. marker; 5. Nb5R13; 6. Nb5G22; 7. Nb5M35; 8. Ncb5or-b5. All bands are between 17.5 and 6.6 kD marker bands.

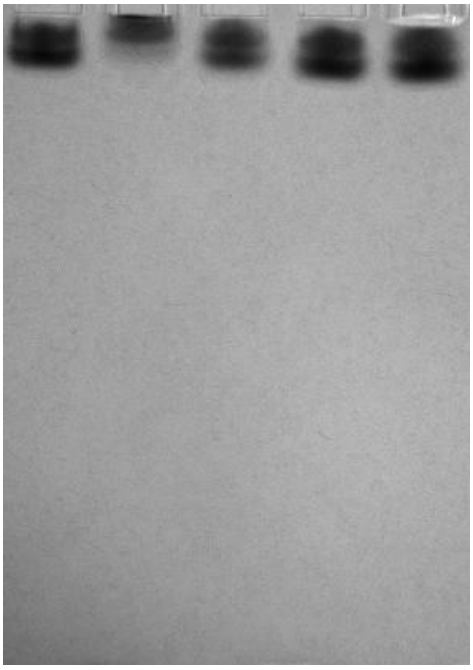

1 2 3 4 5

Native gel of different Nb5: 1. Nb5; 2. Nb5W37A; 3. Nb5LMAA; 4. Nb5R13; 5. Nb5G22. Because of their high pI values, all the proteins were run from positive to negative electrode pole, the opposite of normal polarity, with pH 7.0 for the resolving gel and the running buffer.

Mass spectra:

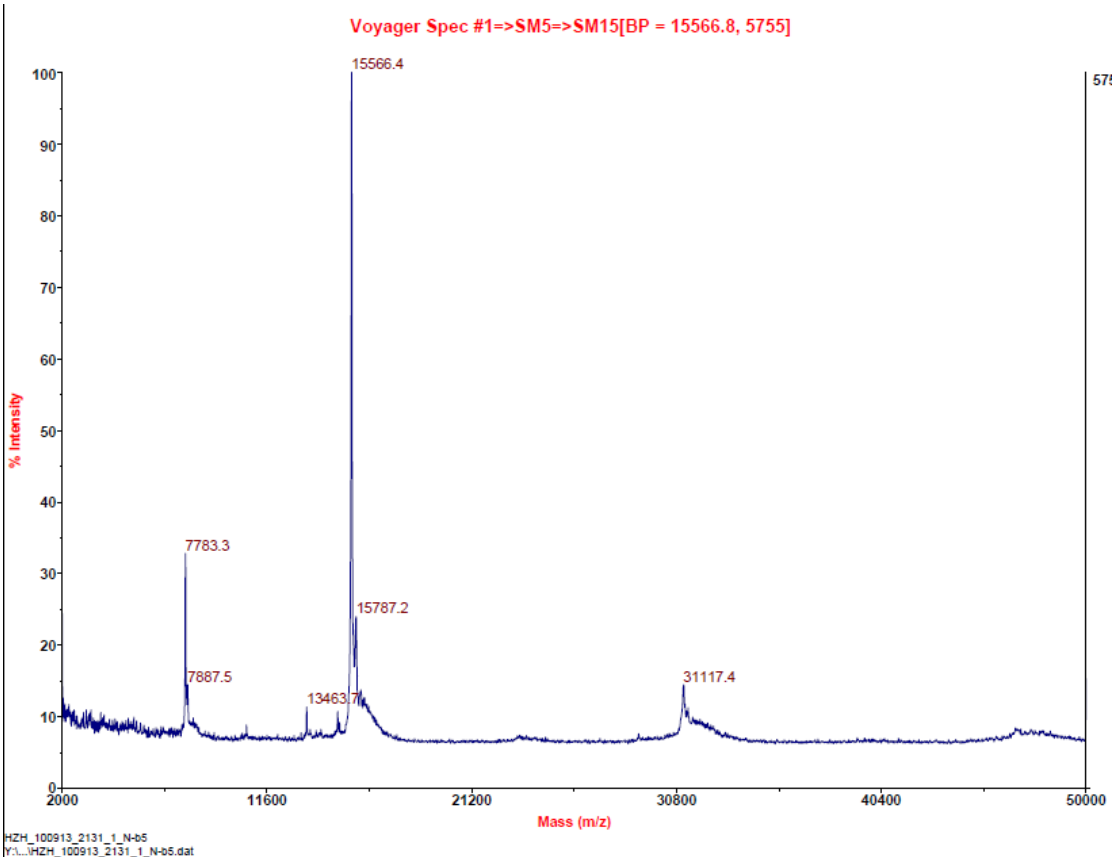

MALDI mass spectra of Nb5: The expected size of Nb5 is 15567, and purified Nb5 is 15566.4.

Sequence of Nb5 (in pET22b):

MLNVPSQSFPAPRSQQRVASGGRSKVPLKQGRSLMDWIRLTKSGKDLTGLKGRLIEVTEE
ELKKHNKKDDCWICIRGFVYNVSPYMEYHPGGEDELMRAAGSDGTELFDQVHRWVNY
ESMLKECLVGRMAIKPAVLK

Sequence of Nb5R13 (in pET22b):

MRSQQRVASGGRSKVPLKQGRSLMDWIRLTKSGKDLTGLKGRLIEVTEEELKKHNKKDD
CWICIRGFVYNVSPYMEYHPGGEDELMRAAGSDGTELFDQVHRWVNYESMLKECLVGR
MAIKPAVLK

Sequence of Nb5G22 (in pET22b):

MGRSKVPLKQGRSLMDWIRLTKSGKDLTGLKGRLIEVTEEELKKHNKKDDCWICIRGFV
YNVSPYMEYHPGGEDELMRAAGSDGTELFDQVHRWVNYESMLKECLVGRMAIKPAVL
K

Preparation of Ncb5or-b5R

Protein expressions:

1. Grown 10 ml culture (in LB media) of *E.coli* BL21(DE3) that harbors pET19bNcb5or-b5R at 37 ^{o}C overnight with a shaking speed of 225 rpm.

   Note: Scratch the surface of glycerol stock with autoclaved tips and dip the tip into media containing 100 μg/ml ampicillin. Glycerol stock is very convenient. Try to do this quickly to avoid thawing of glycerol stock.

2. 10 ml culture is inoculated into 2 L TB media, supplemented with 100 μg/ml ampicillin and 100 uM riboflavin. Shake the 2 L of culture at 37 ^{o}C at a speed of 225 rpm until OD600 is close to 1. Usually it takes about 3 hour.

   Note: Choose flask with right size for media. The media should be stirred once put into the shaker.

3. Cool the culture at 4 ^{o}C until it is colder than room temperature. Add IPTG to the culture with final concentration of 0.5 mM. Shake it at 15 ^{o}C with a speed of 150 rpm overnight.

   Note: IPTG and ampicillin can be made as stock of 1 M and 100 mg/ml, respectively, with autoclaved water. Stocks need to be filtered (0.2 um) and aliquot, and can be stored in -20 ^{o}C. Riboflavin can be dissolved with autoclaved water. The stock is stored at 4 ^{o}C with a concentration of 100 mM. No filtration is required.

4. Once the induction is done, cool the culture to 4 ^{o}C. Pellet the cells down by centrifugation at 4 ^{o}C at 5000 g for 15 min. Remove the supernatant.

   Note: Each centrifuge bottle can hold about 400 ml. It is fine to keep adding more culture

after removing the supernatant each time.

5. Freeze cell pellet in mixture of dry ice and ethanol. Store it at -80 ^{o}C until process.

Protein purification at 4 ^{o}C or cold room:

6. Resuspend the cell pellet with 40 ml lysis buffer (50 mM Tris-HCl, pH 8, 500 mM NaCl, 10 mM imidazole and half tablet of **EDTA-free** protease inhibitor cocktail from Sigma) by pipetting up and down. Try to avoid air bubble and make resuspension homogenous.

   Note: High salt concentration can prevent aggregate of Ncb5or-b5R. EDTA can strip Ni in the column.

7. Break cells by using French press (Thermal). Right before the disruption, add 1 mM PMSF to the resuspension and mix well by invert tube several times. The chamber (or cell) of French press holds 35 ml maximal and needs to be pre cool at 4 ^{o}C. The pressure is set to 1000 psi. Each sample should be loaded to the chamber twice to get fully disrupted.

8. Load the lysate into centrifuge tubes (each can hold 30 ml maximal). Spin the lysate at 4 ^{o}C at 15000 g for 45 min. Save the supernatant and have it filtered with 0.45 um filter.

9. Appropriate amount of Ni-NTA (QIAGEN) is added to a gravity column containing tube connection. Make sure that the surface is even. Let 10 column volumes (CV) of water flow through the column to make the resin compact. Equilibrate the column with 3 CV of lysis buffer (step 6).

   Note: All the buffers running through the column needs to be filtered.

10. The filtered sample is loaded to the Ni column with about 4 ml Ni-NTA beads (QIAGEN) by

a constant pump at a rate of 1 ml/min. During loading, yellow color can be observed at the top of column.

11. Wash the column with washing buffer (50 mM Tris-HCl, 500 mM NaCl, 20 mM imidazole and 1 mM PMSF, pH 8). About 20 CV of washing buffer is loaded to flow through the column by the constant pump at a rate of 1 ml/min until A280 of flow though is below 0.1 (use washing buffer as blank). After washing step, the resin should show yellow on the top and blue in rest of part.

    Note: PMSF needs to be newly added because it is not stable in aqueous solution. However, PMSF can be stable in isopropanol for half a year.

12. Elute the protein with more that 3 CV of elution buffer (50 mM Tris-HCl, 500 mM NaCl, 200 mM imidazole, 1 mM PMSF, pH 8) driven by the constant pump at a rate of 1 ml/min. Collect all the fractions and pool the yellow fractions together.

    Note: For some fractions with light color, if you are not sure, you can scan them and check A461 (absorbance of FAD).

13. Clean the column with 5 CV of cleaning buffer (50 mM Tris-HCl, 500 mM NaCl, 500 mM imidazole, pH 8). Remove cleaning buffer with 3 CV of water. Fill the column with 3 CV of 20% ethanol.

    Note: Ethanol may not be compatible with salt. Every time from ethanol to salt or from salt to ethanol, cleaning the column with water is necessary.

14. Concentrate the pooled yellow fractions with 1 mM PMSF to less than 0.5 ml. The concentrated sample is injected into sample loop with syringe and loaded to Size Exclusion

100 column by FPLC system (GE Healthcare Life Sciences). Before loading, the column is equilibrated with 1.1 column volume of running buffer. The running buffer is 20 mM Tris-HCl, pH 7, 500 mM NaCl, 0.1 mM EDTA. The flow rate is 0.2 ml/min. Collect and pool the yellow fractions within the dominant UV peak.

Note: Concentration without PMSF can cause minor degradation. If Size Exclusion 100 column is not available, use Superdex 75 with the same parameters.

15. Concentrate protein to 1 ml with supplement of 1 mM PMSF. Dilute with the same buffer for gel filtration and concentrate to 1 ml again with 1 mM PMSF.
16. Aliquot the concentrated protein, freeze them with liquid nitrogen, and store them in -80 ^{o}C. The yield for Ncb5or-b5R is about 2 mg/L.

SDS-PAGE and native gel:

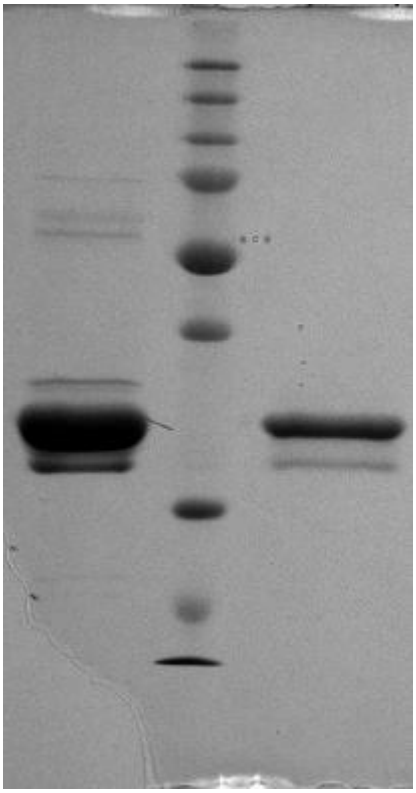

1 2 3

SDS-PAGE of Ncb5or-b5R: 1. Ncb5or-b5R after Ni column; 2. marker; 3. Ncb5or-b5R after size exclusion.

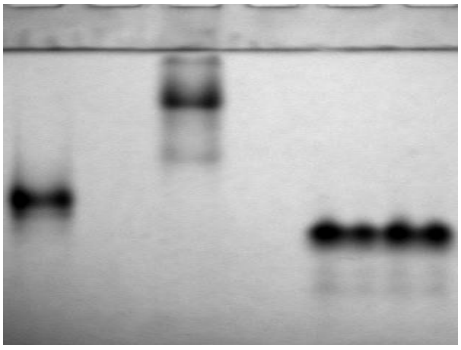

1 2 3

Native gel: 1. Ncb5or-CS/b5R; 2. Ncb5or-b5R; 3. Ncb5or-b5.

Mass spectra:

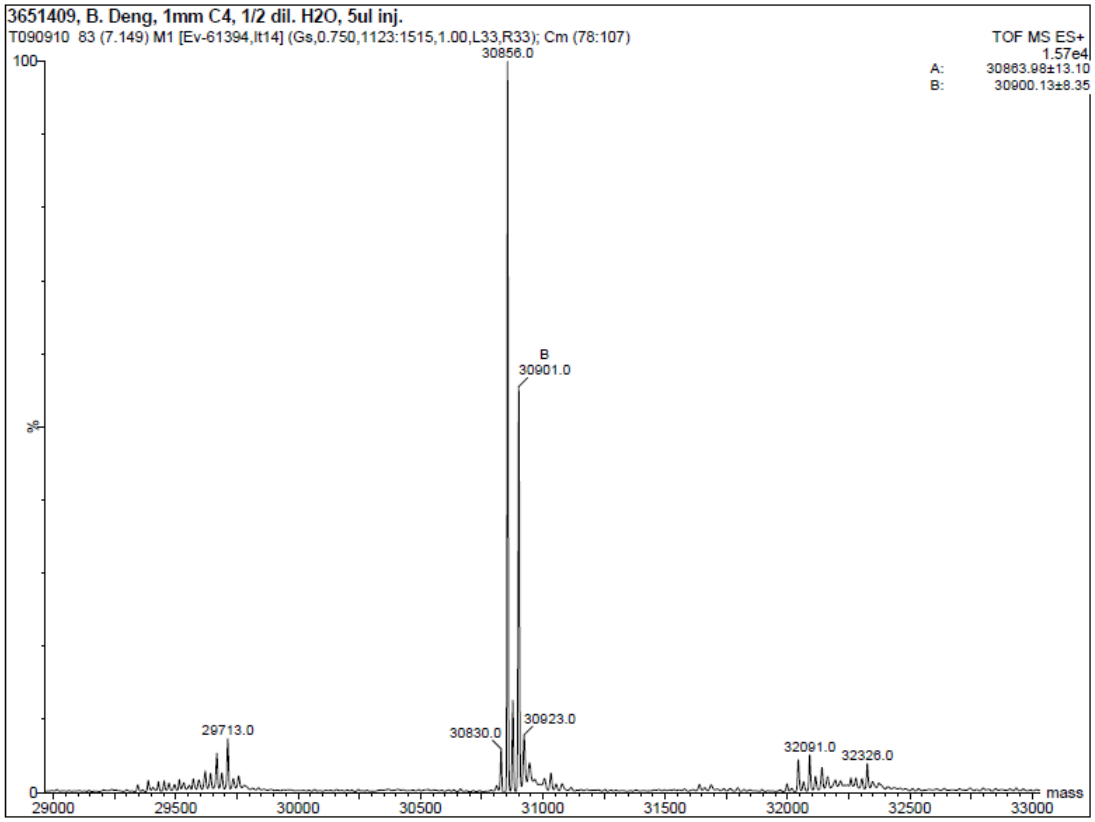

Positive ESI of Nb5or-b5R: the expected size is 30897.

Sequence of Ncb5or-b5R (in pET19b):

MGHHHHHHKNHNSLIPRKDTGLYYRKCQLISKEDVTHDTRLFCLMLPPSTHLQVPIGQH

VYLKLPITGTEIVKPYTPVSGSLLSEFKEPVLPNNKYIYFLIKIYPTGLFTPELDRLQIGDFV

SVSSPEGNFKISKFQELEDLFLLAAGTGFTPMVKILNYALTDIPSLRKVKLMFFNKTEDDII

WRSQLEKLAFKDKRLDVEFVLSAPISEWNGKQGHISPALLSEFLKRNLDKSKVLVCICGP

VPFTEQGVRLLHDLNFSKNEIHSFTA

Preparation of Ncb5or-CS/b5R

Protein expressions:

1. Grown 10 ml culture (in LB media) of *E.coli* BL21(DE3) that harbors pET19bNcb5or-CS/b5R at 37 ^{o}C overnight with a shaking speed of 225 rpm.

   Note: Scratch the surface of glycerol stock with autoclaved tips and dip the tip into media containing 100 μg/ml ampicillin. Glycerol stock is very convenient. Try to do this quickly to avoid thawing of glycerol stock.

2. 10 ml culture is inoculated into 2 L TB media, supplemented with 100 μg/ml ampicillin and 100 uM riboflavin. Shake the 2 L of culture at 37 ^{o}C at a speed of 225 rpm until OD600 is close to 1. Usually it takes about 3 hour.

   Note: Choose flask with right size for media. The media should be stirred once put into the shaker.

3. Cool the culture at 4 ^{o}C until it is colder than room temperature. Add IPTG to the culture with final concentration of 0.5 mM. Shake it at 15 ^{o}C with a speed of 150 rpm overnight.

   Note: IPTG and ampicillin can be made as stock of 1 M and 100 mg/ml, respectively, with autoclaved water. Stocks need to be filtered (0.2 um) and aliquot, and can be stored in -20 ^{o}C. Riboflavin can be dissolved with autoclaved water. The stock is stored at 4 ^{o}C with a concentration of 100 mM. No filtration is required.

4. Once the induction is done, cool the culture to 4 ^{o}C. Pellet the cells down by centrifugation at 4 ^{o}C at 5000 g for 15 min. Remove the supernatant.

   Note: Each centrifuge bottle can hold about 400 ml. It is fine to keep adding more culture

after removing the supernatant each time.

5. Freeze cell pellet in mixture of dry ice and ethanol. Store it at -80 ^{o}C until process.

Protein purification at 4 ^{o}C or cold room*:*

6. Resuspend the cell pellet with 40 ml lysis buffer (50 mM Tris-HCl, pH 8, 300 mM NaCl, 10 mM imidazole and half tablet of **EDTA-free** protease inhibitor cocktail from Sigma) by pipetting up and down. Try to avoid air bubble and make resuspension homogenous.

   Note: High salt concentration can prevent aggregate of Ncb5or-CS/b5R. EDTA can strip Ni in the column.

7. Break cells by using French press (Thermal). Right before the disruption, add PMSF to the resuspension to the concentration of 1 mM and mix well by invert tube several times. The chamber (or cell) of French press holds 35 ml maximal and needs to be pre cool at 4 ^{o}C. The pressure is set to 1000 psi. Each sample should be loaded to the chamber twice to get fully disrupted.

8. Load the lysate into centrifuge tubes (each can hold 30 ml maximal). Spin the lysate at 4 ^{o}C at 15000 g for 45 min. Save the supernatant and have it filtered with 0.45 um filter.

9. Appropriate amount of Ni-NTA (QIAGEN) is added to a gravity column containing tube connection. Make sure that the surface is even. Let 10 column volumes (CV) of water flow through the column to make the resin compact. Equilibrate the column with 3 CV of lysis buffer (step 6).

   Note: All the buffers running through the column needs to be filtered.

10. The filtered sample is loaded to the Ni column with about 4 ml Ni-NTA beads (QIAGEN) by a constant pump at a rate of 1 ml/min. During loading, yellow color can be observed at the top of column.
11. Wash the column with washing buffer (50 mM Tris-HCl, 300 mM NaCl, 20 mM imidazole and 1 mM PMSF, pH 8). About 20 CV of washing buffer is loaded to flow through the column by the constant pump at a rate of 1 ml/min until A280 of flow though is below 0.1 (use washing buffer as blank). After washing step, the resin should show yellow on the top and blue in rest of part.

    Note: PMSF needs to be newly added because it is not stable in aqueous solution. However, PMSF can be stable in isopropanol for half a year.
12. Elute the protein with more that 3 CV of elution buffer (50 mM Tris-HCl, 300 mM NaCl, 200 mM imidazole, 1 mM PMSF, pH 8) driven by the constant pump at a rate of 1 ml/min. Collect all the fractions and pool the yellow fractions together.

    Note: For some fractions with light color, if you are not sure, you can scan them and check A461 (absorbance of FAD).
13. Clean the column with 5 CV of cleaning buffer (50 mM Tris-HCl, 300 mM NaCl, 500 mM imidazole, pH 8). Remove cleaning buffer with 3 CV of water. Fill the column with 3 CV of 20% ethanol.

    Note: Ethanol may not compatible with salt. Every time from ethanol to salt or from salt to ethanol, cleaning the column with water is necessary.
14. Dialyze the pooled sample against 1 L of buffer containing 10 mM Tris-HCl, pH 8, 150 mM

NaCl, 0.1 mM EDTA overnight.

Note: 150 mM NaCl usually is enough for preventing aggregate of Ncb5or-CS/b5R overnight. If the binding to Q column is not good, decrease salt concentration to 100 mM.

15. Add appropriate amount of Q Sepharose to a gravity column with tube connection to pack 4 ml column. Make sure the surface is even. Make the resin compact by flowing 10 column volumes (CV) of water. Equilibrate the column with 3 CV of 10 mM Tris-HCl, pH 8.
16. Take out the sample from the dialysis bag, and dilute it 5 fold with buffer A (10 mM Tris-HCl, pH 8, 1 mM PMSF).

    Note: Dilution makes salt concentration of 30 mM. The protein can bind to Q column but is not stable for long. The purification needs to be done as soon as possible. PMSF needs to be newly added because it is not stable in aqueous solution. However, PMSF can be stable in isopropanol for half a year.
17. The dilute sample is loaded to the Q column with about 4 ml Q Sepharose resin by a constant pump at a rate of 1 ml/min. During loading, yellow color can be observed at the top of column.
18. Wash the column with 2 CV of buffer A containing 1 mM PMSF to remove unbound proteins.

    Note: From this step, the pump can be removed and flow will be driven by gravity. Usually add 1 CV each time. Too much buffer above column can make flow too fast.
19. Elute the protein with increased concentration of NaCl. The buffers all contain 10 mM Tris-HCl, pH 8, 1 mM PMSF. The concentrations of NaCl are 50 mM, 100 mM, 150 mM, 200 mM, 250 mM and 300 mM. 2 CV of buffer at each concentration are used and are added

separately (twice) to avoid fast flow. Collect all the fractions and pool the yellow fraction together.

Note: If the color is too light, scan the fractions and pick ones with high reading at A461. Discard the boundary fractions whose A461/A280 is too low compared to fractions in the center.

20. Add 150 mM NaCl to the pooled sample. Concentrate protein down to 1 ml with 1 mM PMSF.
21. Aliquot the concentrated protein, freeze them with liquid nitrogen, and store them in -80 ^{o}C. The yield for Ncb5or-CS/b5R is less than 1 mg/L.

SDS-PAGE

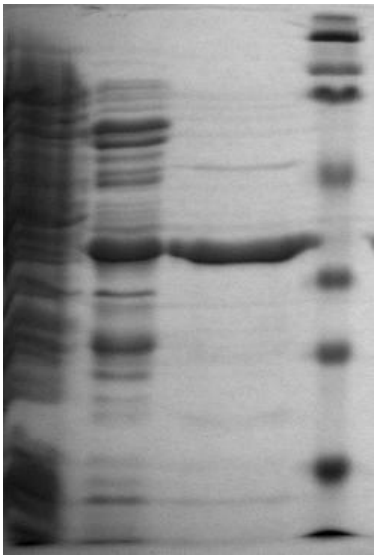

1 2 3 4

SDS-PAGE of Ncb5or-CS/b5R: 1. Supernatant; 2. Ncb5or-CS/b5R after Ni column. 3. Ncb5or-CS/b5R after Q column; 4. Marker.

Mass spectra:

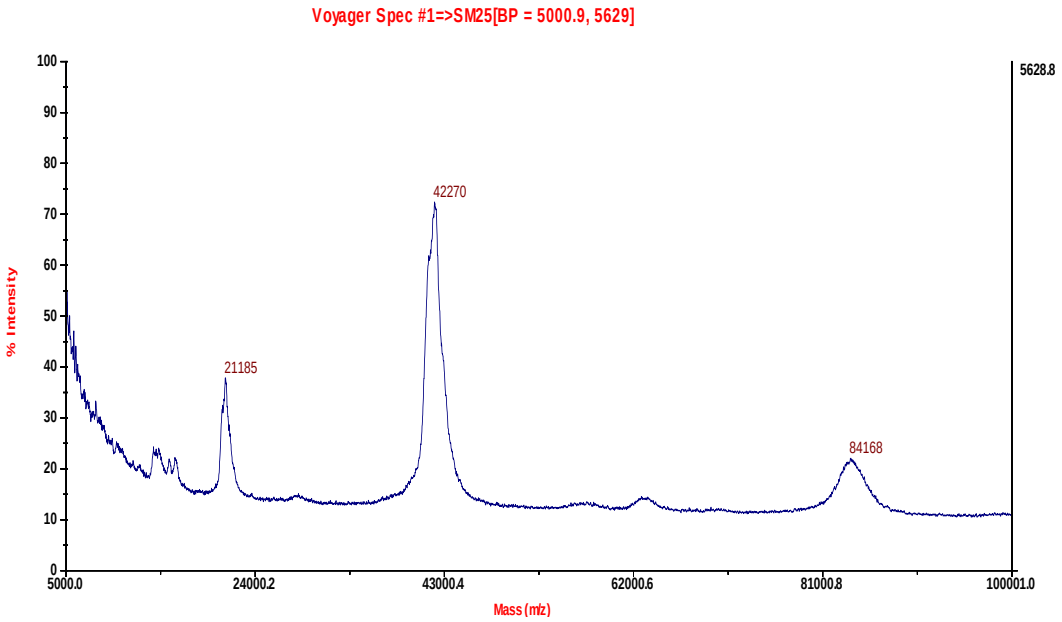

MALDI mass spectra of Ncb5or-CS/b5R: expected size is 41931.

Sequence of Ncb5or-CS/b5R (in pET19b):

MGHHHHHHGPSYPSYDWFQTDSLVTIAIYTKQKDINLDSIIVDHQNDSFRAETIIKDCLYL

IHIGLSHEVQEDFSVRVVESVGKIEIVLQKKENTSWDFLGHPLKNHNSLIPRKDTGLYYRK

CQLISKEDVTHDTRLFCLMLPPSTHLQVPIGQHVYLKLPITGTEIVKPYTPVSGSLLSEFKE

PVLPNNKYIYFLIKIYPTGLFTPELDRLQIGDFVSVSSPEGNFKISKFQELEDLFLLAAGTGF

TPMVKILNYALTDIPSLRKVKLMFFNKTEDDIIWRSQLEKLAFKDKRLDVEFVLSAPISEW

NGKQGHISPALLSEFLKRNLDKSKVLVCICGPVPFTEQGVRLLHDLNFSKNEIHSFTA

Preparation of Cyb5R3

Protein expressions:

1. Grown 10 ml culture (in LB media) of *E.coli* BL21(DE3) that harbors pET19bCyb5R3 at 37 ^{o}C overnight with a shaking speed of 225 rpm.

   Note: Scratch the surface of glycerol stock with autoclaved tips and dip the tip into media containing 100 μg/ml ampicillin. Glycerol stock is very convenient. Try to do this quickly to avoid thawing of glycerol stock.

2. 10 ml culture is inoculated into 2 L TB media, supplemented with 100 μg/ml ampicillin and 100 uM riboflavin. Shake the 2 L of culture at 37 ^{o}C at a speed of 225 rpm until OD600 is close to 1. Usually it takes about 3 hour.

   Note: Choose flask with right size for media. The media should be stirred once put into the shaker.

3. Cool the culture at 4 ^{o}C until it is colder than room temperature. Add IPTG to the culture with final concentration of 0.5 mM. Shake it at 15 ^{o}C with a speed of 200 rpm overnight.

   Note: IPTG and ampicillin can be made as stock of 1 M and 100 mg/ml, respectively, with autoclaved water. Stocks need to be filtered (0.2 μm) and aliquoted, and can be stored in -20 ^{o}C. Riboflavin can be dissolved with autoclaved water. The stock is stored at 4 ^{o}C with a concentration of 100 mM. No filtration is required.

4. Once the induction is done, cool the culture to 4 ^{o}C. Pellet the cells down by centrifugation at 4 ^{o}C at 5000 g for 15 min. Remove the supernatant.

   Note: Each centrifuge bottle can hold about 400 ml. It is fine to keep adding more culture

after removing the supernatant each time.

5. Freeze cell pellet in mixture of dry ice and ethanol. Store it at -80 ^{o}C until process.

Protein purification at 4 ^{o}C or cold room:

6. Resuspend the cell pellet with 40 ml lysis buffer (50 mM Tris-HCl, pH 8, 500 mM NaCl, 10 mM imidazole and half tablet of **EDTA-free** protease inhibitor cocktail from Sigma) by pipetting up and down. Try to avoid air bubble and make resuspension homogenous.

   Note: Low salt concentration can be used for this protein. EDTA can strip Ni in the column.

7. Break cells by using French press (Thermal). Right before the disruption, add 1 mM PMSF to the resuspension and mix well by invert tube several times. The chamber (or cell) of French press holds 35 ml maximal and needs to be pre cooled at 4 ^{o}C. The pressure is set to 1000 psi. Each sample should be loaded to the chamber twice to get fully disrupted.

8. Load the lysate into centrifuge tubes (each can hold 30 ml maximal). Spin the lysate at 4 ^{o}C at 15000 g for 45 min. Save the supernatant and have it filtered with 0.45 um filter.

9. The filtered sample is loaded to HisTrap HP column (5 ml) by ÄKTAxpress purification system (GE Healthcare Life Sciences) at 4^{o}C. The flow rate is 1 ml/min for all the steps. The program is:

   Inlet A: linked to buffer A (20 mM Tris-HCl, pH 8, 500 mM NaCl, 10 mM imidazole)

   Inlet B: linked to buffer B (20 mM Tris-HCl, pH 8, 500 mM NaCl, 500 mM imidazole)

   Inlet S: linked to sample

   Column equilibrium: 5 column volumes (CV) of buffer A

Washing: 20 CV of 5% buffer B

Linear gradient elution: from 10% buffer B to 100% buffer in 10 CV

Auto collection: 2 ml of each fraction in 96-well plate

Note: Buffer A and B need to be filtered with 0.2 um filter. Before starting, pump wash of inlet A, B and S is necessary. Pressure limit is set to 0.5 MPa to avoid damage of system. Targeted protein is usually eluted around 200 mM imidazole.

10. Collect all the fractions and pool the yellow fractions within the dominant UV peak. Concentrate the pooled sample to less than 1.5 ml.
11. The concentrated sample is injected into sample loop with syringe and loaded to Superdex 200 column (120 ml) by FPLC system (GE Healthcare Life Sciences). Before loading, the column is equilibrated with 1.1 column volume of running buffer. The running buffer is 20 mM Tris-HCl, 500 mM NaCl, 0.1 mM EDTA, pH 7. The flow rate is 0.5 ml/min. Collect and pool the yellow fractions within the dominant UV peak. Concentrate protein down to 1 ml.
12. Aliquot the concentrated protein, freeze them with liquid nitrogen, and store them in -80 ^{o}C. The yield for Cyb5R3 is about 10 mg/L.

SDS-PAGE:

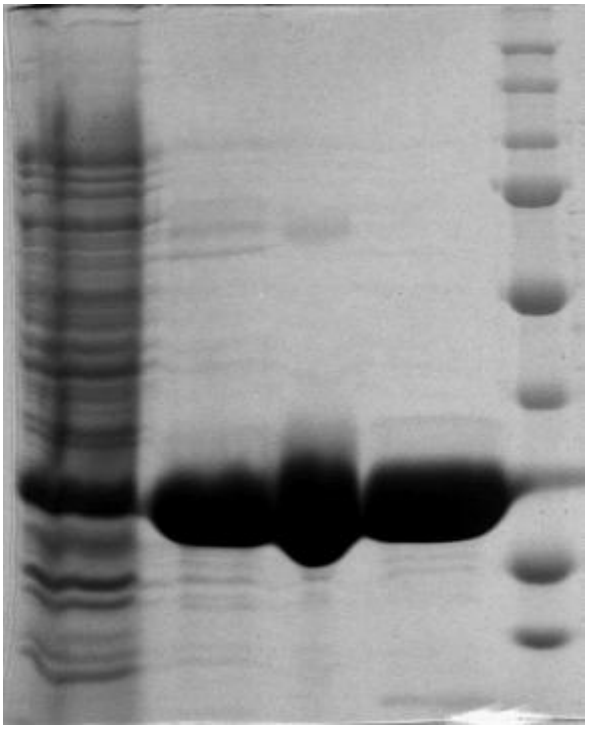

1 2 3 4 5

SDS-PAGE of Cyb5R3: 1. supernatant; 2. Cyb5R3 after Ni column; 3. Cyb5R3 without BME; 4. Cyb5R3; 5. maker.

Mass spectra:

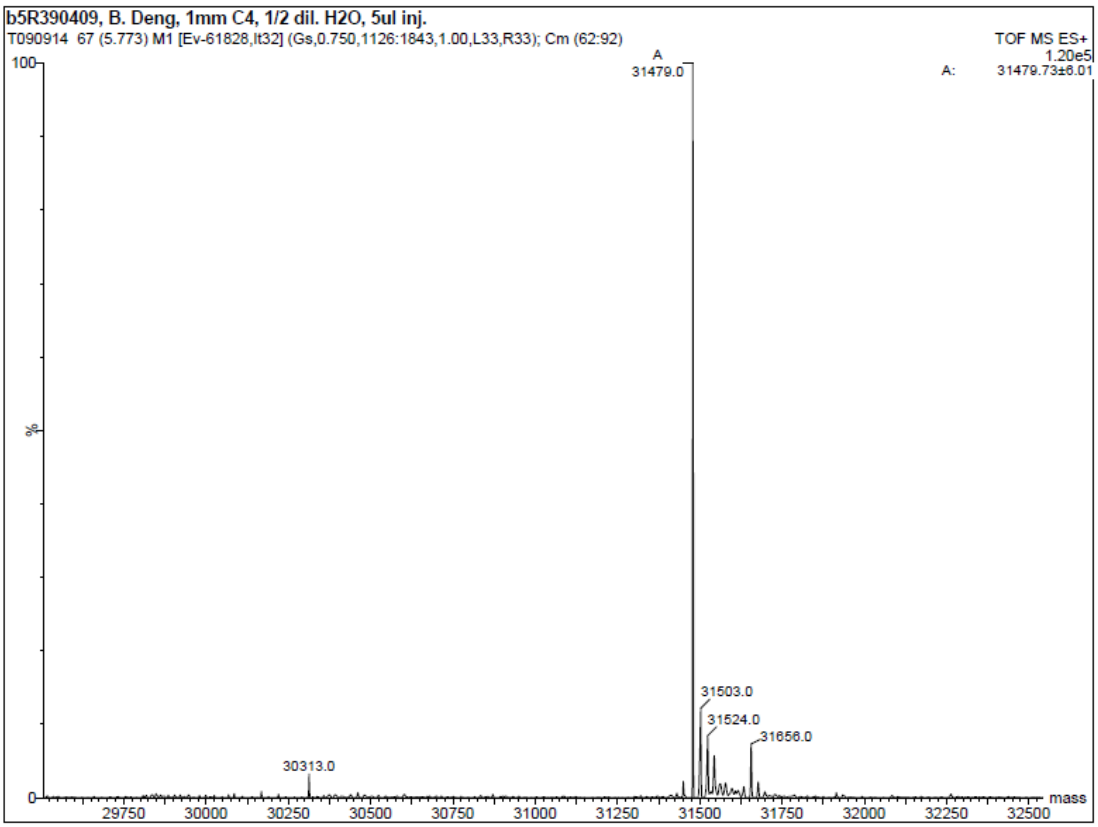

Positive ESI of Cyb5R3: the expected size is 31610.6. The initial Met is cleaved.

Sequence of Cyb5R3 (in pET19b):

MGHHHHHHMITLESPDIKYPLRLIDREIISHDTRRFRFALPSPQHILGLPVGQHIYLSARID

GNLVVRPYTPISSDDDKGFVDLVIKVYFKDTHPKFPAGGKMSQYLESMQIGDTIEFRGPS

GLLVYQGKGKFAIRPDKKSNPIIRTVKSVGMIAGGTGITPMLQVIRAIMKDPDDHTVCHL

LFANQTEKDILLRPELEELRNKHSARFKLWYTLDRAPEAWDYGQGFVNEEMIRDHLPPP

EEEPLVLMCGPPPMIQYACLPNLDHVGHPTERCFVF

Preparation of Ncb5or and D50Ncb5or

Protein expressions:

1. Preparation of Ncb5or, Ncb5orW114A and D50Ncb5or is almost identical.
2. 60 ml culture (in LB media) of *E.coli* BL21(DE3) which harbor the plasmid are grown at 37 ^{o}C overnight with a shaking speed of 225 rpm.

   Note: Scratch the surface of glycerol stock with autoclaved tips and dip the tip into media containing 100 μg/ml ampicillin. Glycerol stock is very convenient. Try to do this quickly to avoid thawing of glycerol stock.
3. 60 ml culture is inoculated into 6 L TB media, supplemented with 100 μg/ml ampicillin and 100 μM riboflavin. Shake the 2 L of culture at 37 ^{o}C at a speed of 225 rpm until OD600 is close to 1. Usually it takes about 3 hour.

   Note: Choose flask with right size for media. The media should be stirred once put into the shaker.
4. Cool the culture at 4 ^{o}C until it is colder than room temperature. Add IPTG to the culture with final concentration of 0.5 mM. Shake it at 15 ^{o}C with a speed of 150 rpm overnight.

   Note: IPTG and ampicillin can be made as stock of 1 M and 100 mg/ml, respectively, with autoclaved water. Stocks need to be filtered (0.2 μm) and aliquot, and can be stored in -20 ^{o}C. Riboflavin can be dissolved with autoclaved water. The stock is stored at 4 ^{o}C with a concentration of 100 mM. No filtration is required.
5. Once the induction is done, cool the culture to 4 ^{o}C. Pellet the cells down by centrifugation at 4 ^{o}C at 5000 g for 15 min. Remove the supernatant.

Note: Each centrifuge bottle can hold about 400 ml. It is fine to keep adding more culture after removing the supernatant each time.

6. Freeze cell pellet in mixture of dry ice and ethanol. Store it at -80 ^{o}C until process.

Heme titration:

7. Resuspend the cell pellet with 40 ml lysis buffer (50 mM Tris-HCl, pH 8, 300 mM NaCl, 10 mM imidazole and half tablet of **EDTA-free** protease inhibitor cocktail from Sigma) by pipetting up and down. Try to avoid air bubble and make resuspension homogenous.

   Note: EDTA can strip Ni in the column.

8. Break cells by using French press (Thermal). Right before the disruption, add 1 mM PMSF to the resuspension and mix well by invert tube several times. The chamber (or cell) of French press holds 35 ml maximal and needs to be pre cool at 4 ^{o}C. The pressure is set to 1000 psi. Each sample should be loaded to the chamber twice to get fully disrupted.
9. Load the lysate into centrifuge tubes (each can hold 30 ml maximal). Spin the lysate at 4 ^{o}C at 15000 g for 45 min. Save the supernatant and have it filtered with 0.45 μm filter.
10. The protein is not expressed as all holo-form. Heme needs to be added. The first step is heme titration to determine amount of heme added to the sample. Take 1 ml from supernatant and dilute it 2 fold with the lysis buffer. The final volume is 2 ml and is held in a wide cuvette. Drop a small stir bar to the bottom of cuvette and let it rotate at grade 7 so that the whole volume can be stirred. Scan the cuvette from 600 nm to 300 nm. Usually the reading at 424 nm is about 0.4. **Slowly** add 5 μl of 0.5 mg hemin solution (dissolved in DMSO) and let stir

bar rotate for **2 min**. Scan the cuvette again in the same range and check the reading at 424 nm. Usually there is increase of 0.15. Repeat adding of heme and scanning until increase of reading at 424 nm is within 0.1. Add 5 μl of 0.5 mg hemin solution again. If the increase at 424 nm is still within 0.1, stop the heme titration. Calculate total volume of hemin added.

Note: Keep the stir bar rotate to avoid heme aggregate. After each adding, stirring of 2 min is necessary. Keep an eye on the region between 300 nm and 400 nm. If the reading of this range increases fast, it is a sign of stopping. In Ncb5or or D50Ncb5or, the heme is reduced from lysate.

11. Based the result of titration, calculate how much of 5 mg hemin solution (dissolved) to be added to the supernatant. Adding of 5 mg hemin should be divided into at least 4 times. There is an interval of 5 min between two adding. Before the first adding, the sample (supernatant) needs to be warmed to close to room temperature. Put the end of tip into sample, **slowly** push pipette and **gently** release hemin into the sample. During one adding, gently tilt the tube several times to make hemin homogenous. Keep manual agitate like this every 2 min. Wait for 5 min before next adding. When it is finished, the sample should change from yellow to orange.

    Note: Heme adding is the only step to be done at room temperature during sample process and purification. This is to avoid precipitation of DMSO. Slow adding is important to prevent heme aggregate which crashes protein. Stir bar can deactivate the FAD domain. Instead of stir bar, I use manual agitate here.

12. Centrifuge the sample titrated with heme at 4 ^{o}C at 20000 rpm for 2 hour. Save supernatant

and filter it with 0.45 μm syringe filter.

Protein purification at 4 ^{o}C or cold room*:*

13. Appropriate amount of Ni-NTA (QIAGEN) is added to a gravity column containing tube connection. Make sure that the surface is even. Let 10 column volumes (CV) of water flow through the column to make the resin compact. Equilibrate the column with 3 CV of lysis buffer (step 6).

    Note: All the buffers running through the column needs to be filtered.

14. The filtered sample is loaded to the Ni column with about 4 ml Ni-NTA beads (QIAGEN) by a constant pump at a rate of 1 ml/min. During loading, orange color can be observed at the top of column.

15. Wash the column with washing buffer (50 mM Tris-HCl, 300 mM NaCl, 20 mM imidazole and 1 mM PMSF, pH 8). About 20 CV of washing buffer is loaded to flow through the column by the constant pump at a rate of 1 ml/min until A280 of flow though is below 0.1 (use washing buffer as blank). After washing step, the resin should show yellow on the top and blue in rest of part.

    Note: PMSF needs to be newly added because it is not stable in aqueous solution. However, PMSF can be stable in isopropanol for half a year.

16. Elute the protein with more that 3 CV of elution buffer (50 mM Tris-HCl, 300 mM NaCl, 200 mM imidazole, 1 mM PMSF, pH 8) driven by the constant pump at a rate of 1 ml/min. Collect all the fractions and pool the orange fractions together.

Note: For some fractions with light color, if you are not sure, you can scan them and check A413 (absorbance of heme).

17. Clean the column with 5 CV of cleaning buffer (50 mM Tris-HCl, 300 mM NaCl, 500 mM imidazole, pH 8). Remove cleaning buffer with 3 CV of water. Fill the column with 3 CV of 20% ethanol.

    Note: Ethanol may not be compatible with salt. Every time from ethanol to salt or from salt to ethanol, cleaning the column with water is necessary.

18. Dialyze the pooled sample against 1 L of buffer containing 10 mM Tris-HCl, pH 8, 50 mM NaCl, 0.1 mM EDTA overnight.

    Note: 50 mM NaCl usually is enough for preventing aggregate of Ncb5or or Ncb5orW114A overnight. For D50Ncb5or, I use 100 mM.

19. Add appropriate amount of Q Sepharose to a gravity column with tube connection to pack 4 ml column. Make sure the surface is even. Make the resin compact by flowing 10 column volumes (CV) of water. Equilibrate the column with 3 CV of 10 mM Tris-HCl, pH 8.

20. Take out the sample from the dialysis bag, and dilute it 5 fold with buffer A (10 mM Tris-HCl, pH 8, 1 mM PMSF).

    Note: Dilution decreases salt concentration to make protein bound to column. PMSF needs to be newly added because it is not stable in aqueous solution. However, PMSF can be stable in isopropanol for half a year.

21. Once dilution, the sample is immediately loaded to the Q column with about 4 ml Q Sepharose resin by a constant pump at a rate of 1 ml/min. During loading, orange color can

be observed at the top of column.

22. Wash the column with 2 CV of buffer A containing 1 mM PMSF to remove unbound proteins.

    Note: From this step, the pump can be removed and flow will be driven by gravity. Usually add 1 CV each time. Too much buffer above column can make flow too fast.

23. Elute the protein with increased concentration of NaCl. The buffers all contain 10 mM Tris-HCl, pH 8, 1 mM PMSF. The concentrations of NaCl are 50 mM, 100 mM, 150 mM, 200 mM, 250 mM and 300 mM. 1 CV of buffer at each concentration is used. Collect all the fractions and pool the orange fractions together.

    Note: For D50Ncb5or, 2 CV of buffer at each concentration can be used to increase separation. If the color is too light, scan the fractions and pick ones with high reading at A413. The ratio of A413/A280 is about 1 for pure protein. Purity of each fraction can be judged by this criterion.

24. Add 150 mM NaCl to the pooled sample. Concentrate protein down to 1 ml with 1 mM PMSF.

    Note: For crystallization, instead of PMSF, other long-last protease inhibitor can be used.

25. Aliquot the concentrated protein, freeze them with liquid nitrogen, and store them in -80 ^{o}C. The yield for Ncb5or and D50Ncb5or is about 0.5 mg/L. A413/A280 is about 1 for Ncb5or, and is a little above 1 for D50Ncb5or.

SDS-PAGE and native gel:

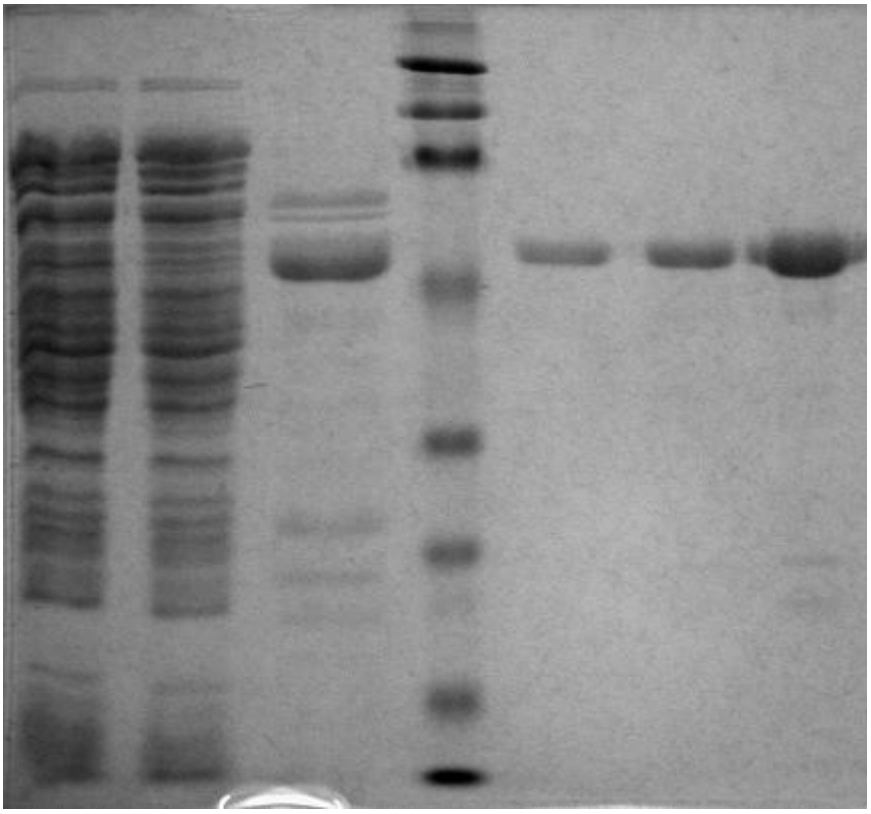

1 2 3 4 5 6 7

SDS-PAGE of Ncb5or: 1: supernatant; 2. flow through of Ni column; 3. Ncb5or after Ni column; 4. marker; 5, 6, 7. different loading amount of Ncb5or after Q column.

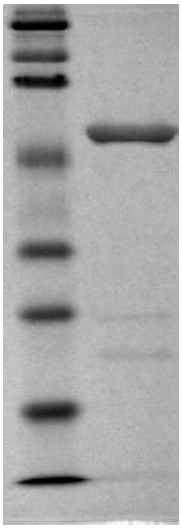

SDS of Ncb5orW114A

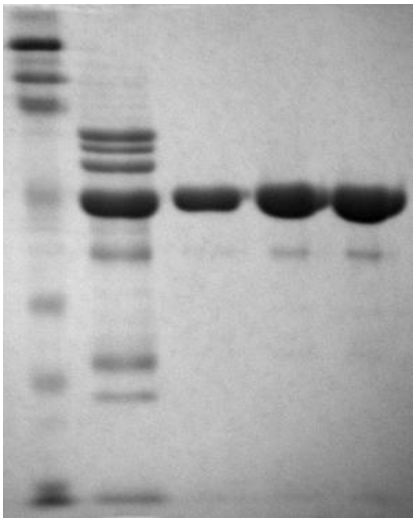

1 2 3 4 5

SDS-PAGE of D50Ncb5or: 1. marker; 2. D50Ncb5or after Ni column; 3, 4, 5. D50Ncb5or after Q column

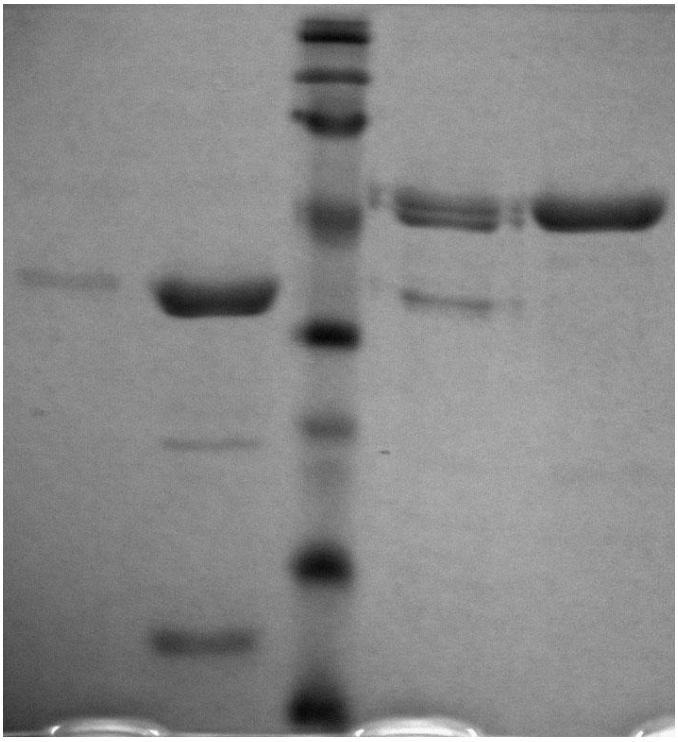

-	+	-	-	FPLC (high pressure)
-	-	+	-	PMSF (short-life inhibitor)
-	-	-	+	Inhibitor cocktail (long-life)

SDS-PAGE of Ncb5or under different purification conditions for more than 1 week: FPLC can generate high pressure and accelerate protein degradation. PMSF can protect protein from degradation in short time. Protease inhibitor cocktail from Sigma has long time of protection.

Native gel of Ncb5or

Native gel of D50Ncb5or

Sequence of Ncb5or (in pET19b):

MGHHHHHHMLNVPSQSFPAPRSQQRVASGGRSKVPLKQGRSLMDWIRLTKSGKDLTGL

KGRLIEVTEEELKKHNKKDDCWICIRGFVYNVSPYMEYHPGGEDELMRAAGSDGTELF

DQVHRWVNYESMLKECLVGRMAIKPAVLKDYREEEKKVLNGMLPKSQVTDTLAKEGPS

YPSYDWFQTDSLVTIAIYTKQKDINLDSIIVDHQNDSFRAETIIKDCLYLIHIGLSHEVQEDF

SVRVVESVGKIEIVLQKKENTSWDFLGHPLKNHNSLIPRKDTGLYYRKCQLISKEDVTHD

TRLFCLMLPPSTHLQVPIGQHVYLKLPITGTEIVKPYTPVSGSLLSEFKEPVLPNNKYIYFLI

KIYPTGLFTPELDRLQIGDFVSVSSPEGNFKISKFQELEDLFLLAAGTGFTPMVKILNYALT

DIPSLRKVKLMFFNKTEDDIIWRSQLEKLAFKDKRLDVEFVLSAPISEWNGKQGHISPALL

SEFLKRNLDKSKVLVCICGPVPFTEQGVRLLHDLNFSKNEIHSFTA

Sequence of D50Ncb5or (in pET19b):

MGHHHHHHMKGRLIEVTEEELKKHNKKDDCWICIRGFVYNVSPYMEYHPGGEDELMR

AAGSDGTELFDQVHRWVNYESMLKECLVGRMAIKPAVLKDYREEEKKVLNGMLPKSQ

VTDTLAKEGPSYPSYDWFQTDSLVTIAIYTKQKDINLDSIIVDHQNDSFRAETIIKDCLYLI

HIGLSHEVQEDFSVRVVESVGKIEIVLQKKENTSWDFLGHPLKNHNSLIPRKDTGLYYRK

CQLISKEDVTHDTRLFCLMLPPSTHLQVPIGQHVYLKLPITGTEIVKPYTPVSGSLLSEFKE

PVLPNNKYIYFLIKIYPTGLFTPELDRLQIGDFVSVSSPEGNFKISKFQELEDLFLLAAGTGF

TPMVKILNYALTDIPSLRKVKLMFFNKTEDDIIWRSQLEKLAFKDKRLDVEFVLSAPISEW

NGKQGHISPALLSEFLKRNLDKSKVLVCICGPVPFTEQGVRLLHDLNFSKNEIHSFTA

Section D: Enzymatic Assays

Preparation of Liver Microsomes and Mitochondria with Density Gradient

1. Use one mouse liver (0.7 – 2 g, fresh or frozen[1]) per isolation. Do NOT mix different livers since each may have different amount of SCD1 protein.
2. Cut liver into small pieces in ice-cold PBS with sharp razor blade to remove blood.
3. Use Dounce homogenizer (loose pestle) to grind up (with 15x up-down-strokes) each liver in 3 ml (or > 3X vol of liver) ice-cold Buffer A (50 mM HEPES, pH7.4, 1 mM EDTA, 0.25 M sucrose, 1 mM PMSF, + protease inhibitor cocktail).
4. Spin down nuclei and cell debris with 3000 g / 15' in cold microcentrifuge.
5. Collect the cloudy upper phase (Post Nuclear Supernatant, PNS) for ultracentrifugation.
6. To increase the recovery, resuspend the debris pellet in < 2.5 ml ice-cold Buffer A, homogenize for 15x strokes, and spin to collect more microsomes (pool with the first PNS extraction, total < 5.5 ml)
7. To collect light subcellular organelle mixture (SOM, including mitochondria / microsomes / peroxisomes), use 5.2 ml pooled PNS sample for ultracentrifugation with SW55Ti rotor and PEG open-top tube under 100,000g (28.6K on Optima Ultra) / 40' / 4 ^{o}C (keep 0.2 ml to confirm [protein] by Western).
8. When the spin is going on, prepare a 10-30% Histodenz density gradient (4.2 ml total in Buffer A / tube) by using 2.2 ml of 30% and 2.0 ml of 10% for the bottom and top reservoir, respectively. Be slow and consistent across tubes! Each needs ~ 3.2 ml 30% stock.

9. Resuspend gently and thoroughly each SOM pellet with 0.5 ml 5% Histodenz. Be gentle by using transfer pipet of wide opening! Avoid air bubbles!
10. Load carefully the entire SOM resuspension on top of gradient (do not disturb!)
11. To separate microsomes from mitochondria with gradient, spin tubes in SW55Ti rotor under 100,000g (28.6K on Optima Ultra) / 18 hours / 4 ^{o}C
12. Take tubes out of the rotor carefully and check the separation of two bands: top = microsome (pinkish yellow, light), bottom = mitochondria (yellow, heavy)
13. Transfer each band into a new tube and add Buffer A to dilute histodenz.
14. Collect organelles by ultracentrifugation (100,000g / 40' / 4 ^{o}C)
15. Resuspend each microsome pellet gently and thoroughly with ~ 0.5 ml Buffer B (0.1 M Tris-HCl, pH 7.2) for SCD activity assay and Western.
16. Determine protein concentration with sample (20 μl of diluted 1/10 – 1/20) and Bio-Rad reagents (1.5 ml each) against BSA standard (20 μl of 0- 1000 μg/ml).
17. Use 80 μg PNS or 10-20 μg microsomes per lane for Western.

Note:

[1] It is important to keep 20-50 mg each liver for RNA preparation with Trizol and qPCR of other functional markers, e.g., SCD1, SCD2, b5, b5R, SREBP1, etc.

Assays of Mitochondrial Function

Preparation of reduced cytochrome c:

1. Swell Sephadex G25 powder[1] in dH2O at 20C for at least 30 minutes with occasional gentle shaking. Remove broken beads (they stay on top in solution whereas intact beads sink to the bottom more easily).
2. Change to 20 mM K-PO4 (pH7.0) buffer and resuspend beads gently by inverting the tube (50 ml good). Pour bead suspension into a long and narrow column (such as 0.7 cm X 15 cm [2]) which contains buffer.
3. Let beads settle by natural flow and gravity force to form a good bed with a flat surface on top.
4. Seal up the top of column to flush the column with at least 2x column volume of buffer to get ready.
5. Oxidized cytochrome c is suspended in 20 mM K-PO4 (pH7.0) buffer at a concentration of 15 mM (100 mg in 0.55 ml, 12 kDa).
6. Add enough granules of ascorbate powder (in ~ 2:1 molar ratio for ascorbate: cytochrome *c*) for reduction immediately before separation on the G-25 column.
7. Observe the color change from brownish red (oxidized) to pinkish red (reduced). Load the mixture solution gently onto the top flat surface of column bed* when it is starting to get dry. Keep the loading zone compact and less than 10% of column volume (preferably ~ 5%).
8. Rinse the sample tube with trace amount of buffer and load it onto the column[3] when all the concentrated samples have entered the bed.
9. Load the buffer gently after the above rinse solution has entered the column[3]. Seal up the top of

column to wash the column with buffer with a drop-wise flow-rate.

10. Watch the migration of red (cytochrome *c*) band along the column and collect the red drops (0.2 ml / tube).
11. Pool the most concentrated (reddish) collections together (~ 1.5 ml total for a 5 ml column) and less concentrated ones together (~ 1.0 ml total for a 5 ml column, normally representing the tail of band).
12. Measure the concentration and purity for diluted samples (~ 20 μM final) with Vis-UV scan (see below).
13. Make small aliquots: ~ 100 ul per 2-mL vials with black cap and PTFE/Silicon liner (12x32 mm, Fisher Cat # NC99087188, 200 ul insert (Fisher Cat # 03-375-1D) can be added for easy withdraw of solution.
14. Fill up each vial with N2 and keep at -80C.

Cytochrome c Oxidase Assay:

1. 20 mM potassium phosphate buffer (pH 7) is pre-incubated at 30 ^{o}C.

2. 20 ul 10 mg/ml dodecyl maltoside (DM) and reduced cytochrome c are mixed in 20 mM potassium phosphate assay buffer (pH 7).

3. 40 μg mitochondrial proteins are added to start the reaction. The total assay volume was 1 ml and initial A550 was 0.68.

4. The decrease of A550 was monitored by the Cary 50 Bio UV-Visible Spectrophotometer for 2-3 min until A550 dropped to about 0.22 and became stable. The pseudo first order rate constant

k was calculated by the kinetic program from the Cary 50 Bio UV-Visible Spectrophotometer, and then k was divided by 0.04 mg (amount of mitochondrial protein) to get a.

$$a\ (min^{-1}mg^{-1}) = k\ (min^{-1})/0.04\ (mg)$$

Citrate Synthase Assay:

1. 100 mM Tris-HCl buffer (pH 8) is Pre-incubated at 30 ^{o}C.

2. 10 ul 10 mM 5,5'-dithio-bis (2-nitrobenzoic) acid (DTNB, dissolved in 100 mM Tris-HCl buffer, pH 8), 4 μl 10% Triton X-100 and 5 μg mitochondrial proteins are mixed in 100 mM Tris-HCl buffer (pH 8).

3. 10 μl 5 mM acetyl-CoA (dissolved in deionized water) and 10 μl 50 mM fresh oxalacetic acid (OAA, dissolved in deionized water) are added to start the reaction.

4. The total assay volume was 1 ml and A412 was monitored for 2 min. The longest linear range was selected to calculate the slope (min^{-1}). Then b was obtained as the formula below:

$$b\ (min^{-1}mg^{-1}mM) = slope\ (min^{-1})/(protein * \varepsilon_{412\ DTNB} * 1\ cm)$$

mitochondrial protein amount=0.005 mg

$\varepsilon_{412\ DTNB} = 13.6\ mM^{-1}cm^{-1}$

Note:

[1]Each gram of beads can swell into ~ 10 ml suspension

[2]The column bed volume is about 5 ml.

[3]When loading onto the column, be extremely gentle to avoid disturbing the flat top surface.

Assay of Fatty Acid Desaturation with Liver Microsomes

1. Use 60-100 μg microsome protein per reaction and 2 reactions for each data point: one with 100 nmole stearoyl-CoA (10 mM FFA stock), the other none; 1 umole (or more) NADH or NADPH and 0.5 ml total (Buffer B) each
2. Add the above components to a new glass tube in the following order (all on ice): (1) Buffer B; (2) microsomes; (3) FFA
3. Initiate the reaction by QUICKLY adding NADH, mixing and starting 37 ^{o}C bath.
4. Stop the reaction at 5' promptly by putting tubes on ice-water and adding 2 ml BHT/methanol to each tube as soon as possible
5. Add 100 nmole FFA 17:0 (internal standard) to each tube and continue extraction: add 4 ml choloform, vortex 20', spin 5', transfer upper phase (aqueous) for retraction with 2 ml methanol / 4 ml choloform, and collect clear bottom phase from both extraction into new tubes for dry-down under N2. To increase FFA recovery: Retract; Do NOT use filter or KCl!
6. Perform transmethylation with 1 ml BF3 each tube (for FFA and PL) at 100 ^{o}C /15'
7. Add 1 ml HPLC-H2O to each tube and 2 ml Pentane for FAME extraction
8. Dry down the FAME content in 2-ml vial under N2 and dissolve with clean Dicholoromethane (60 μl each) and transfer to new inlet for auto injection.
9. Fill up each tube with N2 and keep at -80 ^{o}C until GC analysis

Electron Transfer Assay

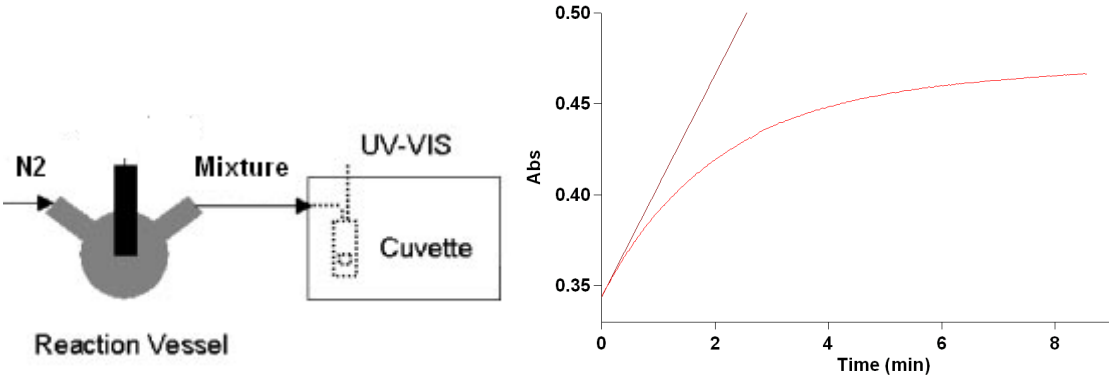

1. Electron transfer assay is performed under anaerobic condition. Protein containing the b5 domain and 50-100 μM NADH are mixed in 5 mM phosphate (pH 7) in the reaction vessel. Drop a mini stir bar into the vessel. The central of vessel is sealed with a rubber stopper. The left side and right side of vessel are sealed by two soft rubber stoppers. Use needles to penetrate each side. The left side is considered as the inlet and the right side is considered as outlet. Let N_2 flow from inlet to the vessel and then to the cuvette. Make sure there is no leakage in the middle. Before entering the vessel, N_2 needs to flow though water. Adjust the flow to see about 5 bubbles per second. Keep the stir bar rotate at grade 7 for at least 15 min to remove oxygen from reaction mixture.

   Note: Heme in the protein will not be reduced by NADH within at least 1 hour. The stir bar will not deactivate the heme protein, but direct bubbling of mixture will deactivate the heme protein. If only initial rate is needed, 15 min of degassing is enough. To get a whole good curve, degassing of at least 30 min is required. In the case of Ncb5or-b5 reduction by Ncb5or-CS/b5R, the rate is too slow to get the whole curve. Usually just calculate the initial slope (rate).

2. Once the degassing is done. Turn down the N_2 flow to see 1 or 2 bubbles per second. Use airtight syringe to inject about 5 μl reductase into the reaction mixture from inlet. The needle of syringe needs to touch the mixture. Usually the final volume is 1.5 ml. Once the injection is done, push the need at outlet into the mixture. The pressure accumulated in the vessel will push the mixture into the cuvette connected. Once the cuvette is filled, start to monitor heme reduction usually at 424 nm. The dead time is about 15 s. It is the first-order reaction. Choose right amount of reductase so that the reaction is not too fast or not too slow. Usually duration is about 10 min.

   Note: Long time of stirring by stir bar can deactivate reductase which contains FAD. Reductase needs to be injected.

3. To calculate the initial slope, set the calculation to zero order in the kinetic program. Choose a short period to calculate the slope. For example, use 0-0.1 min to calculate. If 0 is too noisy. Use the following interval for calculation. For example, 0.1-0.2.

Section E: Biophysical Tools

Circular Dichroism spectra

1. CD spectra are very useful to detect secondary structure (far UV region), tertiary structure by aromatic residues (near UV region), heme environment (Soret region) and FAD environment (about 460 nm).
2. To perform CD spectra, sample should go through buffer exchange to be dissolved in phosphate buffer, pH 7. Nb5 (mutants), Ncb5or-b5 (mutants), Ncb5or or D50Ncb5or is dissolved in 10 mM phosphate buffer, pH 7. Ncb5or-b5R or Ncb5or-CS/b5R is dissolved in 50 mM phosphate buffer, pH 7 due to lower solubility.

   Note: Use dialysis at 4 ^{o}C (about 6 hour) for Ncb5or, D50Ncb5or, Ncb5or-b5R and Ncb5or-CS/b5R. They are susceptible to cleavage and easy to form aggregate during concentration if using concentrator for buffer exchange. For Nb5 and Ncb5or-b5, it is fine to use concentrator for buffer exchange. Sample should be kept on ice before scanning. If final concentration of chloride after dilution with the phosphate buffer is below 1 mM, no buffer exchange will be required.
3. Measurement of CD spectra is performed by JASCO-815 spectropolarimeter at room temperature. First turn on the nitrogen flow feeding the light source and set flow rate (15 cubic feet) as the instruction. Second turn the water pump with cool the machine. After 5 min, turn on the CD spectropolarimeter, light the lamp and let the light source stable for at least 30 min.
4. Start scanning of each sample and corresponding buffer as blank. The parameters are: 50

nm/min of scanning rate, 1 nm of bandwidth and 2 s of response time. Usually scanning rate * response should be close or smaller than bandwidth. For far UV region, 1mm cuvette is used. Under the condition of 1 mm light path, 10 μM protein with about 100 residues can give descent signal. If data are reported as unit of mdeg, divide the value by the protein concentration (μM) and then times 1000000 to get molar ellipticity. Divide molar ellipticity by the number of residues to get ellipticity per residue (only valid for light path of 1 mm and unit with mdeg). For UV and visible regions, 1 cm cuvette is used. On the condition of 1 cm light path, 10 μM of protein can give signal if there is any. For FAD region, it requires about 10 μM protein, but all forms with the b5R domain from Ncb5or have low yield. If data are reported as unit of mdeg, divide the value by the protein concentration (μM) and then times 100000 to get molar ellipticity (only valid for light path of 1 cm and unit with mdeg).

Thermal Denaturation

1. Thermostability of protein containing the b5 domain is defined by tendency of heme loss with increase of temperature.
2. The percent of heme loss (Y axis) is monitored by the decrease in A413 and plotted as a function of temperature. Thermal denaturation experiments are performed on a Varian Carey 100 Bio UV/Visible spectrophotometer equipped with a Peltier-thermostated multiple-cell holder and a dedicated temperature probe accessory (± 0.1 °C).
3. Sample is dissolved in 50 mM potassium phosphate, pH 7 with A413 about 0.7. Record the reading of A413 as A_0. The total volume is 1 ml. The protein solution is in 1 ml quartz cuvette with 1 cm of light path.

   Note: Protein concentration can affect Tm. For usual comparison, A413 is between 0.5 and 1.
4. Fit the cuvette to the cell where air can be circulated by the heater pump. Load the temperature probe accessory onto the top of cuvette. Use an adaptor to seal the cuvette. The adaptor has a hole in the center which can barely allow the insertion of temperature probe. Dip the probe into the solution and fix the probe.

   Note: Cuvette should be sealed during increase of temperature to avoid evaporation.
5. Increase temperature from 25 °C to 99 °C with an interval of 2 °C. Record each temperature and the corresponding absorbance (A) at 413 nm. Record absorbance of 413 nm (A_t) at 99 °C. Calculate percentage of folded protein by the following formula:

$$\% \text{ folded} = (A - A_t)/(A_0 - A_t)$$

Note: thermal program is available for Cary spectrophotometer. Make sure the temperature

recorded is the probe temperature not the block temperature.

6. Fit %folded and temperature (x) into the equation to solve thermal denaturation midpoints (T_m values):

%folded=

(a1*x+b1)+(exp((-t*s/(273+x))+(c*t/(273+x))+s-c-(c*ln(t/(273+x)))))*((a2-a1)*x+(b2-b1))/(1+exp((-t*s/(273+x))+(c*t/(273+x))+s-c-(c*ln(t/(273+x)))))

t in the equation is T_m

Protein Crystallization

1. Protein needs to be purified to a homogeneous state with a purity of more than 95%.
2. The concentration is 20 mg/ml for Ncb5or-b5, about 40 mg/ml for Nb5, 10 mg/ml for Ncb5or, 10 mg/ml for D50Ncb5or and 10 mg/ml for Ncb5or-CS/b5R. Ncb5or-b5 and Nb5 are dissolved in 20 mM Tris-HCl pH 7. Ncb5or, D50Ncb5or and Ncb5or-CS/b5R are dissolved in 20 mM Tris-HCl (pH 7), 300 mM NaCl plus protease inhibitor cocktail from Sigma.

   Note: It is better to not use phosphate buffer to dissolve sample which may cause phase separation without getting any crystal. Long-last protease inhibitor should be used for Ncb5or, D50Ncb5or and Ncb5or-CS/b5R even Nb5 to protect them from degradation. Currently the cocktail is used, but it also contains other small peptide which may interfere with crystal formation. Since the degradation is prevented by PMSF, long-last protease inhibitor like AEBSF with similar effect can be used.
3. Crystal is screened in Compact Jr. sitting drop 96-well plate. Beside each well, there is one small reservoir. So in one plate, 96 conditions will be screened for crystal. For each reservoir, add 75 μl each buffer from Emerald Biosystems or Hampton.
4. For screening at 4 ^{o}C only: seal the plate and pre cool the buffers at 4 ^{o}C for at least 5 min.
5. Drop 0.5 μl concentrated protein to each well with a pipette allowing multiple adding.
6. Transfer 0.5 μl buffer in each reservoir to the corresponding well. Before adding, make each tip touch each droplet of protein in each well so that 0.5 μl of protein can be mixed with 0.5 μl of each buffer.
7. Seal the plate and put it into either 20 ^{o}C or 4 ^{o}C.

Note: It is recommended to set up screenings at both 4 ^{o}C and 20 ^{o}C. Once set up, you should see more than 30% of wells contain precipitations; otherwise the protein concentration is low.

8. Check each well for crystal under microscope every 3 days or every week.

Pictures of crystals or objects:

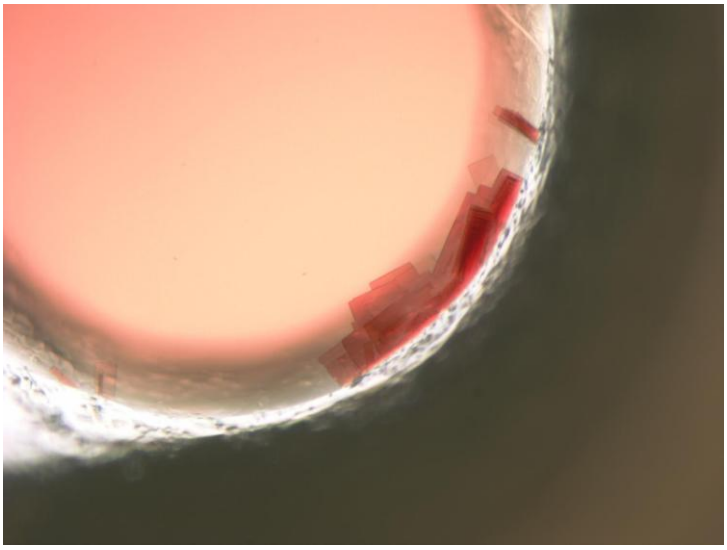

Crystals of Ncb5or-b5 (Wiz2, #41)

Ncb5or (Wiz2, #4)

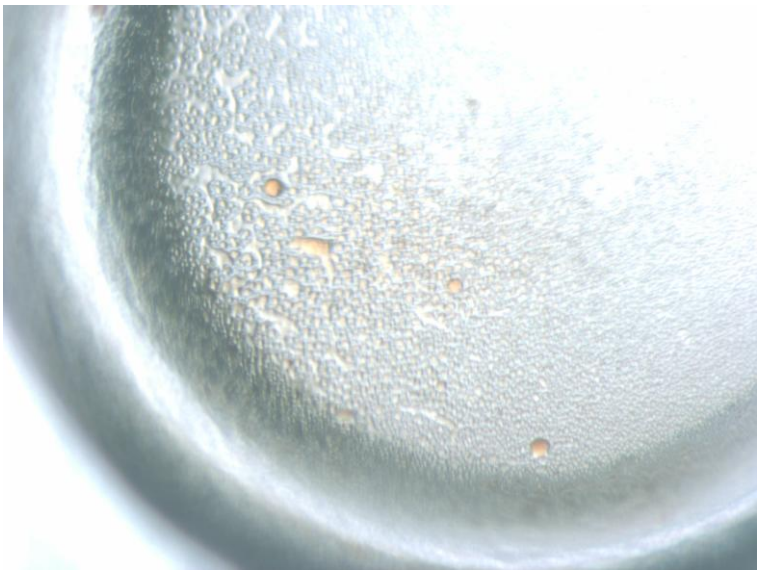

Ncb5or (Wiz2, #16)

D50Ncb5or (Wiz1, #28)